INVESTIGATING THE ROLE OF RUNX1 IN HAIR FOLLICLE STEM CELL DEVELOPMENT AND HOMEOSTASIS

A Dissertation

Presented to the Faculty of the Graduate School

of Cornell University

In Partial Fulfillment of the Requirements for the Degree of

Doctor of Philosophy

by

Karen Marie Osorio

February 2010

INVESTIGATING THE ROLE OF RUNX1 IN HAIR FOLLICLE STEM CELL DEVELOPMENT AND HOMEOSTASIS

Karen Marie Osorio, Ph.D

Cornell University, 2010

Tissue specific stem cells are functionally defined as cells that can self renew and differentiate for the entire life of the organism. As an entry point to understand whether a subset of regulatory pathways is responsible for the functional properties of adult stem cells I analyzed the function on the skin of the transcription factor Runx1, a master regulator of hematopoietic stem cell emergence. I discovered that Runx1 is expressed in the hair follicle from the beginning of its development, at the placode stage, and there on is expressed throughout the life of the organism. Besides its follicular expression Runx1 is highly expressed in the mesenchymal compartment of the skin during morphogenesis but this expression decreases and is completely gone postnatally. By employing tissue specific ablation, lineage tracing studies and cell culture experiments I delineated Runx1 function in the skin at two different stages hair morphogenesis and regeneration.

During embryonic hair morphogenesis I uncovered that two distinct population of Runx1 expressing cells are becoming specified. One population will contribute to the formation of the embryonic hair rudiment while the second population will contribute to definitive compartment of the hair follicle the ORS and bulge. This lineage tracing studies helped elucidating the behavior of adult HFSCs during embryonic development.

Analysis of an epithelial conditional Runx1 knock out (cKO) during hair morphogenesis showed that Runx1 is important during embryonic hair morphogenesis to promote hair follicle induction, *in vivo* and *in vitro* cell proliferation and, *in vitro* keratinocyte cell migration. This developmental role of Runx1 is accomplished in part by modulating the activity of the canonical Wnt signaling pathway, known to be necessary in the skin for normal hair follicle morphogenesis and homeostasis. Furthermore, during adulthood, Runx1 promotes HFSCs activation during normal tissue homeostasis but is not necessary for the injury-triggered stem cell activation mechanism. Collectively all these results demonstrated that besides the HSCs Runx1 function is necessary in a second population of hair follicle stem cell of the bulge.

BIOGRAPHICAL SKETCH

Karen Osorio, daughter of Juan Osorio and Evelyn Martinez, was born in Caguas, Puerto Rico on May 13, 1982. She graduated from Notre Dame High School in 2000 and earned her undergraduate degree in Biology from Universidad de Puerto Rico, Rio Piedras Campus. As an undergraduate student, she worked as a Research Assistant, under the supervision of Dr. Jose Lasalde, investigating the structure of of α4 and α7 subunits of neuronal nicotinic acetylcholine receptors (nAChR). She participated in several summer internship programs in the United States.

In 2002, Karen worked as a Research Assistant at Hunter College, CUNY under the guidance of Dr. Peter Moller. She investigated *Sexual Dimorphisms in the Weakly Electric Fish Mormyrus rume prosboscirostris*. In 2003, she worked as a Research Assistant at Columbia University on *Comparative Studies of the Cysteine Rich Domain Neuregulin-1 in Heterozygous and Wild Type Mice.*

In 2004, Karen graduated with honors from the University of Puerto Rico and moved to Ithaca, New York to attend graduate school at Cornell University and to pursue a Ph D in Genetics and Development. Through the past five years, she has worked under the mentorship of Tudorita Tumbar understanding the role of the transcription factor Runx1 in hair follicle stem cells.

This work is dedicated to those who were there at the beginning of my training and sadly will not be there to see the end result; to my mother and deceased father Juan Osorio, both strong believers in education; and, finally to the two pillars of my life, my mother Evelyn and sister, Carla.

ACKNOWLEDGMENTS

No one earns a doctorate without the help and support of others. I am deeply grateful to all those who took special interest in my progress and contributed in one way or another to my academic and personal development during these past five and a half years. Completion of this dissertation was not possible without the support of many people, particularly my thesis advisor, Doina Tumbar. Through her academic training, trust in my independence to carry out research and the provision of funds to support my investigation, I was able to reach my highest academic potential. I am also indebted to others.

To Ken Kemphues, it was an honor to have you on my committee thank you for the career choice advice that you provided. To Paul Soloway, thank you for the challenging questions that you asked at my seminars. To Lee Kraus, thank you for providing materials that rapidly advanced my research.

I also want to thank my dear friends at the lab for their unrelenting support. To Dave McDermitt for being an excellent lab manager. To my lab mates Jay, Dave, Ying, Song, Deidre, Shu, Morgan, Nikita, Conny, Janice, Charlene and Karin who made the lab feel like a second home**.** To my lab neighbors Maho, Manuel, and Christina for making the mornings and evenings interesting. To Jim Smith for providing perspective as a graduate student and training me to use the FACS machine. To Sanjeev Whagmare for his advice and scientific help. To Gary Isaacs for setting the example of how to teach people, provide advice, materials, and establish protocols. To Nirav for being a great friend and a great colleague.

To Jose Lizardi, my undergraduate student mentor and greatest inspiration for many years. To Dr. Mariana Wolfner for giving me rides to the university every once in a while and providing academic advice. To Dr. Kate Whitlock and John Ewer for their kindness and support during difficult times.

To my mother Evelyn for her unconditional love, guidance, and support. To my sister Carla for her great friendship. To my family in Puerto Rico, especially Arlene, Isadora, Andres, Gero and Ivy for looking after my mother when I could not be there. To Chelsea, my first English speaking friend in Ithaca who helped me to improve my communication skills. To my dear friend Omar Corujo for his emotional support. To Carla Arroyo for being there for me many times. To Nelson, Josean and Felipe, extraordinary friends who cared for my well-being when I was very ill. To Pilar, German, Eli, Juan Camilo, Omar, Beni, Anthony, Nick, Henrique, Jenn, Suzzane, Nadia, Geisa, Ritsdeliz ,Gabriela, Alexis, Marie, Ryan, and Will who made my Ph. D experience a most rewarding one.

TABLE OF CONTENTS

LIST OF FIGURES

LIST OF ABBREVIATIONS

AML1: Acute Myeloid Leukemia 1

BrDU: Bromo Deoxyuridine

CBFB: Core Binding Factor B

cKO: conditional Knock Out

CNS: Central Nervous System

Col-1: Collagen 1

DP: Dermal Papilla

E: Embryonic Day

ECM: Extracellular Matrix

EPU: Epidermis Proliferative Units

FACS: Fluorescent Activated Cell Sorting

FN: Fibronectin

GFP: Green Fluorescent Protein

HF: Hair Follicle

HFSC: Hair Follicle Stem Cells

HS: Hair Shaft

HSC: Hematopoietic Stem Cells

IFE: Interfollicular Epidermis

iKO: inducible knock out

IRS: Inner Root Sheath

Inf: Infundibulum

ISC: Intestine Stem Cells

K1:Keratin 1

K5: Keratin 5

K14: Keratin 14

K17:Keratin 17

LRCs: Label Retaining Cells

NSC: Neural Stem Cells

ORS: Outer Root Sheath

PD: Postnatal Day

PDL: Poly-D-Lysine

RD: Runt Domain

SC: Stem Cells

SG: Sebaceous Gland

SNO: spindle shape N-cadherin positive osteoblastic cells

SGZ: Subgranular Zone

SVZ: Subventricular Zone

CHAPTER1

TISSUE-SPECIFIC STEM CELLS AND THE SKIN

Introduction to stem cells

The development of an organism, including its tissue regeneration, relies on the function of specialized cells called stem cells. A stem cell is unique in its ability to both self-renew and differentiate. This happens through symetric cell division, to generate two identical daughter cells, or to generate an identical daughter cell and a more differentiated one through asymmetric cell division. In vertebrates there are three different types of stem cells: the fertilized zygote, embryonic stem cells, and tissue-specific stem cells. These cells differ in their potential and time of occurrence during development. The fertilized egg and the descendants of its first two divisions are totipotent in that these are the only cells capable of forming the complete organism with its extra-embryonic tissue. The embryonic stem cells, isolated from the inner cell mass of the blastocyst stage embryo, can only give rise to the three germ layers, endoderm, ectoderm and mesoderm. These pluripotent cells are only transient in that they change character as soon as organogenesis begins. Somatic and adult stem cells occur later in development in their respective tissue of origin. Although these cells have a more restricted lineage potential (unipotent, bipotent or multipotent), they are found throughout the lifetime of the organism, replenishing tissues of constant cellular turnover and contributing to tissue repair in case of injury.

Characteristics of tissue stem cells

Stem cells are only a small fraction of the total cell population of a particular

tissue. Some adult tissue-specific stem cells are slow cycling *in vivo.* This slow cycling activity allowed their identification by label retention "pulse-chase" experiments: cells are exposed to either tritiated thymidine or a bromo-deoxyuridine (BrdU), a DNA analog, during the pulse period and the tissues are then analyzed at different time points (or chases) following the pulse. Rapidly dividing cells or transient amplifying cells dilute the BrdU label, while the slow-cycling cells retain the label. These label-retaining cells (LRCs) have been identified as stem cells: not only do they exhibit the slow-cycling behavior typical of stem cells, but transplantation assays show their ability to reconstitute the differentiated cell lineages of a tissue. Using this method, slow cycling cells have been identified in several tissues including the central nervous system (CNS), blood, intestine, hair follicle, muscle, lung, and cornea (Alison and Islam, 2009; Cotsarelis et al., 1990; Duan et al., 2008; Walker et al., 2009). Not all adult tissue stem cells are slow cycling. In the intestine it was recently shown by lineage tracing analysis that the crypt base cells, that rapidly divide *in vivo* can generate all the lineages of intestine cell(Barker et al., 2007; Fuchs, 2009). Regardless of whether they have slow cycling activity *in vivo*, adult stem cells are highly clonogenic *in vitro* (Figure 1.1C).

Figure 1.1. Tissue-specific stem cells

A.Two types of divisions undergone by tissue-specific stem cells 1.) Symmetric cell division to produce two identical daughter cells (expansion of the stem cell pool) or to produce two more differentiated daughter cells (exhaustion of the stem cells). 2.)Asymmetric cell division to produce an identical daughter cell and a differentiated daughter cell (maintenance of the stem cell pool).

B. Tissue stem cells have different potentials: they can be unipotent (only generating one type of lineage), bipotent (generating two lineages), or multipotent (generating more than three lineages throughout the life of the organism).

C. Functional properties of tissue-specific stem cells. *In vivo* the majority of tissue stem cells are slow cycling while *in vitro* they are highly clonogenic.

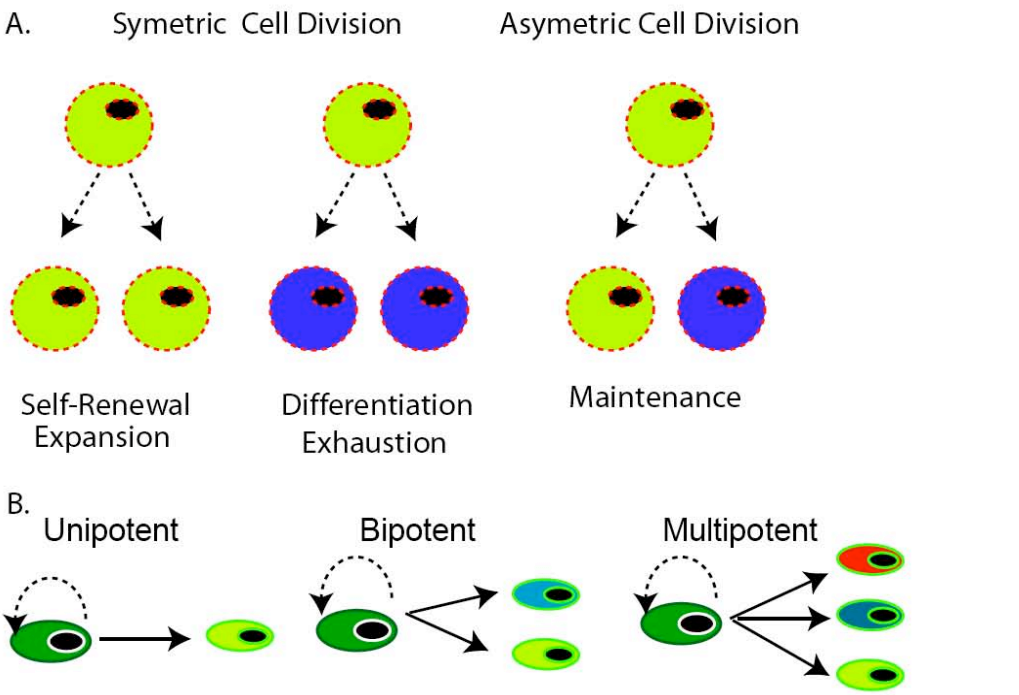
A.
Symetric Cell Division
Asymetric Cell Division
Self-Renewal
Expansion
Differentiation
Exhaustion
Maintenance
B.
Unipotent
Bipotent
Multipotent
C.
Stem Cell Properties
In vivo
Infrequently Divide
Self Renew
Make progenitor cells
Progenitor Cells
In vitro
Rapidly Divide
Self Renew
Make large colonies

The stem cell niche

The concept of a stem cell "niche"was used to explain the clonogenic behavior of stem cells *in vitro*. The stem cell niche is the anatomic location where stem cells are found in any given tissue. Its main function is to regulate stem cell behavior during homeostasis and injury. The niche often involves a proliferative restrictive microenvironment that prevents the stem cells from undergoing exhaustion or overproliferation. In *Drosophila melanogaster* the germline stem cell niche is composed of a support cell, called the hub in the testis and the cap cell in the ovary, surrounded by a cluster of somatic cells (Alison and Islam, 2009; Li and Xie, 2005; Moore and Lemischka, 2006; Walker et al., 2009). Though in mammalian tissues the stem cells niches are more complicated and are under intensive investigation, their primary function remains to provide anchorage and signaling cues that control the fate and the number of the stem cells in a particular tissue.

In the blood, HSCs are physically attached to a group of spindle shape N-cadherin positive osteoblastic cells (SNO) in the trabecular bone. It was shown that mice that have more SNOs (Zhang et al., 2003) or expressed high levels of Jagged 1 (Calvi et al., 2003), a Notch signaling ligand, have an elevated number of HSCs. In the brain, adult neural stem cells reside in the subventricular (SVZ) and subgranular (SGZ) zones of the hippocampus. In the subventricular zone the niche is composed of SVZ astrocytes, ependymal cells, endothelial cells that will form the blood vessels , the neuroblast, and the transitory amplifying progenitors cells (Conover and Notti, 2008; Duan et al., 2008). Numb and Numblike are two factors known to regulate stem cells in the SVZ niche by promoting survival of neuroblast cells (Alison and Islam, 2009).

The subgranular zone niche is composed of the endothelial cells that form the blood vessels, neurons, and SGZ astrocytes (Conover and Notti, 2008). In the muscle, mechanical, electrical, and chemical signals from the myofiber together with the interstitial cells and the basal lamina form the niche for their stem cells called satellite cells (Kuang et al., 2008).

In the intestine and the hair follicle the information about the cellular components of the stem cell niche is less understood. In the intestine, the stem cells are located in the lower region of a structure called the crypt of Lieberkühn. Crypt Base Cells (CBCs) and cells in the +4 position (as measured from the bottom of the crypt and above the specialized type of cell called the Paneth cells) can self renew and differentiate into all the lineages of the crypt-villus unit. It has been proposed that the endothelial cells and the myofibroblast cells surrounding the epithelial cells of the crypt are niche cells. In the hair follicle it is accepted that the bulge is the residence for adult tissue stem cells. However, the support cells in the bulge or in the surrounding dermis still need to be elucidated.

Since all adult stem cells, irrespective of their tissue of origin, share the ability to self-renew and to remain in a relatively undifferentiated state (Alison and Islam, 2009; Alonso and Fuchs, 2003; Moore and Lemischka, 2006), it is possible that a common subset of regulatory pathways are responsible for maintaining cells in a stem cell state. In support of this notion are studies showing transdifferentiation, wherein adult stem cells residing in one tissue contributed to the replenishment of another tissue. Further, transcriptional profiling studies have revealed an overlapping set of genes expressed by

ESCs, HSCs, and NSCs, thus suggesting a potential "stemness" molecular signature (Ivanova et al., 2002; Ramalho-Santos et al., 2002). A subsequent cross comparison of these studies indicated that only a single gene, α6-integrin, consistently overlapped all three populations (Cai et al., 2004; Doherty et al., 2008; Evsikov and Solter, 2003; Fortunel et al., 2003; Ivanova et al., 2002; Ramalho-Santos et al., 2002; Vogel, 2003). A more recent comparison of 12 distinct adult stem cell populations revealed a broader notion of stemness: tissue-specific stem cells were enriched for genes involved in maintaining intracellular processes, while differentiated cells were enriched for genes that aid in communicating with or modifying the extracellular environment (Doherty et al., 2008). Nevertheless the concept of stemness is still used to describe the common attributes and regulatory pathways shared by tissue-specific stem cells (Alison and Islam, 2009; Cai et al., 2004; Fuchs, 2009; Mikkers and Frisen, 2005). Discovering the molecular regulators that affect self renewal and differentiation in the distinct populations of stem cells will help define stemness factors and the common attributes and regulatory pathways shared by tissue-specific stem cells (Alison and Islam, 2009; Cai et al., 2004; Fuchs, 2009; Mikkers and Frisen, 2005).

Tissue stem cells during embryonic development

Most of the knowledge about the behavior and interaction of tissue-specific stem cells with their niche and about their proliferation and self renewal capabilities comes from studies done on fully developed organs. Thus, little is known about the behavior and ontogeny of tissue-specific stem cells during development. When during development do adult tissue-specific stem cells become specified? Are these cells molecularly distint from their progenitors?

What are the mechanisms regulating self renewal in fetal and adult stem cells? Are early tissue-specific stem cells more versatile or less restricted than their adult counterparts? Do these cells also exist within a niche? If yes, when is the niche established and what role does it have during organ development? Answers to these questions might affect the development of cell transplantation-based therapy where the cells from the host and recipient are not always matched by age.

In the blood system, definitive HSCs (those defined by their ability to reconstitute the blood sytem of a lethally irradiated mouse) appear in the mouse at around E10.5 in the aorta gonad mesonephros area, in the placenta, and in the umbilical and vitelline vessels (Dzierzak and Speck, 2008; Speck, 2002). After their emergence, HSCs migrate to the fetal liver and ndergo a series of maturation and expansion processes that allow them to survive, engraft, and self renew in their adult niche, the bone marrow (Mikkola and Orkin, 2006). Besides their niche, fetal HSCs differ from adult HSCs in their proliferative potential and in the expression of surface markers (Dzierzak and Speck, 2008; Mikkola and Orkin, 2006; Speck, 2002). Gfi-1, Tel/Etv6, and Bmi1 are three transcriptional regulators that affect adult, but not fetal, HSCs (Hock et al., 2004a; Hock et al., 2004b; Park et al., 2003). On the contrary Sox17 exerts its effect only in the fetal, but not in the adult, HSCs. Furthermore dissapearence of Sox17 expression in HSCs correlates with acquisition of a less proliferative state (Kim et al., 2007).

In the CNS, neural stem cells arise from a primary pool of neuroepithelial cells. Similar to HSCs, these neuropethial cells have a period of expansion that

results in the thickening of the developing brain. At the onset of neurogenesis (neuron formation) the neuroepithelial cells transform into radial glial cells that persist in the neonatal brain and give rise to oligodendrocytes, neurons, parenchymal astrocyctes, ependymal cells, and subventricular zone (SVZ) astrocytes (Alvarez-Buylla et al., 2008; Kriegstein and Alvarez-Buylla, 2009; Merkle and Alvarez-Buylla, 2006). The SVZ astrocytes functions as NSCs in the adult brain suggesting that fetal and adult NSCs have a common origin (Duan et al., 2008; Merkle and Alvarez-Buylla, 2006). Similar to HSCs, fetal and adult NSCs rely on different mechanisms to control self renewal. One example comes from studies done on the transriptional regulator Bmi1 that affects the maintenance of adult, but not fetal, NSCs. More studies need to be done in order to understand the regulators of both stem cell populations.

Skeletal muscle formation depends on two waves of myogenesis, respectively known as embryonic and fetal myogenesis. Prior to their initiation a group of cells in the dermamyotome, the epithelial sheath that gives rise to the dermis , trunk, and limb muscles, continue to proliferate in a undifferentiated state throughout development until becoming enveloped into a myofiber and acquiring satellite cell positions postanatally (Buckingham et al., 2003; Otto et al., 2009). The survival and expansion of these satellite cell progenitors require the function of the transcription factors Pax7 and Pax3 (Buckingham et al., 2003; Otto et al., 2009). However, this is not true in the adult muscle, were inactivation of Pax7 and Pax3 does not compromise muscle regeneration (Lepper et al., 2009).

Although in the stem cell field it is accepted that the events that occur during

development are recapitulated during tissue regeneration, it is becoming clear that the genetic requirements for the regulation of stem cell and its progenitors at both stages differ.

The skin: a model system to understand stem cell function during development, homeostasis, and injury

The skin is the largest organ in the body and together with its appendages, sebaceous gland (SG) , nail, teeth, and hair follicles (HFs), forms the integumentary system. The main function of the skin is to protect the organism against dehydration, mechanical insults, and microbial infections. In order for these functions to be maintained, the upper most differentiated layers of the skin are constantly being replaced by new cells. The skin, as in all continually renewing tissue, relies on the activity of the stem cells for the constant replacement of differentiated cells in the interfollicular epidermis (IFE), SG, and hair follicle.

The skin itself is composed of two main compartments: the epidermis and the dermis. The epidermis and its appendages, SG, hair follicle, and sweat glands are derived from the ectoderm layer. The dermis is derived from the mesoderm and neural crest cells in the embryo. The epidermis begins to form at E9.5 when a single layer of ectodermal cells acquire epidermal fate. These cells symmetrically divide to maintain the basal layer or asymmetrically divide and differentiate into the suprabasal spinous, granular, and stratus corneum layers of the skin. This process, called stratification, requires the activation of different transcriptional processes and its end result is the formation of the barrier function. In mice the barrier function is completed at

embryonic (E) day E18.5 but needs to be constantly maintained throughout life.

The epidermal stem cells (EpiSCs), thought to be located in the basal layer of epidermis on top of the basement membrane, are responsible for replenishing the pool of basal layer cells and also for continuing the stratification process. Initially it was proposed that EpiSCs resided within domains called epidermis proliferative units (EPU). These EPU consisted of one stem cell surrounded by ~10 progenitors or transient amplifying cells and overlaid by suprabasal cells. Lineage tracing analysis in which epidermal keratinocytes were infected with a LacZ-containing virus confirmed the organization of basal cells into these discrete columnar EPU units (Blanpain and Fuchs, 2006; Ghazizadeh and Taichman, 2001). This current model of stem cell organization was challenged in 2007, when a mathematical model used to fit the data of the fate of genetically labeled epidermal cells predicted that the maintenance of the basal layer relied only on one type of cell (Clayton et al., 2007). It is still a matter of debate whether epidermal stem cells do exist in the basal layer and if they do exist where they reside.

Some of the factors that regulate the balance of proliferation and stratification in the basal layer of the epidermis are well characterized. A homologue of the p53 tumor suppressor gene, p63, is required for the maintenance of the epidermis (Mills et al., 1999; Yang et al., 1999). Analyses of two different p63 null mouse strain showed severe abnormalities that included among others a fragmented epidermis, lack of epidermal stratification, and a complete absence of hair follicles (Mills et al., 1999; Yang et al., 1999). Besides p63, basal layer

cells are regulated by miRNAs, methyltransferases like Ezh2 and transription factors such as p21 and AP2 (Ezhkova et al., 2009; Fuchs, 2007; Koster and Roop, 2007; Yi et al., 2008).

The hair follicle

The hair follicle is one of the epidermal appendages of the skin that together with the sebaceous gland and the arrector pili muscle constitutes the pilosebaceous unit. The hair follicle consists of an upper region, which is permanent, and a lower region, which undergoes periodic cycles of growth and degeneration throughout life (Figure1.2) (Muller-Rover et al., 2001; Schneider et al., 2009). The permanent region consists of the infundibulum, isthmus, sebaceous gland (SG), and bulge. The infundibulum is the region of the follicle close to the epidermis that encloses the hair canal. The isthmus comprises the middle part of the upper follicle that extends from the opening of the sebaceous gland duct to the insertion of the arrector pili muscle. The lower part of the permanent region contains the bulge, which is the niche for hair follicle stem cells.

In the lower, non-permanent part of the hair follicle reside the early progenitors of bulge cells, matrix cells. Once committed to a particular lineage, matrix cells differentiate into the hair shaft or inner root sheath. The hair shaft is composed of the medulla, cortex, and cuticle and is surrounded by the inner root sheath (IRS). The main function of the IRS, composed of the Henle, Huxley, and cuticle layers, is to provide support to hair formation. The transcription factor Gata3 (Kaufman, et al., 2003) together with the activity of Bmp and Notch signaling are essential for the proper specification of the IRS

(Kobielak et al., 2003; Kulessa et al., 2000; Pan et al., 2004).The companion layer separates the IRS from the outer most layer of the hair follicle, the outer root sheath (ORS). Although the function of the companion layer is not understood it has been proposed that it helps maintain the integrity of the IRS and ORS (Poblet et al., 2005). The ORS, continuous to the basal layer of the epidermis, is residence for the sebaceous gland and adult hair follicle stem cells. The transcription factor Sox9 has been involved in the specification of the ORS in the adult.

Hair follicle morphogenesis

An adult hair follicle is the end result of a series of reciprocal mesenchymal-ectodermal interactions that begins in the embryo (Millar, 2002; Muller-Rover et al., 2001; Schmidt-Ullrich and Paus, 2005; Schneider et al., 2009). This process initiates when epidermal keratinocytes respond to an inductive signal from the underlying dermal cells and organize into a structure known as the hair placode (Millar, 2002; Schmidt-Ullrich and Paus, 2005; Schneider et al., 2009). Continuous down growth and proliferation of the placode cells give rise sequentially to hair germ, peg, and bulbous peg. The bulbous peg continues growing and differentiates into an adult hair follicle.

Four different types of hairs form the pelage of the mouse: guard, awl, auchene, and zig zag. In order to produce all these hair types four successive waves of induction, downgrowth, and differentiation happen in the skin during embryogenesis. The first one starts at E14.5 and gives rise to the primary hair follicles or guard hairs.

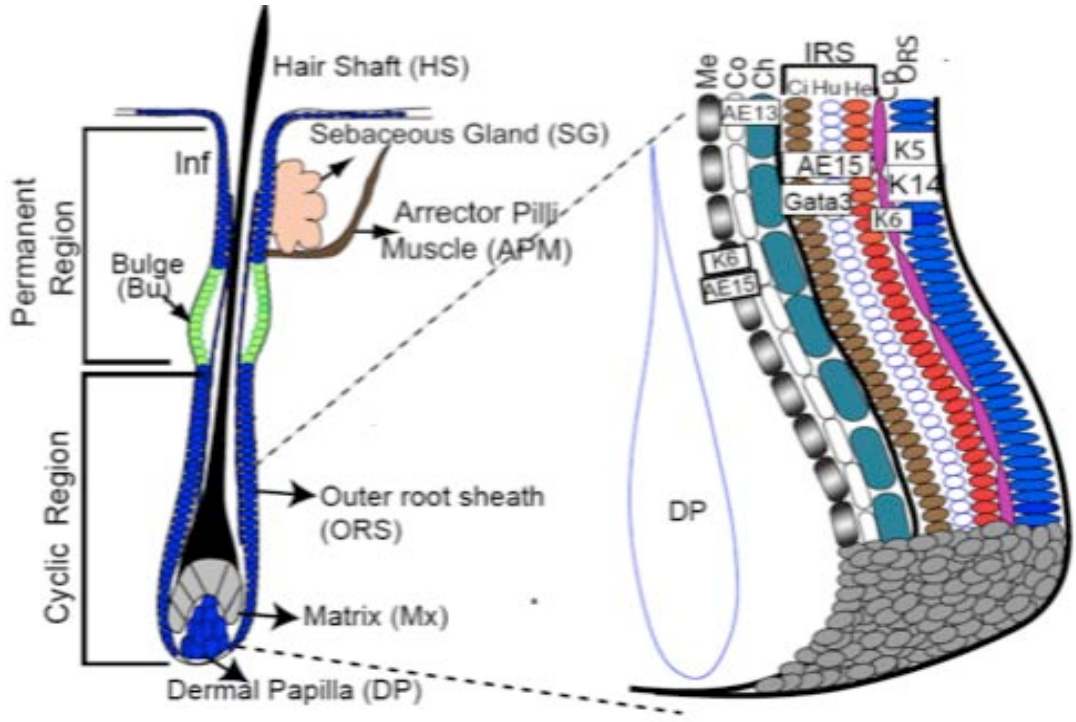

Figure 1.2. The hair follicle.

Illustration of a mature hair follicle and its eight concentric layers of differentiated keratinocytes.

Guard hairs comprise 2-10% of the hair pelage and are unique in that they have sensory function and two sebaceous gland. The second, third, and fourth waves start from E16-postnatal day (PD)0 and give rise to the secondary hair follicles or auchene, awls, and zig zag hair (Schneider et al., 2009). Overall four major signaling pathways ,TNF, TGF-BMP, Wnt and Shh, are responsible for controlling the epidermal-mesenchymal interactions in all hair morphogenetic waves. Hair morphogenesis will continue postnatally until ~ PD17 when the mice enter into the first stage of the adult hair cycle.

Adult hair cycle

The hair follicle undergoes cyclic periods of regression (catagen), quiescence(telogen) and regeneration (anagen) known as the hair cycle. This cyclic process of growth, regression and quiescence is a distinctive characteristic of mature hair follicles that occurs throughout the lifetime of the organism. During the catagen phase the lower part of the hair follicle fully regresses and the dermal papilla (DP), a mesenchymal-derived structure, moves upward to approach the adult stem cell compartment, the bulge. The first catagens last ~3 days in mouse and is followed by the entrance into the telogen phase of the hair cycle. During this phase, the adult stem cells of the bulge complete maturation, express CD34 and Keratin 15 (K15) (Blanpain and Fuchs, 2009; Trempus et al., 2003), and are competent to receive and respond to proliferation cues from the DP (Blanpain and Fuchs, 2009). A new anagen initiates when active stem cells asymmetrically divide and migrate out of the bulge forming transient amplifying matrix cells.

The matrix cells continue to proliferate until they turn on their differentiation programs and regenerate the inner layers of the hair follicle. Unlike in humans, the first postnatal hair cycle after morphogenesis is synchronous in mouse back skin. This feature allows monitoring the genes that affect the hair cycle.

Similarities in hair morphogenesis and cycling

The adult hair cycle, similar to hair morphogenesis, can be divided into three main phases: induction, proliferation, and differentiation (Figure 1.4). In morphogenesis the inductive phase results in a placode formation while in the adult it results in the migration of cells from the bulge to the hair germ. Bmp signaling from the underlying mesenchymal and Wnt signaling in the epithelial compartment control the inductive phase in both the embryo hair development as well as in the adult.

Following the induction phase comes the downgrowth phase characterized by the proliferation and migration of hair progenitors into the dermis. In embryonic hair morphogenesis placode cells rapidly proliferate and invaginate into the dermis forming the hair germ and peg structures. In the adult hair follicle the downgrowth phase occurs once the bulge cells migrate out from the bulge and proliferate to make the hair matrix. These matrix cells continue proliferating into the dermis to eventually enter the differentiation program. Shh signaling is crucial for the downgrowth phase at both stages. During hair morphogenesis Shh is expressed in the placode and during regeneration its expression is polarized in the hair germ.

Figure 1.3. Hair morphogenesis and hair cycle

Embryonic hair development can be divided into eight morphological stages (0-8) that represent the main events occuring during morphogenesis: induction, downgrowth, and differentiation. At the pre-placode stage the cells from the underlying mesenchyme organize beneath the ectodermal layer to send the first inductive signal to the ectoderm. In response to the dermal signal, ectodermal cells organize into the hair placode (stage 1). Placode cells proliferate into the dermis forming the hair germ (stage 2). At these stages a second signal coming from the ectoderm induces the formation of the dermal condensate known as the dermal papilla. The Wnt and Shh signaling pathways are crucial for this downgrowth phase. Besides the formation of the dermal papilla, acquisition of hair polarity and orientation of the hair begins to occur during this downgrowth phase at the hair peg (stages 3-5). The process of terminal differentiation begins at the bulbous peg (stages 6-8), when the different lineages of the hair follicle are being specified. At around PD8 the majority of the hair follicles have reached stage 8 of morphogenesis and continue growing hair until PD17 when they enter their first regression phase (catagen). Catagen is characterized by cell degeneration of the lower part of the hair follicle and is followed by a period of quiescence called telogen. During telogen the bulge compartment is in close proximity to the dermal papilla and will receive signals for a new hair formation phase or anagen. The first telogen phase in mice usually two days, PD20-PD21, and is followed by the anagen phase that lasts around two weeks. A non-active phase of the hair cycle is called the exogen phase, when the old hair is shed out of the hair follicle.

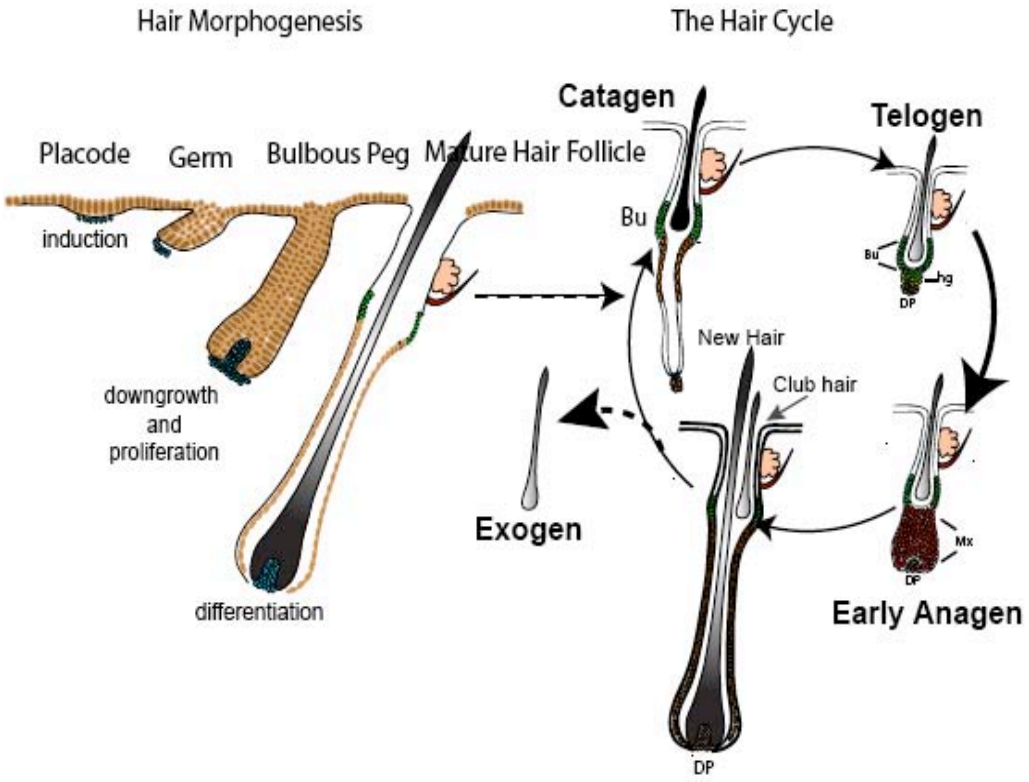
Hair Morphogenesis
The Hair Cycle
Placode
Germ
Bulbous Peg
Mature Hair Follicle
induction
downgrowth
and
proliferation
differentiation
Catagen
Telogen
Bu
hg
DP
New Hair
Club hair
Exogen
Mx
Early Anagen

Blocking Shh signaling during development does not inhibit placode formation but does affect its expansion (Wang et al., 2000). Similarly blocking Shh signaling during regeneration by adding either its inhibitor cyclopamine or anti-Shh antibodies results in a blockage of anagen (Wang et al., 2000). Finally the differentiation phase is when the activation of a combination of signaling cascades will result in the lineage specification and formation of the IRS and hair shaft. Notch and Bmp signaling are key regulators of differentiation at both stages. While Shh, Wnt, Bmp, and Notch appear to be essential for the inductive, downgrowth, and differentiation phases of both hair morphogenesis and regeneration, their activators might be different.

The bulge, the niche of hair follicle stem cells

Several lines of evidence suggest that the bulge area serves as the niche for hair follicle stem cells. In 1990, the bulge was identified as the area of the hair follicle enriched for label retaining cells. Furthermore these LRCs disappeared in response to TPA, a proliferation promoter, indicating that the cells retain the ability to proliferate (Cotsarelis et al., 1990). Experiments in which rosa26-labeled bulge cells transplanted into athymic mice contributed to all layers of the hair follicle, including the ORS and SG, further supported the notion that the bulge region was enriched for stem cells.

Figure 1.4. Similarities between hair morphogenesis and hair cycle

Scheme showing the similarities between the induction, downgrowth and differentiation phases of hair morphogenesis and adult hair cycling. Notice how major pathways like BMP, Wnt and Shh signaling regulate in a similar way the induction and downgrowth phase in both embryo and adult.

Hair Follicle Morphogenesis

Induction

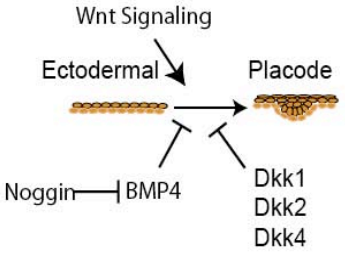

Downgrowth and Proliferation

Proliferation Differentiation

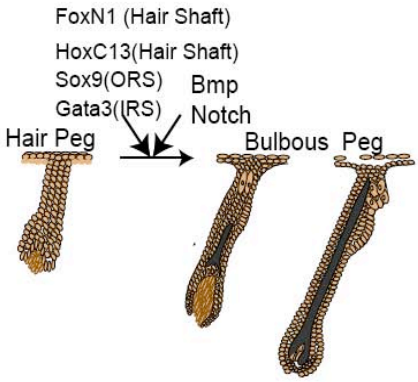

Adult Hair Cycle

Induction

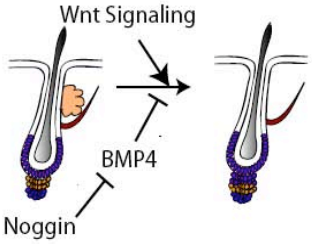

Downgrowth and Proliferation

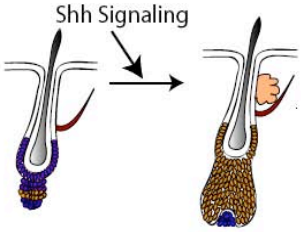

Proliferation Differentiation

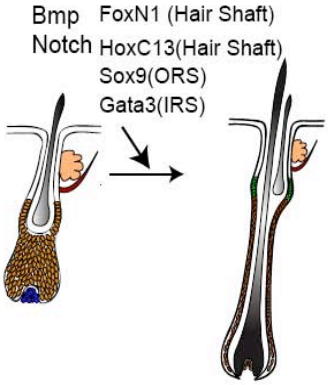

The bitransgenic K5-TetOff;pTRE-H2BGFP mouse strain (Tumbar et al., 2004) has made *in vivo* isolation of slow cycling bulge cells possible: in the presence of doxycycline the tet repressor binds to the tetracycline response elements and shuts down the transcription of H2B-GFP (Tumbar et al., 2004). In this way slow cycling cells will retain the GFP label while rapidly proliferating cells dilute the label below the detectable threshold. Using this approach the slow cycling cells in the bulge were characterized at the molecular level. The authors found that the bulge is enriched for the expression of: 1) extracellular matrix/basement proteins known to participate in niche stem cell interaction, 2) Wnt signaling inhibitors and TgfB-induced factors, 3) cell cycle inhibitors, and 4) a group of transcription factors, some of which are conserved in other adult stem cell populations. The bulge compartment also showed downregulation of genes involved in differentiation and hair fate acquisition.

The multipotency of these bulge cells was tested *in vivo* and *in vitro* by expanding isolated bulge cells that were labeled with either GFP or LacZ *in vitro* and transplanting the back skin of another mouse. Analysis of their descendants showed contribution of labeled cells to all the different compartments of the hair follicle including the sebaceous gland and the bulge. Furthermore in response to a wounding stimulus labeled cells mobilized to repair the wound (Claudinot et al., 2005).

The use of this bitransgenic system also allowed studying the kinetics of cell proliferation of bulge stem cells (1-5 divisions/per cycle) during a complete hair cycle (Tumbar et al., 2004; Waghmare et al., 2008) and determination of the global molecular changes that occur in the bulge compartment during the

telogen to anagen transition (Zhang et al., 2009). Lastly using this bitransgenic system in combination with lineage tracing analysis of single bulge cells allowed determination of the dynamics of proliferation and fate of bulge cells at distinct stages of the hair cycle. Prior to the initiation of a hair cycle, bulge cells migrate away from the bulge without divisions asymmetrically divide, acquire progenitor-like characteristics, and regenerate a new hair. However during anagen bulge cells rely on symmetric cell division to replenish their pool(Zhang et al., 2009). Still, it remains unresolved whether all the cells in the bulge compartment have the same potential, why some cells in the bulge divide only once during a complete hair cycle, whether these singly-divided cells are stem cells or are equivalent to cells that undergoing multiple divisions, and whether the bulge form is comprised of a homogeneous or heterogeneous population of cells.

The sebaceous gland

The sebaceous gland is another appendage of the skin located just above the bulge. The cells from the sebaceous gland (sebocytes) produce oil and sebum that lubricates the hair and skin and inhibits the growth of bacteria. Like the IFE, the sebaceous gland employs a pool of progenitors cells that continually generate these sebum-producing cells.

The transcriptional repressor, Blimp1, is expressed during late embryonic development E17.5 in the skin epithelium. By lineage tracing analysis and cell culture experiments it was shown that Blimp1 marks a pool of progenitor cells that, *in vivo,* can regenerate the whole sebaceous gland and, *in vitro,* form sebocytes colonies that constantly self- renew. Furthermore it was shown that

the absence of Blimp1 in the skin increases the levels of a potent proto-oncogene, c-myc. Mice that lack Blimp1 or over-expressed c-myc in the epithelial compartment of the skin had both abnormalities in the number and size of the sebaceous gland and over-activation of bulge stem cells. It still remains unknown what mechanisms act upstream of Blimp1 to control this population of unipotent progenitors in the SG. Recently another population of bipotent progenitors was found in the upper isthmal region of the hair follicle. These cells expressed Lrig1 and were shown to have high clonogenic potential *in vitro* and to contribute to SG formation and epidermis during normal homeostasis (Jensen et al., 2009). In conclusion the skin is an excellent model system to study stem cell behavior during development homeostasis and injury. Four different populations of epidermal stem cells residing in the skin need to act in concert to become activated and differentiate into the right lineage continuously. How the skin achieves this with a minimal amount of error is a mystery.

Established and potential regulators of hair follicle stem cells

Currently, we are gaining insight into how differentially-regulated genes in the bulge compartment affect hair follicle stem cell behavior. An example is the potent proto-oncogene c-myc that leads to stem cell exhaustion *in vivo* and *in vitro* when overexpressed and also promotes SG fate acquisition (Arnold and Watt, 2001; Gandarillas and Watt, 1997; Waikel et al., 2001). Deletion of epidermal Rac1, a rho guanosine triphosphatase that negatively regulates c-myc, also results in exhaustion of hair follicle stem cells and thus provides a possible indication of how regulatory networks control stem cell behavior in the adult hair follicle (Benitah et al., 2005). Smad4, a co-receptor of the TgfB

signaling , also regulates stem cell behavior. Deletion of Smad4 in the epithelia increases stem cell proliferation that eventually results in stem cell exhaustion (Yang et al., 2009). Sox9 , a member of the SRY gene family characterized by the presence of HMG box, is one of the adult bulge markers expressed during hair morphogenesis. Sox9 function is not required for embryonic hair development. However during postnatal morphogenesis Sox9 is required for the formation of the SG and maintenance of the ORS (Nowak et al., 2008; Vidal et al., 2005).

Stat3 and Lhx2 are two transcription factors involved in the stem cell activation process. While Stat3 epithelial conditional knockout mice have a prolonged telogen that can be reversed by any type of skin injury, Lhx2 knockouts precociously enter anagen suggesting an antagonistic relationship (Rhee et al., 2006; Sano et al., 2000). With this genetic analysis we are beginning to unravel the mechanisms that control hair follicle stem cell activation and maintenance during homeostasis (Blanpain and Fuchs, 2006; Cotsarelis, 2006; Fuchs and Horsley, 2008; Fuchs and Nowak, 2008).

Wnt Signaling promotes activation of stem cells and cell fate acquisition

Wnt proteins belong to a family of cysteine-rich secreted ligands that control a variety of molecular processes including proliferation, differentiation, and cell fate acquisition. In the canonical Wnt signaling pathway, a Wnt ligand activates a series of events that ultimately allow the accumulation and stabilization of B-catenin. B-catenin does not have transcriptional activity by itself, but instead forms an active transcription factor complex with Lef/Tcf

DNA binding proteins and to activate the transcription of its downstream effectors genes.

In the brain, conditional ablation of B-catenin in the cerebral cortex and the hippocampus severely impairs the proliferation of the neural stem cells. In the blood, decreased Wnt activity induced by the overexpression of DKK1 in the osteoblastic niche cells results in increased proliferation of HSCs. In the intestine Wnt signaling is involved in maintaining crypt cells in a proliferative Overall Wnt signaling is a major regulator of tissue-specific stem cells.
Many studies have been done to address the role of the Wnt signaling pathway in the skin during embryonic development and homeostasis. In part this progress has been facilitated by the availability of different genetic tools, such as the BATGAL and TOPGAL (tcf-optimal promoter) reporter mouse strains, that have allowed investigation of the cells and tissues affected by the Wnt signaling. TOPGAL and BATGAL both have a promoter containing multiple tcf/lef1 binding sites upstream of a lacZ gene (DasGupta and Fuchs, 1999; Maretto et al., 2003). Using these reporter mice Wnt activity has been detected at the earliest timepoints of hair morphogenesis. In addition, Lef 1 is first detected in the mesenchymal and epithelial compartments of the skin during the placode stage of embryonic hair morphogenesis (Zhou et al., 1995) and at later stages Lef1 expression is found in the leading edge of the developing follicle (DasGupta and Fuchs, 1999). Mice lacking Lef1 showed severe defects in tissues that require epithelial-mesenchymal interactions that included reduction in total hair density and lack of whiskers in the skin (van Genderen et al., 1994). Furthemore, mice lacking B-catenin in the skin showed a reduction of hair follicle formation during morphogenesis, a lack of hair

cycling in the adult, and a formation of cysts (Huelsken et al., 2001). However, the phenotypes observed in the B-catenin epithelial knockout could be attributed to a defect in both Wnt signaling and E-cadherin mediated cell adhesion. To bypass this problem a stabilized form of B-catenin, which lack the amino terminal domain, was engineered. No phenotype during initial hair morphogenesis was observed in the mice, but at the beginning of a new hair cycle de novo hair follicles formed from the previously developed follicles and eventually turned into tumors (DasGupta et al., 2002; Gat et al., 1998). Ovexpression of Lef1 or a mutated form of Lef1 that lacked its B-catenin binding site under the keratin 14 promoter yielded mice with two distinct phenotypes. With the former the density and orientation of hair follicles was affected during development but not differentiation (Zhou et al., 1995), and with the latter no obvious phenotype was observed during development but during the initiation of a new hair cycle abnormal sebocyte cell fate acquisition was acquired (Merrill et al., 2001). Another interesting fact about the epithelial overexpression of Lef1 and B-catenin was that different phenotypes were observed on different regions of the body indicating the involvement of different interactors.

In the skin, Wnt signaling also regulates hair fate determination during embryonic hair development. In the adult hair cycle, Tcf3 resides in the bulge and the lower ORS while Lef1 is found in the matrix cells (DasGupta and Fuchs, 1999). Overexpressing Tcf3 in the epithelial compartment of the skin suppressed barrier function and terminal differentiation. In addition overexpression of a mutant form of Lef1 that lack the B-catenin binding site promotes sebocyte formation at the expense of follicular formation (Merrill et

al., 2001). All these phenotypic analyses demonstrate how a small misregulation in Wnt signaling can affect hair development, hair cycling, and hair differentiation.

TGF-B signaling: the role of Smads and Bmps in skin restricts activation of stem cell

Bone morphogenetic proteins (Bmps) are secreted proteins that belong to the transforming growth factor-beta superfamily. When bound to their receptors they can either activate the canonical or Smad-dependent signaling cascade or the non-canonical MAPK signaling cascade. In the canonical Bmp pathway, the activated receptor phosphorylates the receptor smads , Smad1, Smad5 and Smad 8, that will interact with the common receptor smad (C-Smad). The C-smad/R-smad complex translocates to the nucleus and activates transcription of the Bmp effector genes. Similar to Wnt signaling, Bmp is another key regulator of proliferation and differentiation in different systems. In the intestine, Bmp signaling inhibits crypt formation.

Analyses of different mouse mutant strains have revealed the role of the Bmp signaling in hair development and homeostasis. During skin development Bmp2 and BmpR1A are both expressed in the hair placode while Bmp4 and Noggin (Botchkarev et al., 1999) are expressed in the mesenchymal compartment. Noggin antagonizes BMP signaling during hair development and when Noggin is ablated the skin shows a severe reduction of hair germ formation accompanied by a reduction of Lef1, cytoplasmic accumulation of B-catenin, and an increase in expression of Bmp2 and Bmp4 (Botchkarev et al., 1999; Botchkarev et al., 2002; Jamora et al., 2003). Furthermore overexpression of Noggin in the matrix cells or conditional ablation of BmpR1A in skin

epithelia showed alteration in the hair follicles due to defects in differentiation (Botchkarev, 2003; Kulessa et al., 2000). These results together demonstrate the importance of Bmp signaling not only for hair follicle initiation but also for differentiation.

The effect of Bmp signaling during tissue homeostasis comes from analysis done on inducible loss of function and gain of function studies. Some of the characteristics of adult HFSCs, such as slow cycling and expression of CD34, are lost upon the conditional loss of BmpR1A. This activation did not result in exhaustion of the stem cell pool suggesting that Bmp signaling is necessary to maintain a quiescent bulge. This observation was supported by the analysis of BmpRIA overexpression in the skin epithelia, which resulted in a blockage of stem cell activation and promotion of hair follicle differentiation (Kobielak et al., 2007).

The family of Runx genes

The Runx genes belong to the mammalian Runt-related family of transcription factors that are highly conserved throughout evolution. These transcription factors share homology in a 128 amino acid region, known as the runt domain (RD), which in humans and mice is encoded by exons 3, 4, and 5. The runt domain is required for their DNA binding activity and also for their interaction with their binding partner, core binding factor B (CBFB).
In mammals there are three Runx genes, Runx1, Runx2, and Runx3, and information about their function comes from analysis done on full knock out mouse strains.

Runx1 is required for the development of adult HSCs and its ablation causes embryonic lethality at E12.5-E13.5 (Okuda et al., 1996; Wang et al., 1996). In addition conditional ablation of this gene contributes to an understanding of its function in different tissues. Runx1 activity is necessary for the development of different subtypes of neurons in the peripheral and central nervous system (Theriault et al., 2004). In the musculoskeletal system, Runx1 maintains muscle homeostasis by repressing genes responsible for muscle atrophy and wasting (Wang et al., 2005). In the epithelial compartment of the skin, Runx1 regulates hair shaft differentiation (Raveh et al., 2006). Runx2 function is essential for osteogenesis and its ablation causes lethality at birth with no osteoblast differentiation (Komori et al., 1997). Runx3 regulates axonal projection to dorsal root ganglia and its absence results in severe motor defects (Inoue et al., 2002; Li et al., 2002). In addition Runx genes control the balance of proliferation and differentiation in many tissues. In the dorsal root ganlia Runx1 expression is required for the expression of different proteins that regulate nociceptive function. Runx3 controls propioceptive differentiation since its conditional ablation or overexpression resulted in a decrease or increased population of TrkC neurons (Zhong et al., 2006).

Besides their function during development, misregulation in any of these genes can lead to cancer formation. Ablation of Runx1 at later stages of postnatal development affects the maturation and differentiation of platelets and lymphocytes, respectively, as well as an expansion of the myeloid lineages (Growney et al., 2005; Ichikawa et al., 2004). Furthermore, in humans, 30% of acute myeloid leukemia cancer patients carry a mutation in Runx1 and it appears to be highly overexpressed in patients with endometrial carcinoma

(Blyth et al., 2005). Although less is known about the oncogenic role of Runx2, its overexpression results in increase cell migration, survival, and angiogenesis all characteristics of malignant transformations. Runx3 has been associated with the formation of gastric cancer due to excessive proliferation and reduced apoptosis in gastric epithelia (Appleford and Woollard, 2009; Blyth et al., 2005). One characteristic of Runx genes complicating the interpretation of their function is that in some situations they can behave as tumor suppressor while in others they can behave as oncogenes. Their function will always be dependent on the cellular context.

Despite all the knowledge about the Runx family of transcription factors in development, differentiation, proliferation, and cancer formation, their function in stem cells behavior is not well understood. The following chapters describe the function of the transcription Runx1 in the skin and hair follicle stem cells.

CHAPTER2[1]

RUNX1 MODULATES DEVELOPMENTAL BUT NOT INJURY DRIVEN HAIR FOLLICLE STEM CELLS ACTIVATION

Introduction

Adult stem cells (SCs) of regenerative tissue, such as blood, hair, and epidermis are essential for homeostasis and injury repair. They are kept quiescent in specialized microenvironments called niches, which are critical in providing control of proliferation and preventing disease (Fuchs et al., 2004). Major developmental pathways are shared by many tissue SCs, but a common core of specialized "stemness" genes remains largely unknown (Fuchs et al., 2004; Mikkers and Frisen, 2005). In this study, we test the role of a master regulator of hematopoietic stem cells (HSCs) and blood development, the transcription factor Runx1 (Speck and Gilliland, 2002), in hair follicle stem cells (HFSCs).

Runx1 is required for definitive blood formation (Speck and Gilliland, 2002; Speck, 2002), while its disruption in adulthood leads to an apparent increase of the HSCs pool, as defined by cell surface markers (Growney et al., 2005; Ichikawa et al., 2004).

---

[1]This chapter has been published in *Development* (Osorio, KM., Lee, SE., McDermitt, D.J., Waghmare, S.K., Zhang, Y.V., Woo, H.N. and Tumbar, T**.** Development**;** 135, 1059-1068.) and is reprinted with permission. The following is the contribution of each individual author to the manuscript: 1. Karen Osorio all figures (2.1-2.13) 2. Song Eun Lee contributed data for figure 2.9 panel C and D. 3. Dave McDermitt helped in the wounding experiments and cell culture experiments 4.) Sanjeev Waghmare provided data for figure 2.2 A and B 5.) Ying Zhang and Sanjeev Waghmare together with Karen worked on the preparation of figure 2.10 and 2.11. All mouse handling, tissue preparation, genotyping for immunofluorescence and skin preparation for cell sorting were done by Karen. Cell Sorting and analysis was done by Sanjeev Waghmare and immunostaining for BrDU /CD34 and caspase was done by Ying Zhang.

Runx1 is mutated in 20-30% of acute myeloid leukemia and myelodisplastic syndrome patients, and affects cell survival, proliferation, and differentiation (Blyth et al., 2005; Mikhail et al., 2006; Speck and Gilliland, 2002). Runx1 also plays roles in muscle (Wang et al., 2005), nervous system (Theriault et al., 2005), and skin, where it affects hair follicle (HF) shaft structure (Raveh et al., 2006). The role of Runx1 in HFSCs is unknown. embedded deep into the dermis (Cotsarelis, 2006). It is composed of concentric layers or sheaths of mainly epithelial cells (keratinocytes) surrounding the hair shaft. The outer root sheath contains the HFSCs in the bulge region below the sebaceous gland. Bulge cells regenerate the rapidly proliferating matrix progenitor cells that further differentiate into the inner layers of the HF and the hair shaft (Figure 2.1A). As with blood development, the HF life can also be divided into primitive and definitive waves, known as morphogenesis and adult hair cycling, respectively. Morphogenesis is the initial temporary phase of hair shaft production, which provides the cellular architecture that will eventually enclose a powerful SC niche: the bulge (Cotsarelis, 2006; (Cotsarelis et al., 1990; Oshima et al., 2001). At the end of morphogenesis, adult HFSCs complete maturation and enter quiescence. The transition from morphogenesis into the adult stage of hair regeneration is initiated by activation and proliferation of bulge HFSCs.

The adult HF undergoes periodic phases of growth and proliferation (anagen), regression and apoptosis (catagen), and quiescence (telogen) that are synchronously orchestrated in mouse skin during youth and take ~3 weeks to complete (Muller-Rover et al., 2001) (Figure 2.1B). A mesenchymal structure (dermal papillae) functions as a signaling center and contacts the hair germ

structure right beneath the bulge SC niche. The dermal papillae sends signals that are thought to synergize with those from the bulge environment, to activate bulge HFSCs proliferation and hair growth (anagen) (Cotsarelis, 2006; Fuchs et al., 2004; Panteleyev et al., 2001). These activating signals antagonize the inhibitory microenvironment of the bulge, thought to be set up in part by the outer root sheath cells including the bulge and germ themselves (Fuchs et al., 2004; Spradling et al., 2001; Watt and Hogan, 2000), and in part by other cell types surrounding the bulge. Single cell assays and transplantations suggest that bulge SCs contribute to making de novo functional niches (Blanpain et al., 2004). However, it is currently unclear whether all bulge and germ cells are stem and/or early progenitor cells, or some perform specialized niche cell roles.

To address the role of Runx1 in adult HFSCs, we targeted its gene locus in skin epithelial cells (keratinocytes). We show that Runx1 modulates HFSCs activation and suggest an overlap in the transcriptional control of SC function at an analogous developmental stage for hair and blood.

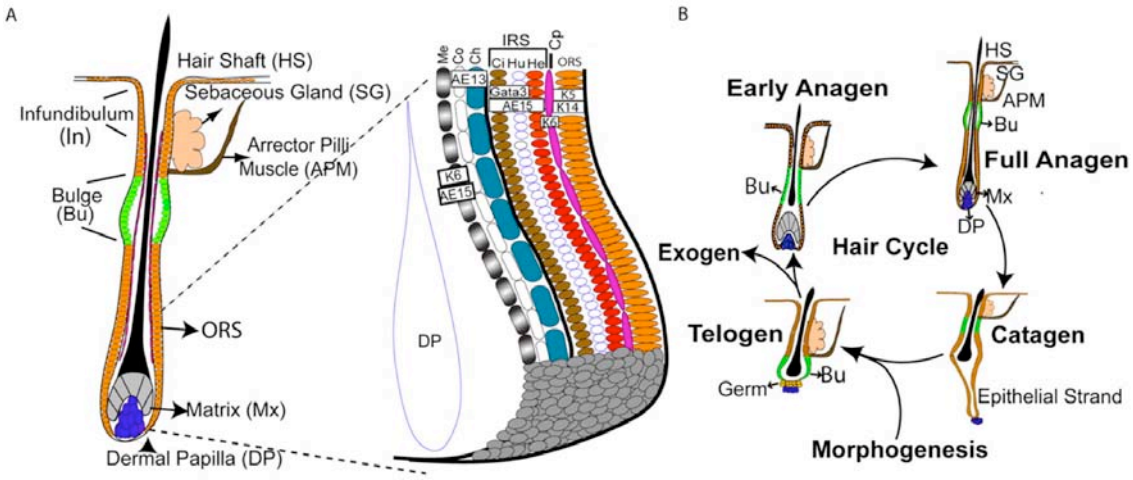

Figure 2.1. Schematics of hair follicle organization (A) and hair cycle (B). The follicle cell layers are depicted in color with appropriate protein marker shown in black-boxed area. SCs are in the bulge and progenitor cells are in the matrix. Differentiated hair lineages: (Cp) companion cell layer; (IRS) inner root sheath; (He) Henle's layer; (Hu) Huxley's layer; (Ci) cuticle of IRS; (Ch) cuticle of hair shaft; (Co) cortex of hair shaft; (Me) medulla. In, infundibulum. Exogen is hair shaft loss.

Materials and Methods

Mice

To generate K14-Cre/*Runx1*$^{\Delta 4/\Delta 4}$mice, we mated hemizygous K14-Cre (CD1) and homozygous *Runx1*$^{Fl/Fl}$ (C57Bl6) mice; F1 K14-Cre/*Runx1*$^{Fl/+}$(CD1C57Bl6) progeny were bred subsequently with *Runx1*$^{Fl/Fl}$ mice. *Runx1*$^{+/LacZ}$ mice were maintained on C57Bl6 background. Genotyping was as described (Growney et al., 2005; North et al., 1999; Vasioukhin et al., 1999). We used littermates wild type (WT) controls housed in cages with knockouts of same sex post weaning at PD (postnatal day) 21. Skin color of animals at PD28 was assessed by visual inspection of the entire back skin, on >24 litters and >129 mice. Mice with any gray patches on the back were scored in anagen.

BrdU labeling

BrdU (5-bromo-3-deoxy-uridine) (Sigma-Aldrich) was injected intraperitoneally at 25μg/g body weight in saline buffer (PBS) at PD20. This was followed by administration of 0.3 mg/ml BrdU in the drinking water. Animals were sacrificed after 3-4 days (N=11 *Runx1*$^{\Delta 4/\Delta 4}$ and 6 WT). Staining of skin sections was described (Tumbar, 2006)

Skin injury

Mouse work was approved by the Cornell University IACUC, and was described (Tumbar et al., 2004). Close shaving of Runx1$^{\Delta 4/\Delta 4}$ skin could result in hair growth, but using scissors avoided this problem. Hair pluck was done with human facial hair removing wax. All wounds were performed lateral of

the midline using a dissection scalpel, and control skin was from the opposite equivalent side of the torso.

Histology, immunofluorescence, and X-Gal staining

Staining of skin tissue for immunofluorescence and hematoxylin and eosin (H&E) were described (Tumbar, 2006; Tumbar et al., 2004). MOM Basic Kit (Vector Laboratories) was used for mouse antibodies. Nuclei were labeled by 4',6'-diamidino-2-phenylindole (DAPI). For 5-Bromo-4-chloro-3-indoxyl-beta-D-galactopyranoside (X-Gal) staining, 10μm skin sections were fixed for 1 min in 0.1% glutaraldehyde and washed in PBS. Incubation in X-gal solution (North et al., 1999) was at 37°C for 12-16 hrs. Antibodies were from (1) rat: a6& ß4-integrins (1:100), CD34 (1:150) (BD Pharmingen), BrdU (1:300, Abcam); (2) rabbit: β-Gal (1:2000, Cappel), K5&K14 (1:1000, Covance), K6 (1:1000), LEF1 (1:250) E. Fuchs, Rockefeller U.), Runx1 (1:8000, Jessel T., Columbia U.), Sox9 (rabbit, 1:100, M. Wegner, Erlangen-Nuernberg U., Germany) (Stolt, et al., 2003), active capase-3 (1:500; R&D Systems), Ki67 (1:100; Novocastra), S100A6 (1:100, Lab Vision), Tenascin C (1:500, Chemicon); (3) guinea pig: K15 (1:5000, E. Fuchs), (4) mouse: AE13 (1:50, Immunoquest), and AE15 (1:10; T.T. Sun, NYU), GATA3 (1:100, Santa Cruz). Secondary Abs were coupled to the following fluorophores: FITC, Texas-Red or Cy5 (Jackson Laboratories).

Microscopy and image processing

Images were acquired using the IP-Lab software (MVI) on a light fluorescence microscope (Nikon) equipped with a CCD 12 bit digital camera (Retiga EXi, QImaging), and motorized Z-stage.To eliminate the out of focus blur, we deconvolved Z-stacks using AutoQuant X software (MVI). Single images and

projections through stacks were assembled and enhanced for brightness, contrast, and levels using Adobe Photoshop and assembled in Illustrator.

Primary cell culture, flow cytometry, and RT-PCR

Skin cells were cultured using low Ca^{2+} keratinocyte E media (Barrandon and Green, 1987), by plating in triplicate 100,000 and 200,000 live (not staining with Trypan Blue) cells on irradiated mouse embryonic fibroblast (passage 4). Keratinocyte colonies and cells were counted using phase contrast microscopy or H&E staining. For flow cytometry cells were stained with biotin-labeled CD34 antibody (eBioscence) followed by Streptavidin-APC (BD-Pharmigen) and with phycoerithrin-labeled α6-integrin (CD49f) antibody (BD Pharmingen), as described (Tumbar, 2006; Tumbar et al., 2004). Live cells were those excluding propidium iodide (PI, Sigma). Fluorescence activated cell sorting (FACS) was performed using BD-Biosciences Aria at Cornell. RNA isolation from sorted cells and RT-PCR of cDNAs were described (Tumbar, 2006; Tumbar et al., 2004).

Western blot

Protein extracts were from skin tissue snap-frozen in liquid N_2 and dissolved in RIPA buffer (1% Triton X-100 in PBS with 10 mM EDTA, 150 mN NaCl, 1% sodium deoxycholate, and 0.1% SDS), protease inhibitors (Protease Inhibitor Cocktail Set III, Calbiochem) and PMSF. Runx1 immunoblotting described in the SuperSignal chemiluminescence kit (Pierce) was done with anti-distal Runx1 (1:1000) (J. Telfer, University of Massachusetts Amherst).

Statistical Analyses

Data are shown as averages and standard deviations. Chi Square test was used for skin color assay (PD29), T-Tests (done with Excel 2003) for colony formation analyses and for FACS of α6+/CD34+ bulge cells. For the growth curve analysis, we used one-factor ANOVA with repeated measures done with MINITAB.

Results

Runx1 expression in hair follicles during stem cell activation

Previously we labeled infrequently dividing putative HFSCs, in transgenic mice that expressed histone H2B-GFP under control of Keratin 5 (K5) driven tetracycline inducible system (Diamond et al., 2000; Tumbar et al., 2004). Microarray analyses of bulge expression profiles revealed Runx1 as a potentially HFSC-increased factor (Tumbar et. al., 2004, and unpublished data). Here we confirmed the up-regulation of Runx1b isoform (Fujita et al., 2001) by RT-PCR of bulge SC populations relative to outside the bulge population (Figure 2.2B). We used H2B-GFP^{high}, and cell surface expression of CD34 and α6-integrin, to define the bulge populations, while H2B-GFP+/α6-integrin+/CD34- cells defined the outside the bulge cells in the basal layer of the epidermis and hair outer root sheath (Trempus et al., 2003; Tumbar et al., 2004) (Figure 2.2A). We isolated skin cells at the telogen-anagen transition (PD49& PD56; Figure 2.2 C, a), 4 weeks after H2B-GFP repression. Since Runx1 was known to be a master regulator of blood stem cells (Speck and Gilliland, 2002; Speck, 2002), we hypothesized that it might also play a regulatory role in hair follicle stem cells.

Figure 2.2 Runx1 expression in HF during SC activation. (**A**) FACS of skin cells after 4 weeks of H2B-GFP repression shows GFP epifluorescence, and surface CD34 and 6-integrin expression. (**B**) RT-PCR for Runx1b in the HFSC pool (CD34+/6+/GFP^{high}) relative to other epithelial skin cells (CD34-/6+/GFP+). (**C**) Skin at second telogen-anagen transition (a) from mice in A. Skin at first telogen-anagen transition (PD21) from Runx1$^{lacZ/+}$ (b) and wild-type (c-e) mice. Staining for Runx1 and Ki67 (d,e) show HFs from serial sections. Arrows (c,d) indicate bulge CD34+/nuclear Runx1+ cell, enlarged in inset. Arrow in e points to a Ki67+ bulge cell, which is indicative of early stage of stem/progenitor cell proliferation (activation). Ep, epidermis; Bu, bulge; hg, hair germ, DP, dermal papillae. Scale bars: 20 μm. Blue is DNA DAPI staining

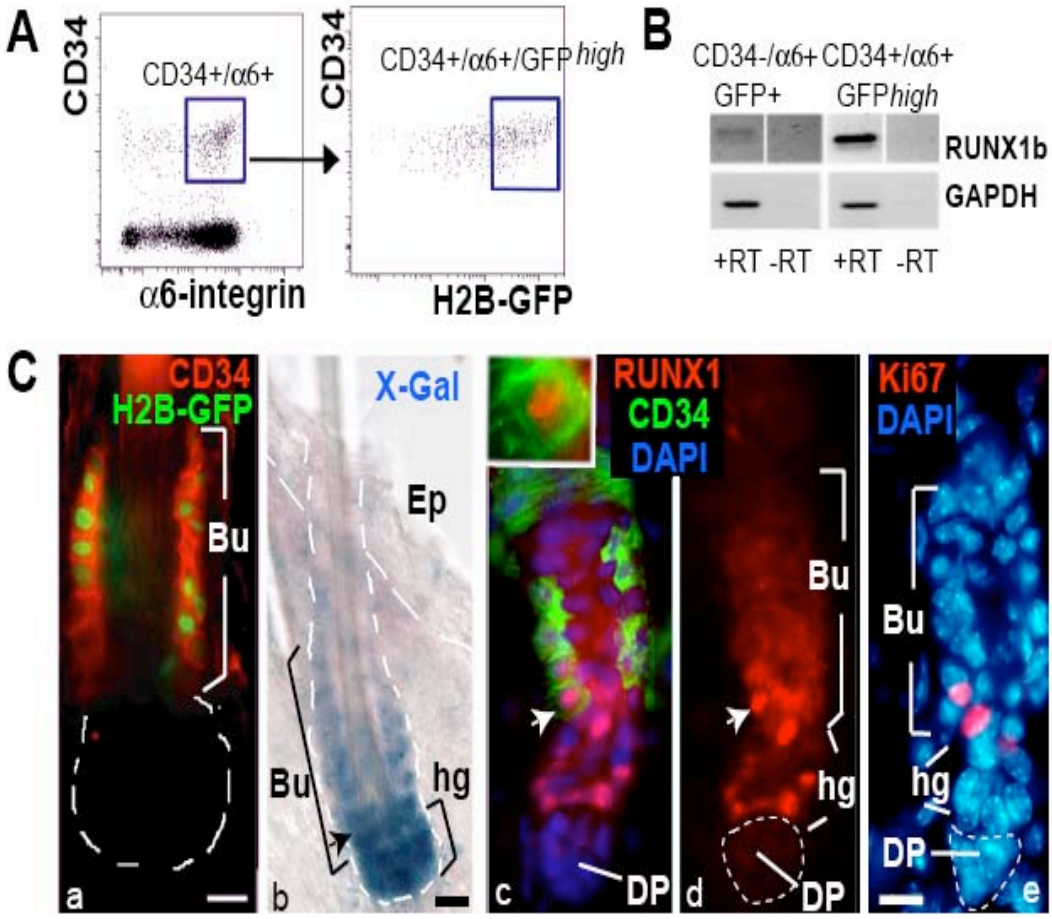
A
CD34
CD34+/α6+
α6-integrin
CD34
CD34+/α6+/GFP high
H2B-GFP
B
CD34-/α6+
CD34+/α6+
GFP+
GFP high
RUNX1b
GAPDH
+RT -RT +RT -RT
C
CD34
H2B-GFP
Bu
a
X-Gal
Ep
Bu
hg
b
RUNX1
CD34
DAPI
c
DP
Bu
hg
d
DP
Ki67
DAPI
Bu
hg
DP
e

To begin to examine its role in HFSCs we first determined Runx1 expression patterns in skin development in $Runx1^{LacZ/+}$ reporter mice previously generated (North et al., 1999). Newborn skin showed Runx1 expression at the epidermal-dermal junction (Figure 2.3A). We also observed Runx1 expression in the bulge, outer root sheath, matrix, and cortex during anagen and in the lower outer root sheath during catagen (Figure 2.3A), as reported (Raveh et al., 2006). The upper HF area (infundibulum) showed variable levels of Runx1, but we found no expression in the interfollicular epidermis. During telogen to anagen transition we found Runx1 expressed in the bulge, as expected from our mRNA analyses of sorted cells. Runx1 levels increased from top to bottom of the hair bulge with maximal expression in the hair germ (Figure 2.2C,b). Moreover, we examined the localization of endogenous Runx1 protein by immunofluorescence with specific antibodies (Chen et al., 2006), at different SC activation stages. Nuclear Runx1 protein overlapped CD34 bulge expression in only a few lower bulge cells during telogen-anagen transition (PD21) (Figure 2.2C, c&d). Furthermore, during anagen (PD24 and P29) more nuclear Runx1+ cells were present throughout the bulge (Figure 2.4B). These differences of Runx1 expression in bulge cells underscore the topological heterogeneity of cells within this area. In particular, the germ and lower bulge, which mark the hair region that proliferates first at the telogen-anagen transition, expressed the highest levels of Runx1.

To determine if Runx1 expression accompanied or preceded the onset of bulge SC proliferation, we stained serial skin sections with antibodies to Runx1 and Ki67, a marker of proliferation.

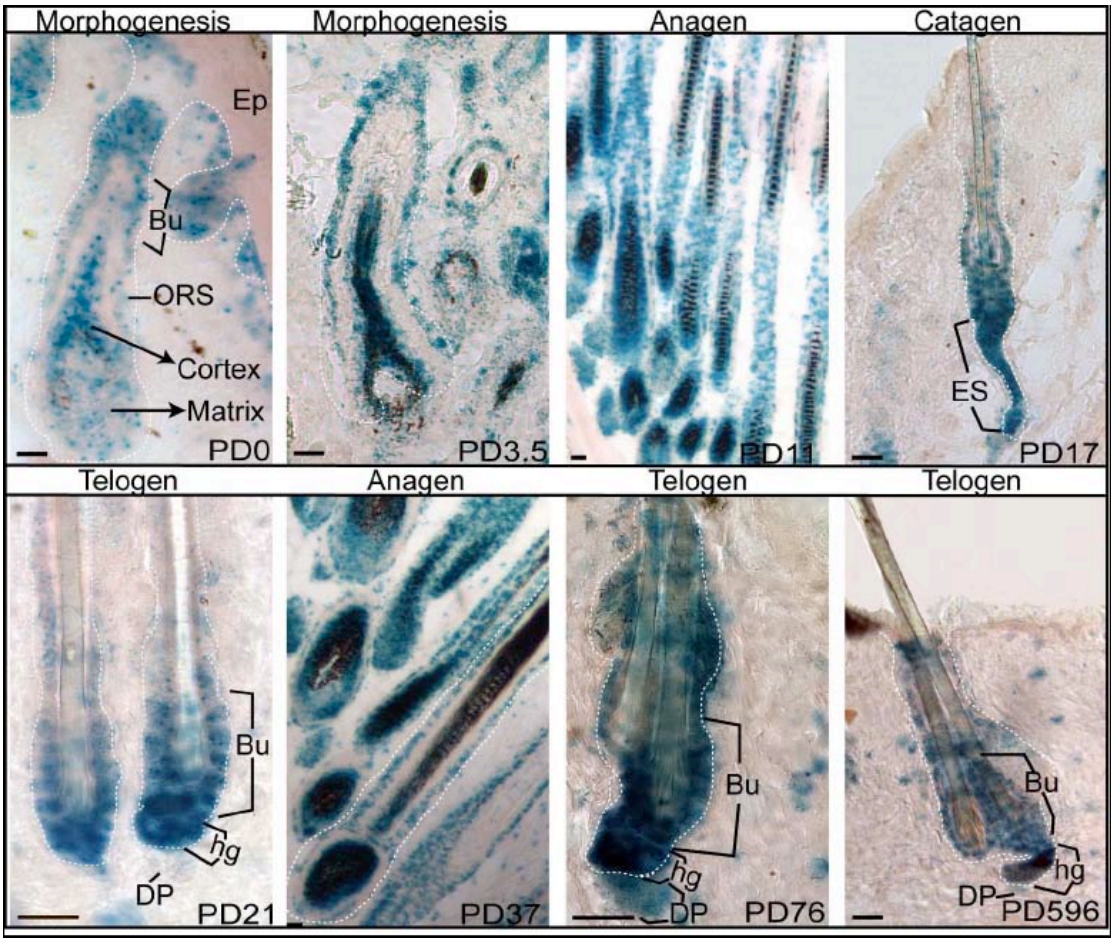

Figure 2.3. *Runx1*$^{LacZ/b+}$ detection during hair development. X-Gal staining of *Runx1*$^{LacZ/+}$ skin documents dynamic *Runx1* expression in hair compartments. Note expression in bulge and other hair compartments during morphogenesis and hair cycle. No expression is found in the epidermis (Ep) but some cells of the dermis underlining the dermal-epidermal junction in newborn skin (PD0) were found positive see De* below broken line demarcating epidermis (Ep) in the upper left corner panel. Bu, bulge; ORS, outer root sheath; DP, dermal papillae; hg, hair germ; ES, epithelial strands; De, dermis.

Nuclear Runx1 was present in ~6-8 cells of hair germ and base of bulge segments, in 50-90% follicles within each skin section. Ki67 staining was found in only 1-2 cells/follicle (Figure 2.2C, e), in ~40% of the follicles (>150 total follicles from 2 back skin regions). Co-staining for Runx1 and Ki67 during different anagen stages revealed that some but not all Runx1+ cells were Ki67+. Conversely we found Ki67+ cells that were Runx1- (Figure 2.4 A2B). Moreover, prominent β-Gal staining of $Runx1^{LacZ/+}$ skin showed Runx1 expression in fully quiescent (Ki67-) hair germs at PD21 (Figure 2.4A). Together these data demonstrate that Runx1 expression precedes the bulge proliferation stage, and suggests a more complex and potentially non-cell autonomous role in cell proliferation.

Runx1 disruption prolongs the hair cycle quiescent phase and impairs HFSCs colony formation

To study Runx1 role in the HF we deleted its function in epithelial cells using Keratin14 (K14) promoter driven Cre mice (Vasioukhin et al., 1999). Under this promoter Cre expression turns on during embryonic hair morphogenesis, and remains active in the basal layer of the epidermis and the outer root sheath of the HF, including the HFSCs. We documented the efficiency of K14-Cre recombination in Rosa26R reporter mice by X-Gal staining (Soriano, 1999), which showed >90% follicles targeted (Figure 2.5A). We crossed the K14-Cre and *Runx1* loxP-containing (floxed) mice, to delete part of the Runt DNA binding domain (Growney et al., 2005).

Figure 2.4. *Runx1* expression in the skin and hair follicle. (**A**) Skin from *Runx1*$^{LacZ/+}$ mice at telogen-anagen transition immunolabeled for β-Gal and proliferation marker Ki67 and counterstained for β4-integrin. Left and right panels are serial sections of the same hair follicles. (**B**) Skin from wild-type mice in anagen (PD24) shows triple co-immunostaining for Runx1 (red), Ki67 (green) and CD34 (blue). Arrows show Runx1+/Ki67+ cells, arrowheads show Runx1+/Ki67−, and asterisk shows Runx1−/Ki67+ cells. Bu, bulge; Mx, matrix; HS, hair shaft; ORS, outer root sheath; Ep, epidermis; hg, hair germ. Scale bar: 50 μm.

A

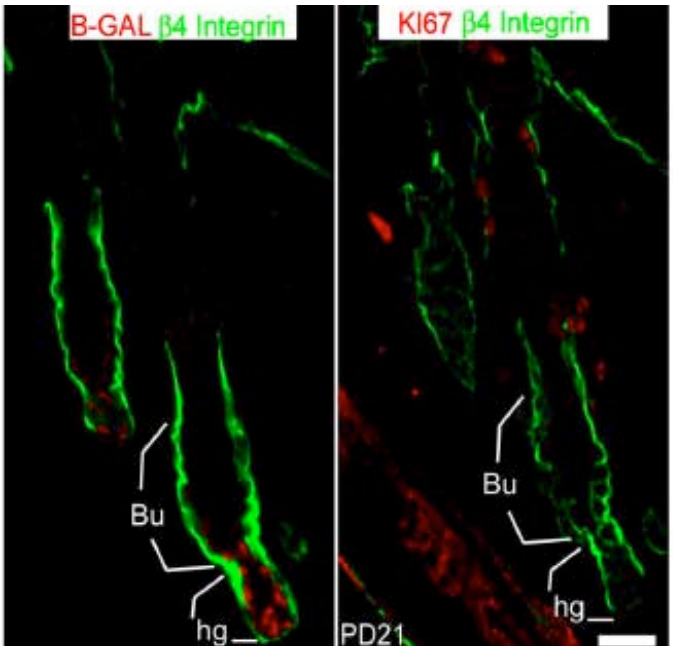
B-GAL β4 Integrin
KI67 β4 Integrin
Bu
hg
Bu
hg
PD21

B

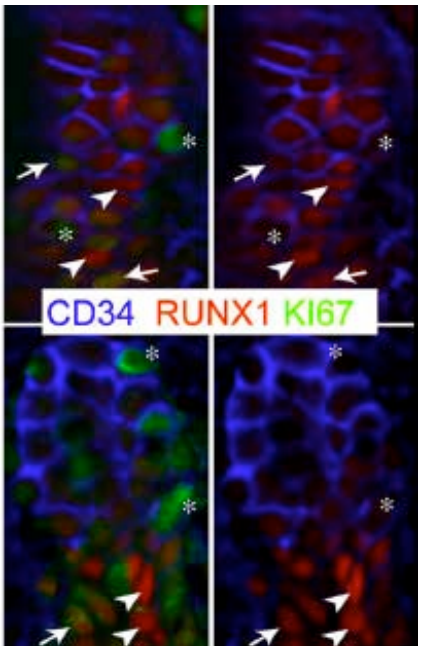
CD34 RUNX1 KI67

To identify mice that carried the *Runx1* mutation we used specific PCR primers (Growney et al., 2005; Vasioukhin et al., 1999). Mice positive for Cre and homozygous for Δ4 deletion were designated *Runx1*$^{\Delta4/\Delta4}$ mutant, while littermates with no excision band (*Runx1*$^{Fl/Fl}$ or *Runx1*$^{Fl/+}$) were labeled as wild type (WT) (Figure 2.5B). Western blot of PD21 protein extract with an antibody to the N-terminus of Runx1 (Telfer and Rothenberg, 2001) showed substantial reduction of full-length Runx1 and a truncated band of ~20 kD (Figure 2.5C). The Runx1 N-terminal domain is known to have a weak transcriptional activity, but is incapable of DNA binding (Blyth et al., 2005; Mikhail et al., 2006). Furthermore, Runx1 immunofluorescence of skin from 4 mutant mice at PD21, PD23 (Figure 2.5D, E) and PD29 (not shown) showed no staining in 92% of follicles. Together, these data showed high efficiency of Runx1 deletion in epithelial cells. *Runx1*$^{\Delta4/\Delta4}$ mice appeared essentially normal in their early postnatal life. By weaning, the mutant mice appeared obviously smaller than WT and heterozygous littermate controls, weighing on average ~30% less at PD21 and PD29 (data not shown). However, Runx1$^{\Delta4/\Delta4}$ showed no premature HF anagen cessation, hair loss or hair thinning, phenotypes commonly associated with severe malnutrition (Rushton, 2002).

The hair shafts began to appear on WT and *Runx1*$^{\Delta4/\Delta4}$ animals skin at ~PD5. Mild structural defects of the hair coat were apparent as described in detail elsewhere in Keratin 5-Cre Runx1 knockout mice ((Raveh et al., 2006), and was consistent with Runx1 expression in hair cortex. To look for effects of *Runx1*$^{\Delta4/\Delta4}$ mutation on HF development, we analyzed the histology of sections from a skin region of the mouse upper right back during morphogenesis and

the first adult hair cycle (Figure 2.5F,G). Skin morphology, expression of Ki67 and differentiated hair cell lineage markers appeared normal in morphogenesis (data not shown). At PD21, both mutant and WT follicles were in catagen VIII (Muller-Rover et al., 2001; Paus et al., 1999) or telogen (Figure 2.5F, 2.6A). Thus, HF morphogenesis appeared largely unperturbed by Runx1 deletion.

Starting with PD21, HFs of the *Runx1*$^{\Delta 4/\Delta 4}$ mice showed a striking phenotype. WT follicles reached full anagen and produced new hair shafts by PD29 (Figure 2.5F,G,H). In contrast, *Runx1*$^{\Delta 4/\Delta 4}$ HFs were quiescent (catagen VIII or telogen) at all time points analyzed past PD21 (Figure 2.5F, 2.6B). The telogen stage in mutant mice encompassed the entire back skin, and unlike WT mice *Runx1*$^{\Delta 4/\Delta 4}$ mice were unable to re-grow hair within two weeks after gentle hair removal with scissors (Figure 2.5H). To quantify this effect we used skin color of PD28-29 mice (Figure 2.5I, 2.13). Whereas 93% of WT mice had grey/black skin indicative of anagen (N=59), 81% of the *Runx1*$^{\Delta 4/\Delta 4}$ mice had pink skin indicative of telogen (N=42). We also found that 94% of *Runx1*$^{\Delta 4/+}$ heterozygous mice showed anagen specific grey/black skin (N=18). The 19% Runx1$^{\Delta 4/\Delta 4}$ mice with anagen follicles were indistinguishable from WT in body weight and hair coat appearance and were likely the result of inefficient Cre-mediated gene disruption. Consistent with this assessment, skin samples from 3 such animals showed normal nuclear Runx1 staining. In addition, we ruled out the possibility that anagen onset in mutant mice was influenced by their lower weight, by comparing skin color of Runx1$^{\Delta 4/\Delta 4}$ animals at PD29 to small WT littermates of similar weight (Figure 2.7).

Figure 2.5. Effect of Runx1 disruption on HF cycle and keratinocyte growth. (A) X-Gal stained skin (blue) from Rosa26R mice shows efficiency of K14-Cre. (B) PCR of genomic DNA shows detection of K14-Cre transgene (top) and Runx1 alleles (bottom): loxP unexcised (Fl), loxP excised (cKO) and loxP untargeted (+).(C) Western blot of total skin protein extract probed with N-terminal Runx1 antibody. (D) Skin sections from PD21 mice show nuclear Runx1 protein (red) in hair germ cells in wild-type but not Δ4 animals. Asterisk indicates hair shaft autofluorescence. (E) Quantification of HFs with nuclear Runx1 expression. (F) Hematoxylin and Eosin stained skin sections at indicated ages demonstrate prolonged telogen in cKO mice. (G) Summary of hair cycle stage determined by microscopy of Hematoxylin and Eosin stained skin sections. In brackets are numbers of mice analyzed. (H) Wild-Type but not cKO mouse skin at PD25 produces new hair during first hair cycle following morphogenesis. (I) One hundred and one wild-type and cKO mice analyzed by skin color at PD29 show 4 mice in telogen (pink skin) when virtually all wild-type mice are in anagen (black skin color) (P<0.001). (J) Bright-field images of Hematoxylin and Eosin stained keratinocytes on feeder cells, 2 weeks post-plating. Wild-type keratinocyte colony is outlined. (K) Growth curve from 100,000 live keratinocytes plated on feeders. $Runx1^{4/4}$ keratinocyte proliferation is impaired (P<0.0001) after 3 weeks in culture. (L) Arrow indicates an example of colony imaged by phase contrast (L). (M) Quantification of primary keratinocyte colonies obtained from equal numbers of WT and 4 plated cells. 4 mutant show impaired colony formation P_{exp1}=0.012; P_{exp2}=0.019. Ep, epidermis; Hf, hair follicle; DP, dermal papillae; hg, hair germ; Bu, bulge. Scale bars: 50 μm.

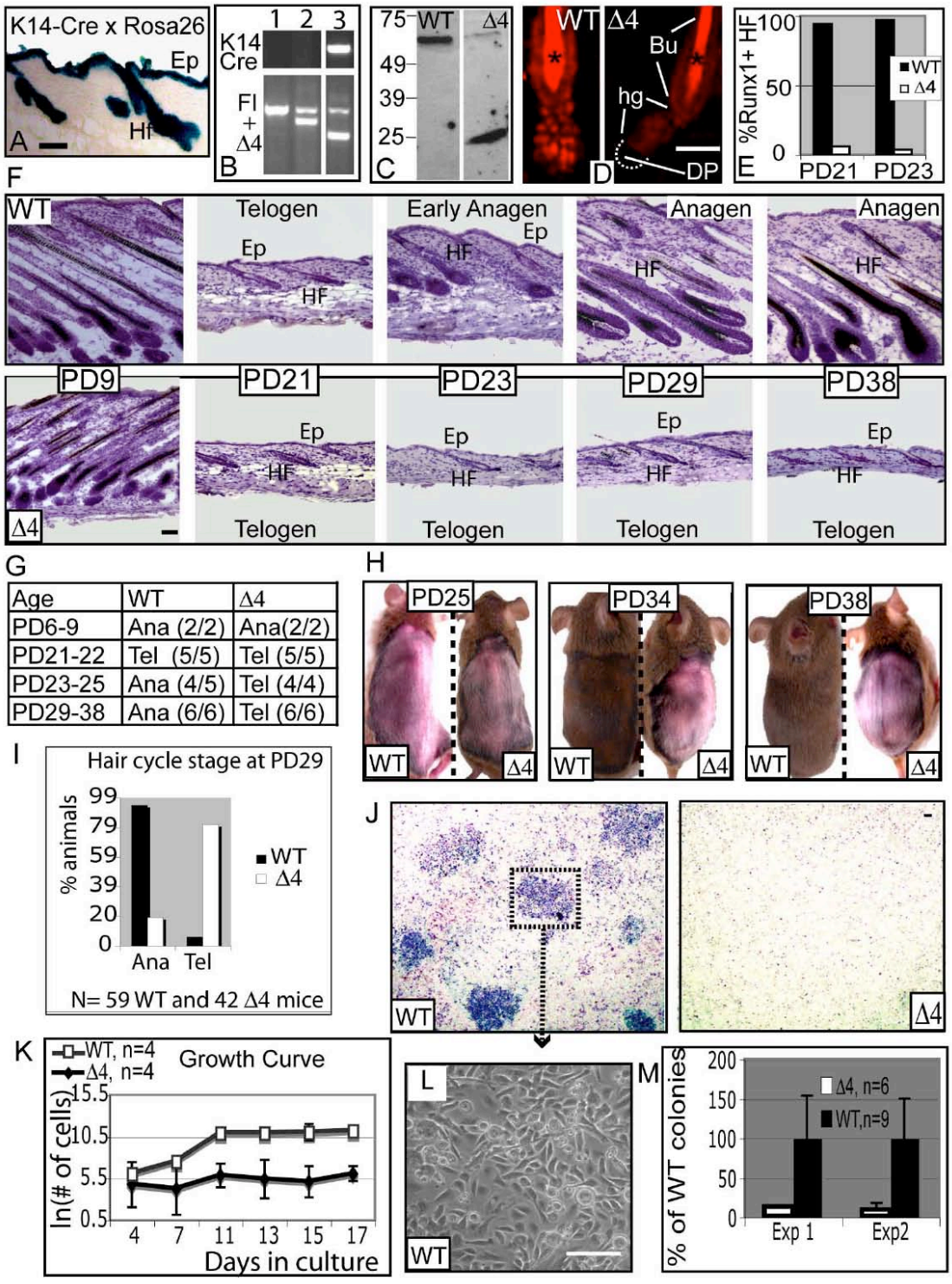

Age	WT	Δ4
PD6-9	Ana (2/2)	Ana(2/2)
PD21-22	Tel (5/5)	Tel (5/5)
PD23-25	Ana (4/5)	Tel (4/4)
PD29-38	Ana (6/6)	Tel (6/6)

Figure 2.6. Remodeling of hair germ structure during prolonged quiescence of *Runx1*$^{\Delta b4/b/\Delta b4}$ follicles. (**A**) H&E staining of PD21 WT and Δ4 skin shows lower ORS or germ morphology consistent with end of catagen (stage VIII) or telogen. Note larger size of germ areas marked by dotted lines in Δ4 follicles. (**B**) H&E staining of Δ4 skin sections shows progressive decrease in germ size and cell numbers at stages indicated. WT follicles are in anagen (Figure. 3F). Images are representative of germ morphology analyzed in *n*=11 animals (3 WT mice PD21, 3 Δ4 mice at PD21 and 5 Δ4 mice at PD23-PD29).

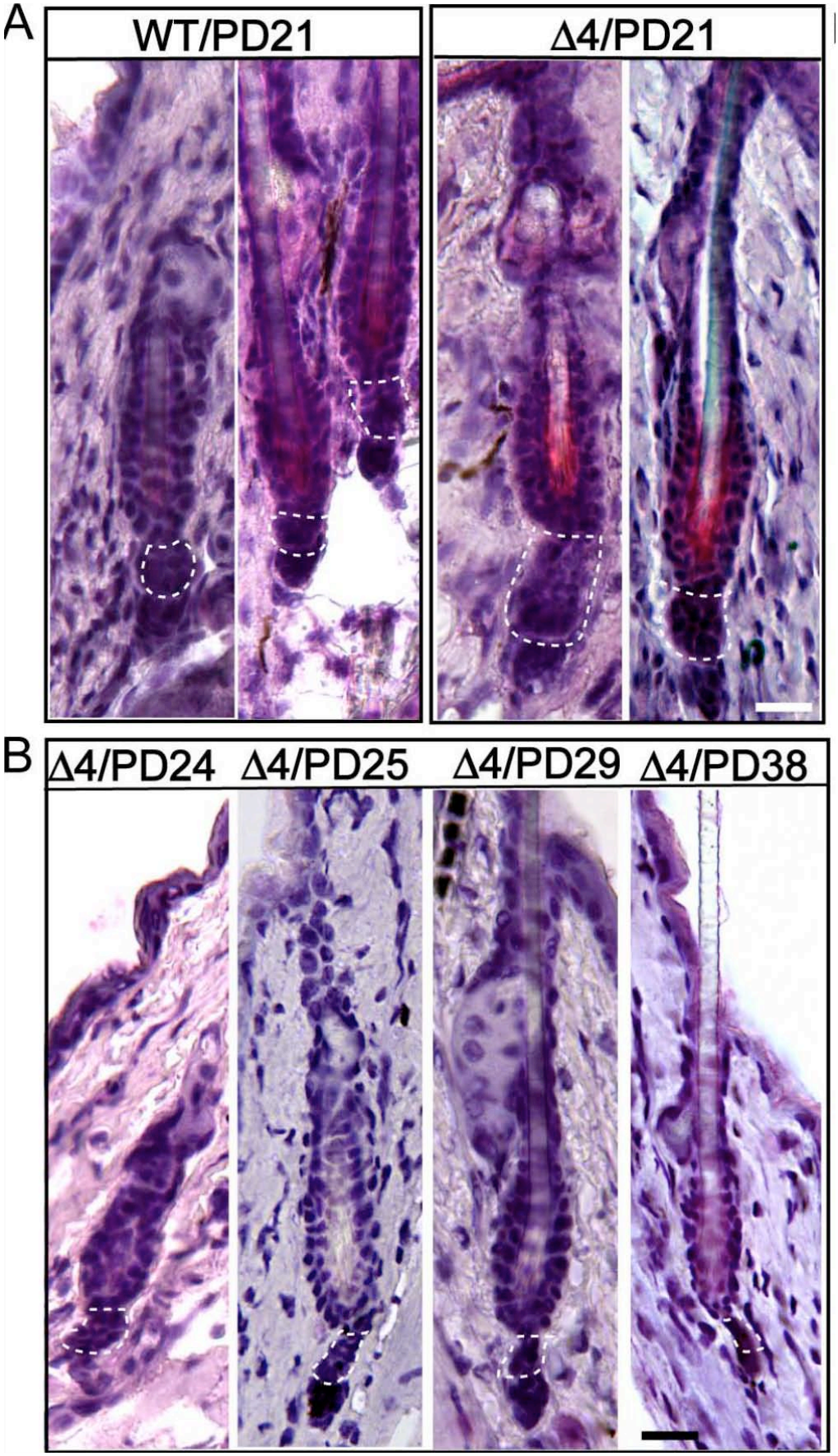
A
WT/PD21
Δ4/PD21
B
Δ4/PD24
Δ4/PD25
Δ4/PD29
Δ4/PD38

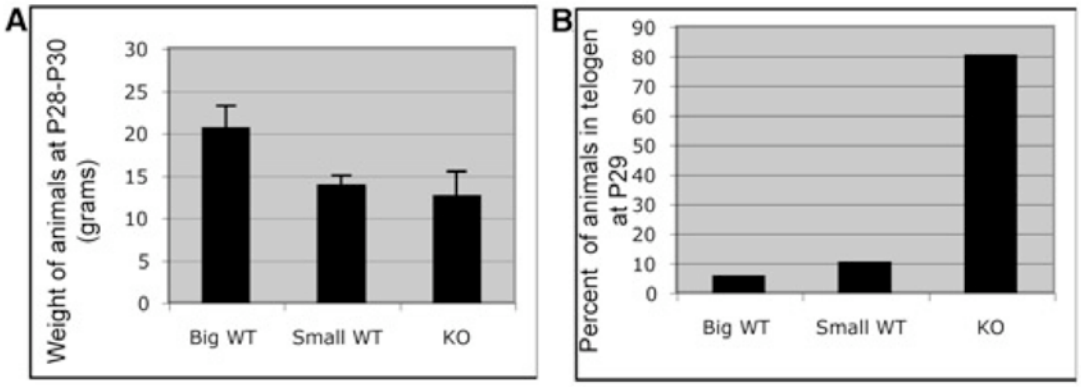

Figure 2.7: Effect of Runx1 disruption on weight and hair differentiation. (**A**) Weight of Δ4 and WT animals at PD28-PD30. Average weight was 12.57g (±2.9) for Δ4 animals (*n*=25), 13.7g (±1.2) for small WTs (*n*=10) and 20.4g (±2g) for big WTs (*n*=19). (**B**) Percentage of animals with telogen (black) skin at P28-30 in the 3 weight categories defined in A. Skin color was assessed by visual inspection of shaved animals. Mice with gray/black patches on the back were scored in anagen.

At PD21 *Runx1*$^{\Delta 4/\Delta 4}$ HFs displayed a slight increase in the number of outer root sheath cells below the bulge (Figure 2.6A), suggesting increased survival of these cells normally destined to die. Apoptotic (caspase positive) cells indicating end of catagen were detectable in the germ cells below the bulge at PD21 in both *Runx1*$^{\Delta 4/\Delta 4}$ and WT (data not shown). Progressive reduction in number of cells and narrowing of the germ-like structure below the bulge became apparent in Runx1$^{\Delta 4/\Delta 4}$ follicles at PD24, 25, 29 and 38 (Figure 2.6B). Moreover, the shrinking "hair germ" displayed 1-2 apoptotic cells in > 40% mutant HFs at PD24, while growing WT follicles showed no caspase staining at this stage (Figure 2.10B, D). Thus, cells shown to normally express Runx1 at high levels display increased survival in Runx1 mutant follicles, suggesting a role of Runx1 in apoptosis of keratinocytes during catagen.

The telogen-like morphology of mutant follicles suggested lack of differentiated hair lineage in the absence of functional Runx1. To determine if Runx1$^{\Delta 4/\Delta 4}$ mutant follicles showed any differentiated cells, we performed immunofluorescence staining with specific hair lineage markers characteristic of anagen phase at PD21 and PD29 (Figure 2.8A). We detected none of these markers, including that of progenitor matrix cells (Ephrin B1), in any of the *Runx1*$^{\Delta 4/\Delta 4}$ follicles. This was consistent with a true telogen block as assessed by hair morphology (Figure 2.5F), and suggested that Runx1 works upstream, at the SC level, in skin keratinocytes. To further analyze this possibility we examined SC behavior by clonogenicity assays. It has been established that generation of large keratinocyte colonies is initiated by independent SC populations of inter-follicular epidermis and HFs (Barrandon and Green, 1987; Gambardella and Barrandon, 2003). Cultured keratinocytes from PD2 mice

showed 80% fewer colonies in *Runx1*$^{\Delta 4/\Delta 4}$ versus WT cells (Figure 2.5J, L, M) and a drastic proliferation defect over time (Figure 2.5K). Most mutant forming colonies were small and eventually stopped growing, and the few that expanded over time amplified from the rare Runx1 untargeted cells (due to ~90% Cre efficiency, data not shown). Since Runx1 is not in inter-follicular epidermis, we expected to obtain some normal growing *Runx1*$^{\Delta 4/\Delta 4}$ keratinocyte colonies derived from this SC compartment, but our culture results did not fit this expectation. The result might be explained by the finding that all cultured keratinocytes, regardless of their HF or inter-follicular origin, expressed Runx1 (not shown). This result suggested that all skin keratinocytes utilize Runx1 for their proliferation in culture.

In summary, the phenotypes observed in vitro and in vivo in the epithelial Runx1 knockout suggests that Runx1 acts in hair follicles at the stem cell level (Figure A6B). Specifically, Runx1 deletion affected the HFSCs' ability to proliferate in vitro and to produce in vivo all differentiated hair lineages including the progenitor-matrix cells at the onset of the adult hair cycling stage. Based on these phenotypes, we hypothesized four possible developmental mechanisms by which *Runx1*$^{\Delta 4/\Delta 4}$ could impair adult HFSCs function to initiate hair cycling: 1) lack of adult HFSCs; 2) lack of activation/proliferation of quiescent HFSCs; 3) impairment of HFSCs differentiation; 4) loss of HFSCs due to lack of maintenance/self-renewal. We next proceeded to test each mechanism.

Figure 2.8 . Lack of all differentiated lineages in Runx1 mutant hair follicles. (A) Runx1$^{\Delta 4/\Delta 4}$ hair follicles show no differentiated cell lineage marker expression. Skin sections from wild type (WT) and mutant (Δ4) animals at PD21 and PD29 (*n*=2 in each group to a total of 8 mice analyzed) show expression of markers indicated in corresponding color. Bu, bulge; hg, hair germ; Dp, dermal papillae, Mx, matrix; IRS, inner root sheath; preC, precortex; Me, medulla. Scale bars: 10 μm (note scale difference in anagen and telogen follicles). *Auto-fluorescence from the hair shaft. Θ, non-specific streptavidin staining of the sebaceous gland. (B) Schematic summarizing the Runx1 phenotypes, which suggest its role at the stem cell level

A

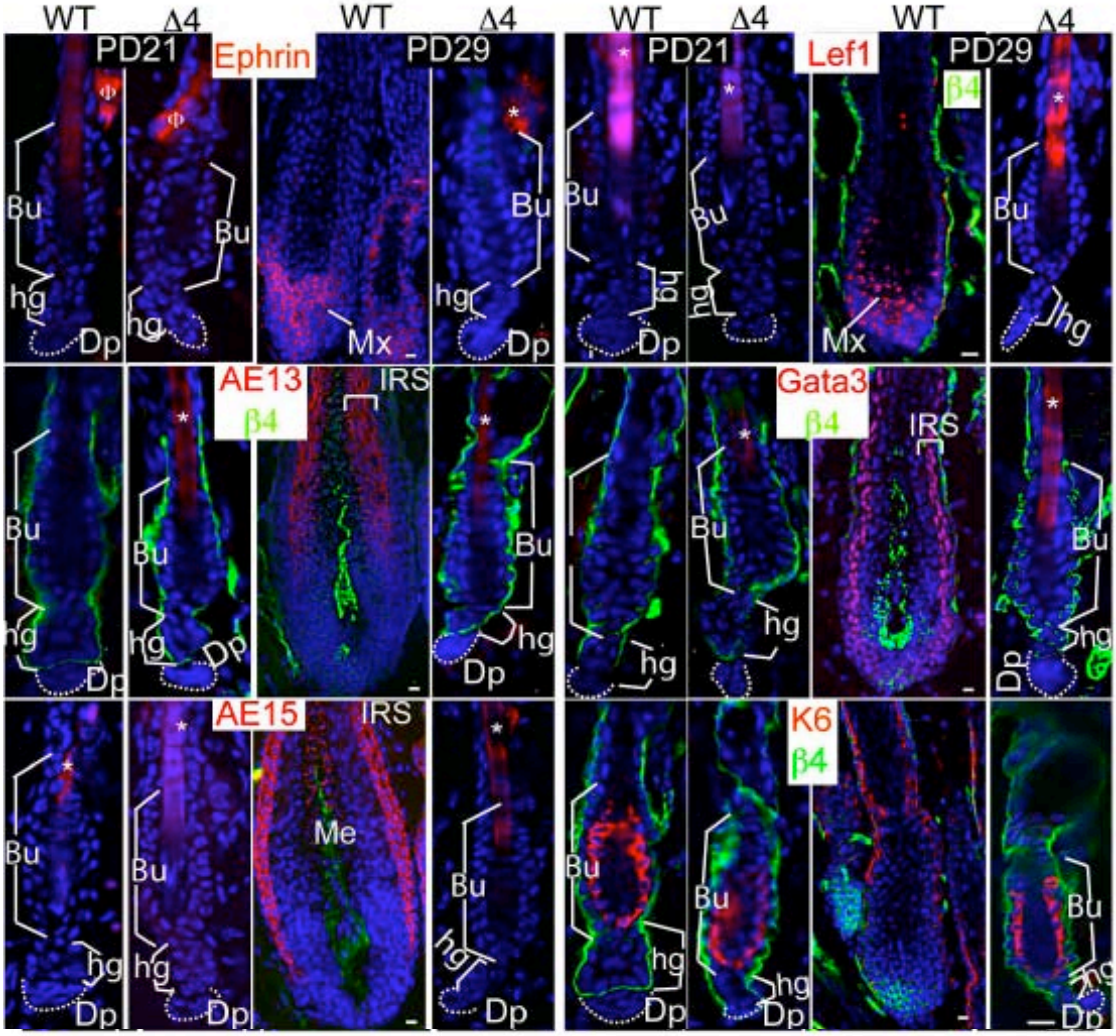
WT
Δ4
PD21
Ephrin
PD29
Lef1
β4
AE13
IRS
Gata3
AE15
Me
K6
Bu
hg
Dp
Mx

B.

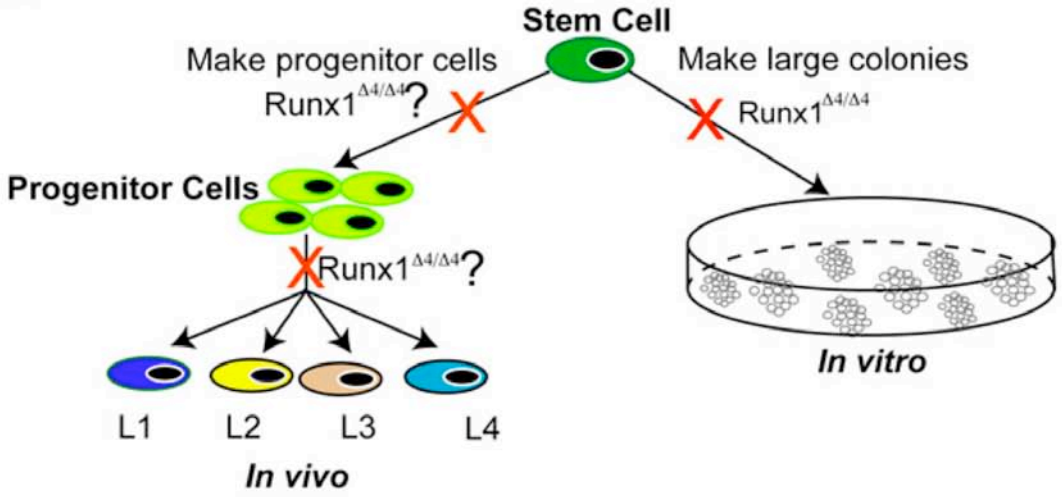
Stem Cell
Make progenitor cells
Runx1Δ4/Δ4?
Make large colonies
Runx1Δ4/Δ4
Progenitor Cells
Runx1Δ4/Δ4?
L1
L2
L3
L4
In vivo
In vitro

HFSCs are present in the Runx1$^{\Delta 4/\Delta 4}$ niche but show deregulation of hair cycle gene effectors

To test the first mechanism we asked whether bulge SCs were either missing or in reduced numbers in *Runx1*$^{\Delta 4/\Delta 4}$ versus WT skin at PD21 during telogen-anagen transition. A significant fraction of bulge cells behaved as SCs in previous functional assays (Gambardella and Barrandon, 2003). Loss of bulge SCs can be accompanied by aberrant expression of known bulge and outer root sheath markers such as CD34, α6- and β4-integrins, Keratin 15 (K15) and 14 (K14), Sox9, S100A6 and Tenascin C. In immunostaining assays at PD21 we detected depletion of Runx1, but no change in expression level of these markers in the bulge (Figure 2.9A). Moreover, these expressions were maintained in the arrested *Runx1*$^{\Delta 4/\Delta 4}$ mutant HFs at PD24 and PD29 (data not shown). The qualitative immunofluorescence results were supported by quantitative FACS analyses (Figure 2.9B) of PD20 WT and mutant skin cells, which showed no significant difference ($p=0.2$) in the frequency of bulge SC population (defined by CD34+/α6-integrin+)(Figure 2.9C). These results suggest that the HFSCs were present at normal numbers in the mutant follicles.

We next examined if the mutant bulge cells displayed perturbation in expression of genes with known hair functions, that might contribute to the Runx1 hair phenotype (Nakamura et al., 2001; Otto et al., 2003; Topley et al., 1999). We analyzed the following specific factors by RT-PCR of bulge and outside the bulge basal sorted cells*: Bcl2, Bdnf, Dkk1, Dvl2, Stat3, Tgf-β1, Noggin, Bmp4, Fzd2, sFRP1, Fyn, Dab2, and p21*. As expected, *Fzd2, sFRP1* and *Dab2* were increased in the WT bulge fraction (not shown), as documented by

our previous microarray analyses (Tumbar et. al, 2004), and this pattern was maintained in the *Runx1*$^{\Delta4/\Delta4}$ cells. While some of the tested genes were unchanged or showed sample-to-sample variation in expression levels in both mutant and WT bulge cells, several were consistently increased in *Runx1*$^{\Delta4/\Delta4}$ bulges (Figure 2.9D,E). The change in expression agrees with the role of these factors as catagen/telogen effectors, or negative regulators of proliferation or hair growth. The exception was a slight but statistically significant increase in *Stat3* expression (also see qRT-PCR, Figure A4E). This disagreed with the prolonged telogen of *Stat3* knockout mice, but might possibly be due to a compensatory effect of mutant bulge cells. *GAPDH* served as a loading control. These results suggest the mis-regulation of some known hair cycle effector genes (Nakamura et al., 2001), in the *Runx1*$^{\Delta4/\Delta4}$ bulge cells.

Taken together these data suggested that *Runx1*$^{\Delta4/\Delta4}$ HFs likely contained the SCs, but these cells probably failed to timely exit the quiescent phase and sustain hair growth, likely due to changes in gene expression known to affect normal hair cycling. This conclusion is supported by functional assays described later in the paper.

Figure 2.9. Analyses of *Runx1*$^{4/4}$ bulge SC numbers and gene expression. (A) Skin sections from wild-type and 4 mice at PD21 show expression of markers indicated at the top (yellow). Bu, bulge; hg, hair germ; DP, dermal papillae. Asterisk indicates background signal of hair shaft. (B) Surface expression of CD34 and 6-integrin by FACS of skin cells at PD20. (C) Summary of FACS experiments in B shows frequency of 4 and wild-type CD34+/6-integrin+ bulge cells in the skin (*P*=0.2 demonstrates no significant differences). (D) Bulge (Bu) and outside the bulge (O/Bl) sorted cells from (B) were used to prepare total RNA and cDNA. RT-PCR analyses show expression levels for genes indicated on the left. +/+ and -/+ designate CD34 and 6-integrin expression in each population. The last four lanes are negative controls without reverse transcriptase. (E) Summary of phenotypes for mutant mice indicated (left column) and gene expression level obtained consistently in wild-type and 4 mice tested (right column). Tm, targeted mutation (knockout); Tg, transgenic (overexpression). Level of expression in *Runx1*$^{4/4}$ bulge is indicated in the right-hand column by + (increase), - (decrease) or N/C (no change). N/A, not applicable.

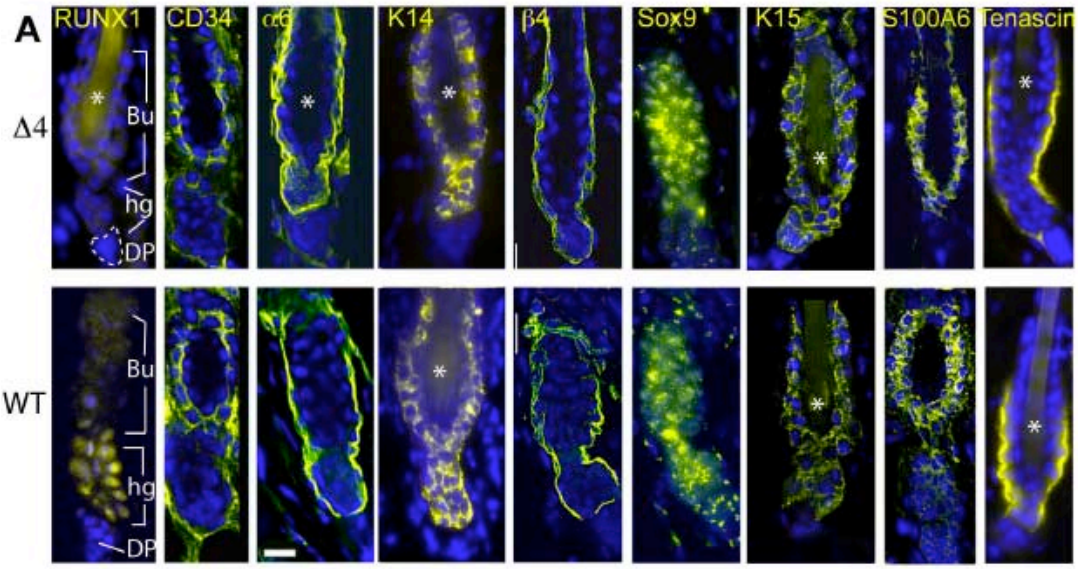

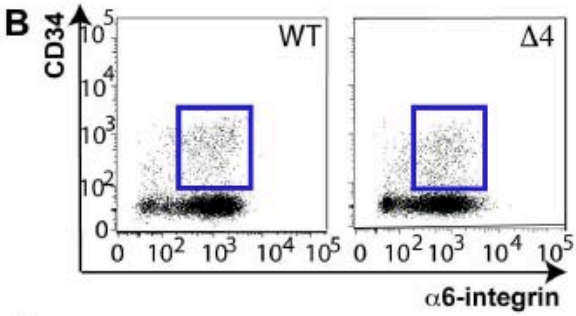

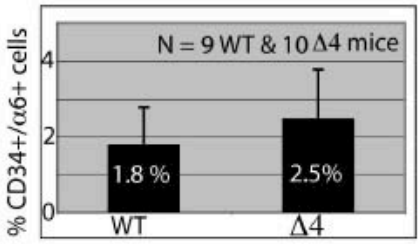

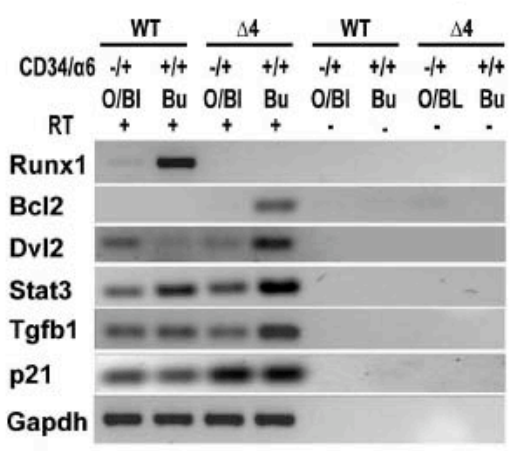

E

Genes	Type	Abnormalities of hair follicles	Level in Runx1$^{\Delta 4}$ Bulge
Runx1	Tm	Prolonged Telogen	- - -
Bcl2	Tg	Prolonged Telogen Premature Catagen	++
Dvl2	Tg	Premature Catagen	++
Stat3	Tm	Prolonged Telogen	+
Tgfb1	Tm Inject	Delayed Catagen Premature Catagen	++
p21	Tm	Increased # of SCs	++
Gapdh	N/A	N/A	N/C

Runx1$^{\Delta 4/\Delta 4}$ bulge stem cells fail to proliferate during telogen-anagen transition

A second possible mechanism for explaining the *Runx1*$^{\Delta 4/\Delta 4}$ phenotypes in vivo and in vitro was a failure to proliferate by either the HFSCs or the early progenitor cells. In the former possibility, *Runx1*$^{\Delta 4/\Delta 4}$ bulge SCs do not divide, and do not give rise to early progenitor cells. In the latter, *Runx1*$^{\Delta 4/\Delta 4}$ bulge SCs divide and make progenitor cells, which in turn fail to proliferate. To distinguish between these scenarios we BrdU labeled skin cells continuously for 4 days at the anagen onset (PD20-PD24), to track cells that divided during this time. We then determined the localization of BrdU+ cells in the hair germ or the bulge. If bulge cells divide but their early progeny cells failed to proliferate further, we expected to see some BrdU+ cells in the CD34+/α6-integrin+ bulge cells. Inspection of skin sections co-stained for BrdU and CD34 at PD23 and 24 revealed that 100% of WT follicles were in anagen, and 67% of these follicles displayed variable numbers of BrdU+ bulge cells. Conversely, *Runx1*$^{\Delta 4/\Delta 4}$ follicles (5/5 mice) were in telogen and showed complete lack (100% follicles) of BrdU in the bulge (Figure 2.11A, B).

Furthermore, all WT follicles displayed bright BrdU+ germ cells, while 90% of Runx1$^{\Delta 4/\Delta 4}$ hair germs had no BrdU+ cells. The remaining 10% contained only 1-2 dim BrdU+ cells (Figure 2.10A), which were likely due to incomplete Runx1 targeting. These BrdU+ germ cells found in the mutant follicles were caspase negative but positive for Keratin 5, normally expressed by epithelial hair germ cells (Figure 2.10C). To understand if we failed to detect activated (BrdU+) bulge cells due to possible apoptosis of these cells, we looked for the expression of caspase in bulge cells at PD24. While we detected 1-2 apoptotic

cells in ~40% *Runx1*$^{\Delta 4/\Delta 4}$ germs (Figure 2.10B) the frequency of apoptotic cells in the bulge was below detection. The WT follicles were in early anagen and contained no apoptotic caspase positive cells (Figure 2.10D). These data supported the first possibility, in which the bulge SCs remained quiescent in the *Runx1*$^{\Delta 4/\Delta 4}$ mutant.

To further examine the failure of bulge SCs to proliferate at their normal activation stage, we counted BrdU positive cells in sorted CD34+/α6-integrin+ bulge cells isolated from mice continuously labeled with BrdU during anagen onset (PD20-PD24). These cells stained for undifferentiated keratinocyte markers K5 and β4-integrin, documenting at least 90% homogeneity of our sorted cells (Figure 2.11C, D). Staining for BrdU revealed 10-30% positive WT cells and 0% BrdU positive *Runx1*$^{\Delta 4/\Delta 4}$ cells (Figure 2.11C, E). In conclusion, these data ruled out the possibility that *Runx1*$^{\Delta 4/\Delta 4}$ mutation allowed SC activation from quiescence, but simply blocked the proliferation of the early progenitor matrix cells. Instead, we showed that Runx1$^{\Delta 4/\Delta 4}$ SCs remained quiescent at a stage when WT SCs undergo developmentally controlled activation.

Figure 2.10. Effect of Runx1 disruption on apoptosis and proliferation. All follicles are from 4-day BrdU-labeled PD24 Δ4 or WT skin as shown on each panel, with quadruple staining. Left and right panels are different stains of the same follicle. Stains are indicated on each image in appropriate color. (**A**) Arrow points to weakly labeled BrdU+ cell in the hair germ, which was negative for caspase co-staining. (**B**) Conversely, caspase positive cell shown by arrow does not have BrdU. (**C**) Caspase-positive cell expresses K5 (arrow). (**D**) WT follicles show proliferating but no caspase+ cells at this stage. DP, dermal papillae. (**E**) Stat3 shows ~2.8 fold increase in bulge cells of 3 Δ4 vs 3 WT animals by qRT-PCR in experiments performed in duplicate ($P<0.1$).

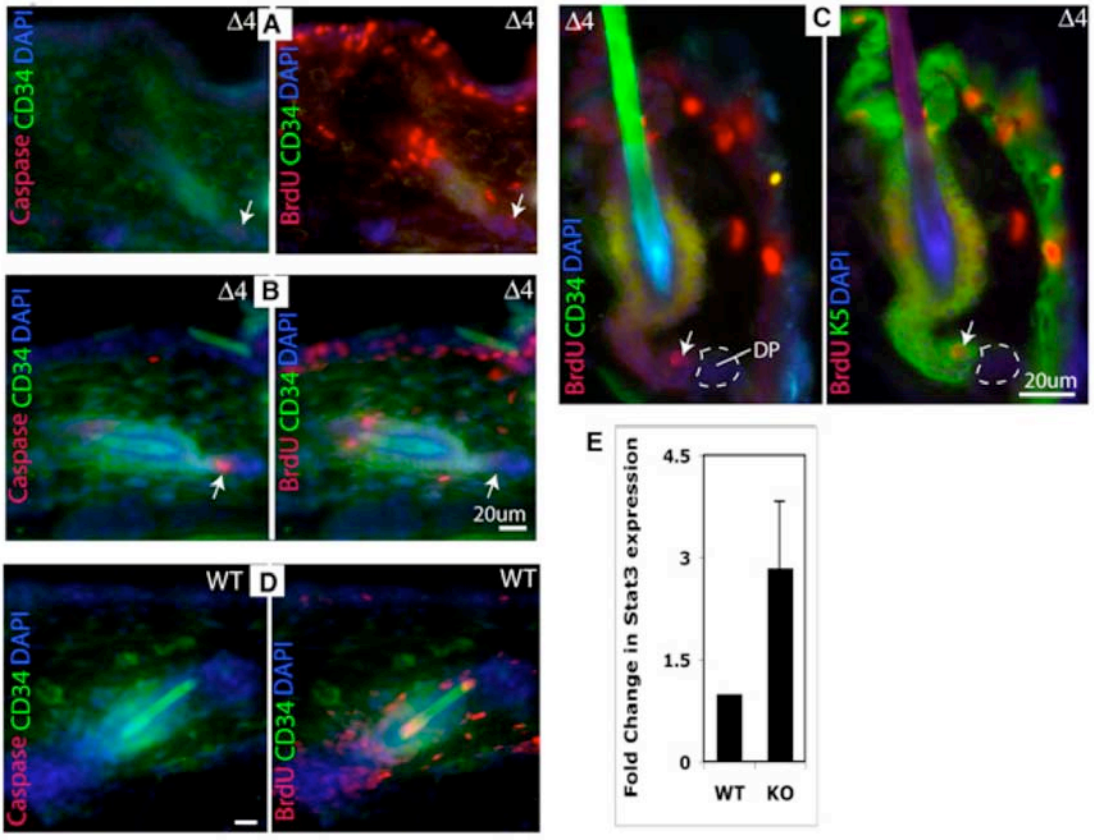
Δ4
A
Caspase CD34 DAPI
Δ4
BrdU CD34 DAPI
Δ4
B
Caspase CD34 DAPI
Δ4
BrdU CD34 DAPI
20um
WT
D
Caspase CD34 DAPI
WT
BrdU CD34 DAPI
Δ4
BrdU CD34 DAPI
DP
C
Δ4
BrdU K5 DAPI
20um
E
Fold Change in Stat3 expression
4.5
3
1.5
0
WT
KO

Figure 2.11. Effect of *Runx1*$^{4/4}$ on bulge SC proliferation. (**A**) Sections from 3- or 4-day-old BrdU-labeled skin (PD20-PD23 or 24) show cells that proliferated during anagen onset. Early anagen wild-type follicle (a,b) shows multiple BrdU+ (red) cells in hair germ and several BrdU+(red) and CD34+ (green) bulge cells (arrows). Telogen *Runx1*$^{4/4}$ follicle shows complete lack of BrdU+ cells in CD34+ bulge cells or germ cells (c,d). Ep, epidermis; Bu, bulge; hg, hair germ; DP, dermal papillae; De, dermis. Asterisk shows hair shaft autofluorescence. (**B**) Fraction of follicles scored on skin section shown in A that displayed BrdU+ cells in bulge or germ. Sixty-seven percent of follicles have BrdU+ bulge cells for wild-type mice and there is a complete lack of BrdU+ bulge cells for 4 mice. Follicles with BrdU+ germ cells are further subdivided into those with more than two BrdU+ cells/germ and one or two BrdU+ cells/germ. Total number of HFs analyzed from five wild-type (black) and five 4 (gray) littermates is shown (802 wild type & 737 4). Error bars underscore variability of BrdU+ follicle fractions in each category. (**C**) CD34+/6-integrin+ cells from mice in A,B were sorted on slides, fixed and stained as described (Tumbar, 2006). There is a high frequency of cells that are double positive for keratin 5 (K5, red) and β4-integrin (β4, green, bottom panel). BrdU+ (red) and DAPI (blue) staining (top panel) shows lack of proliferation in 4 but not wild-type bulge cells. (**D**) Sorted bulge cells from C counted for double expression of epithelial K5 and β4 markers. Un, unsorted live cell control. Number of cells is at the top, ID of mice is at the bottom. (**E**) Quantification of proliferating (BrdU+) sorted bulge cells from (C). Number of cells is at the top, mouse ID is at the bottom. Negative controls were from BrdU-negative mice.

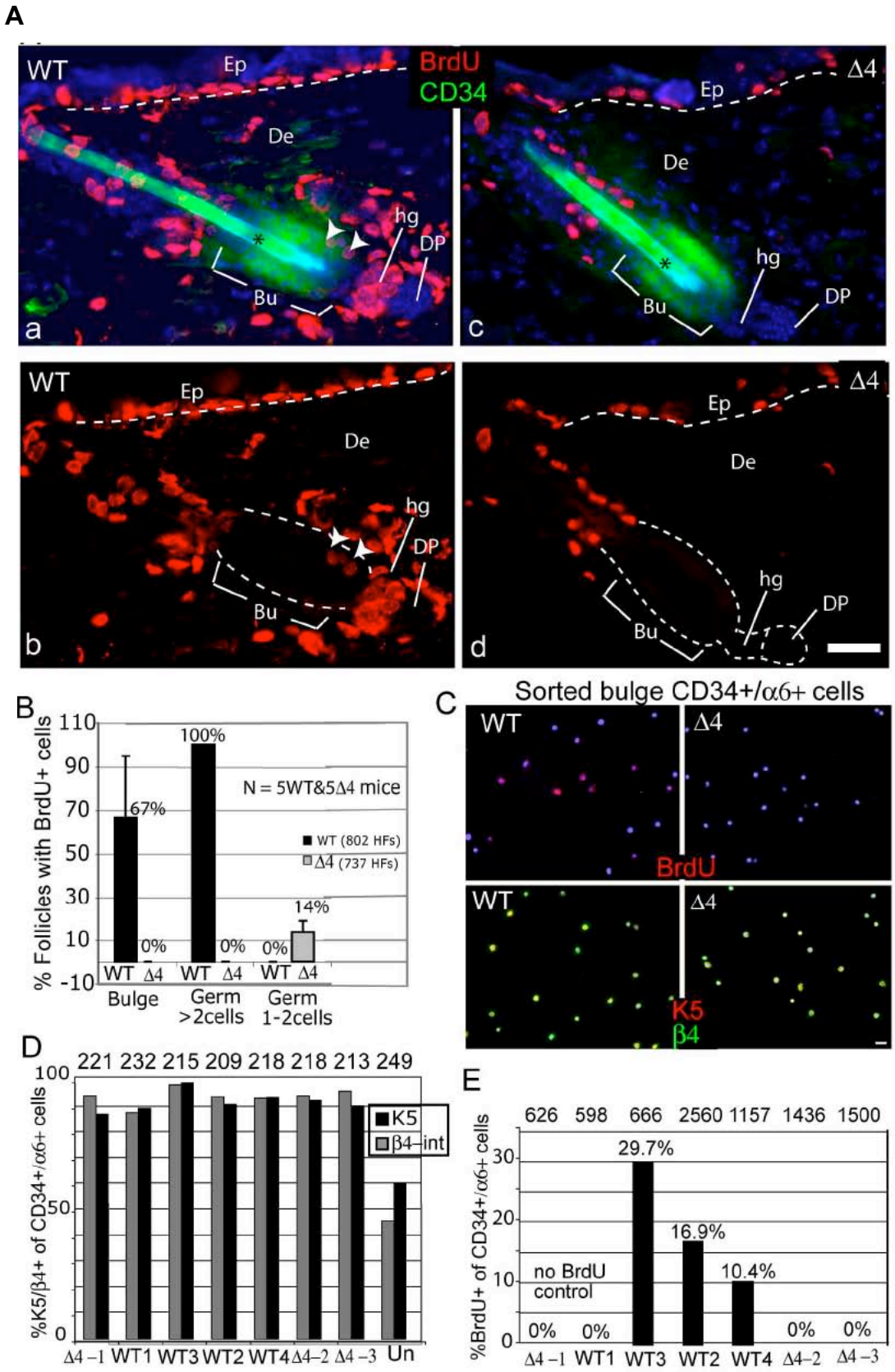
A
WT
Ep
BrdU
CD34
De
hg
DP
Bu
a
Δ4
c
b
d
B
% Follicles with BrdU+ cells
N = 5WT&5Δ4 mice
WT (802 HFs)
Δ4 (737 HFs)
67%
100%
14%
0%
Bulge
Germ >2cells
Germ 1-2cells
C
Sorted bulge CD34+/α6+ cells
BrdU
K5
β4
D
221 232 215 209 218 218 213 249
%K5/β4+ of CD34+/α6+ cells
K5
β4-int
Δ4 –1 WT1 WT3 WT2 WT4 Δ4–2 Δ4 –3 Un
E
626 598 666 2560 1157 1436 1500
%BrdU+ of CD34+/α6+ cells
29.7%
16.9%
10.4%
no BrdU control
Δ4 –1 WT1 WT3 WT2 WT4 Δ4–2 Δ4 –3

Proliferation and differentiation of Runx1$^{\Delta 4/\Delta 4}$ HFSCs in response to skin injury

Our experiments suggested that *Runx1*$^{\Delta 4/\Delta 4}$ SCs failed to respond to normal growth activation signals during the initiation of adult hair cycling phase. If *Runx1*$^{\Delta 4/\Delta 4}$ SCs were functional, one might expect that in response to a different activation signal they would be able to proliferate, differentiate, and generate new hairs (Figure 2.12A). To test this hypothesis we employed skin injury as the source of activation signal (Fuchs et al., 2004). We used a total of 38 *Runx1*$^{\Delta 4/\Delta 4}$ mice and injured by hair plucking, light epidermal scraping or close shaving, and dermis penetrating incision at PD21 or PD29. Any type of skin injury at these stages reversed the *Runx1*$^{\Delta 4/\Delta 4}$ SC quiescence block.

The prolonged telogen described here could be consistent with a role of Runx1 in regulating early stem/progenitor cell fate choice and differentiation to hair cell lineages. Thus, we asked if the injury-triggered hair growth in Runx1$^{\Delta 4/\Delta 4}$ mutants resulted in normal proliferation and differentiation of bulge cells. 4-18 days post-wounding (performed at PD21) we detected Ki67+ proliferating bulge cells, and new hair shaft growth in the wounded area (Figure 2.12B, C, D). The HF had essentially normal morphology and cycled normally (Figure 2.12C). Furthermore, we found all differentiated lineage markers correctly expressed in the newly grown *Runx1*$^{\Delta 4/\Delta 4}$ hair bulbs by immunofluorescence staining (Figure 2.12E). This indicated that Runx1$^{\Delta 4/\Delta 4}$ did not affect the differentiation potential (multipotency) and fate decision of progenitors and HFSCs, a step upstream of the previously shown Runx1 effect on aspects of terminal differentiation (Raveh et al, 2006).

Runx1$^{\Delta4/\Delta4}$ effect on long-term regenerative potential of HFSCs

Finally, to test a fourth possible mechanism for Runx1 action, we examined the long-term regeneration potential of *Runx1*$^{\Delta4/\Delta4}$ HFSCs population, a definitive hallmark of self-renewing SCs. During a time period of >1 year, we induced 4-5 rounds of back skin injury by shaving and light dermabrasion of small epidermal areas (Figure 2.12F). In WT and *Runx1*$^{\Delta4/\Delta4}$ skin hair growth began from the injured area and spread along the entire back skin region (Figure 2.13B). This spreading could result from an activating morphogen released from the growing follicles, which triggered new growth in the surrounding dormant follicles. Follicles eventually re-entered the quiescent phase, as shown by the pink skin color. At this point we repeated the skin wounding in a different region of the skin to reinitiate another cycle of SC activation and hair growth (Figure 2.12F). Occasionally, upon a new injury cycle we found a grey or black patch of anagen skin at the site of a previous wound (Figure 2.13C). This suggested initiation of a new hair cycle in the absence of immediate injury in a skin area that was previously activated by injury to grow hair. An important question is whether HFs would begin cycling spontaneously at later developmental stages in the complete absence of injury. Suggestively, of 10 un-injured mutant mice analyzed between PD42-PD48, 5 were in early anagen while 5 remained in telogen. It is difficult however to rule out the role of spontaneous injury in this delayed anagen initiation (bites, scratching, scraping) since even shaving can trigger hair growth in mutant animals. Addressing un-ambiguously the role of Runx1 in spontaneous hair cycles in older mice will require further investigation.

Taken together these results suggested that during later developmental stages beyond the initiation of the adult phase: 1) *Runx1*$^{\Delta 4/\Delta 4}$ HFSCs maintained their long-term potential, and repeated stimulation did not exhaust the mutant SC pool; 2) *Runx1*$^{\Delta 4/\Delta 4}$ HFSCs activation could occur in the absence of injury, at least in follicles that had already been previously directly initiated via injury, and in follicles found in the vicinity of actively growing hairs.

Discussion

Runx1 modulates hair cycling

In this work we examined the function of Runx1, a hematopoietic SC factor, in the hair follicle. We found that Runx1 is important for normal hair cycling at the transition into adult skin homeostasis. Mice lacking functional Runx1 in skin epithelial cells are able to produce normal hair follicles during morphogenesis, but these follicles displayed a prolonged first telogen. The hair follicle quiescence is rapidly overcome by injury, which triggers proliferation and differentiation of the HFSCs. Importantly the hair growth can spread far into unwounded areas, and can also resume in follicles that have been already removed from quiescence by one round of injury. It remains unclear whether at later developmental time points hair follicles might be capable to cycle spontaneously. The Runx1 mutant phenotype underscores differences in developmental versus injury triggered hair growth, a phenotype also displayed by the Stat3 knockout mouse (Sano et al., 1999; Sano et al., 2000). The relationship between these transcription factors in hair follicles remains to be elucidated.

Figure 2.12. Injury reverses *Runx1*$^{4/4}$ HFSCs block in quiescence.
(A) Schematic of HFSC activation. (B) Back region of 4 mice post-hair plucking shows hair growth in injured area (arrow). (C) Hematoxylin and Eosin staining of 4-skin sections collected from wounded and unwounded (opposite) back regions at time points indicated show progression through the hair cycle. (D) *Runx1*$^{4/4}$ injured skin shows proliferating Ki67+ (red, arrows) of CD34+ bulge cells (green). (E) Staining of skin sections 18 days post-wounding shows normal expression of differentiated hair lineage markers. There is a lack of Runx1 staining (performed in serial sections) in 4 but not in wild-type follicles. (F) Schematic of long-term functional HFSC assay.

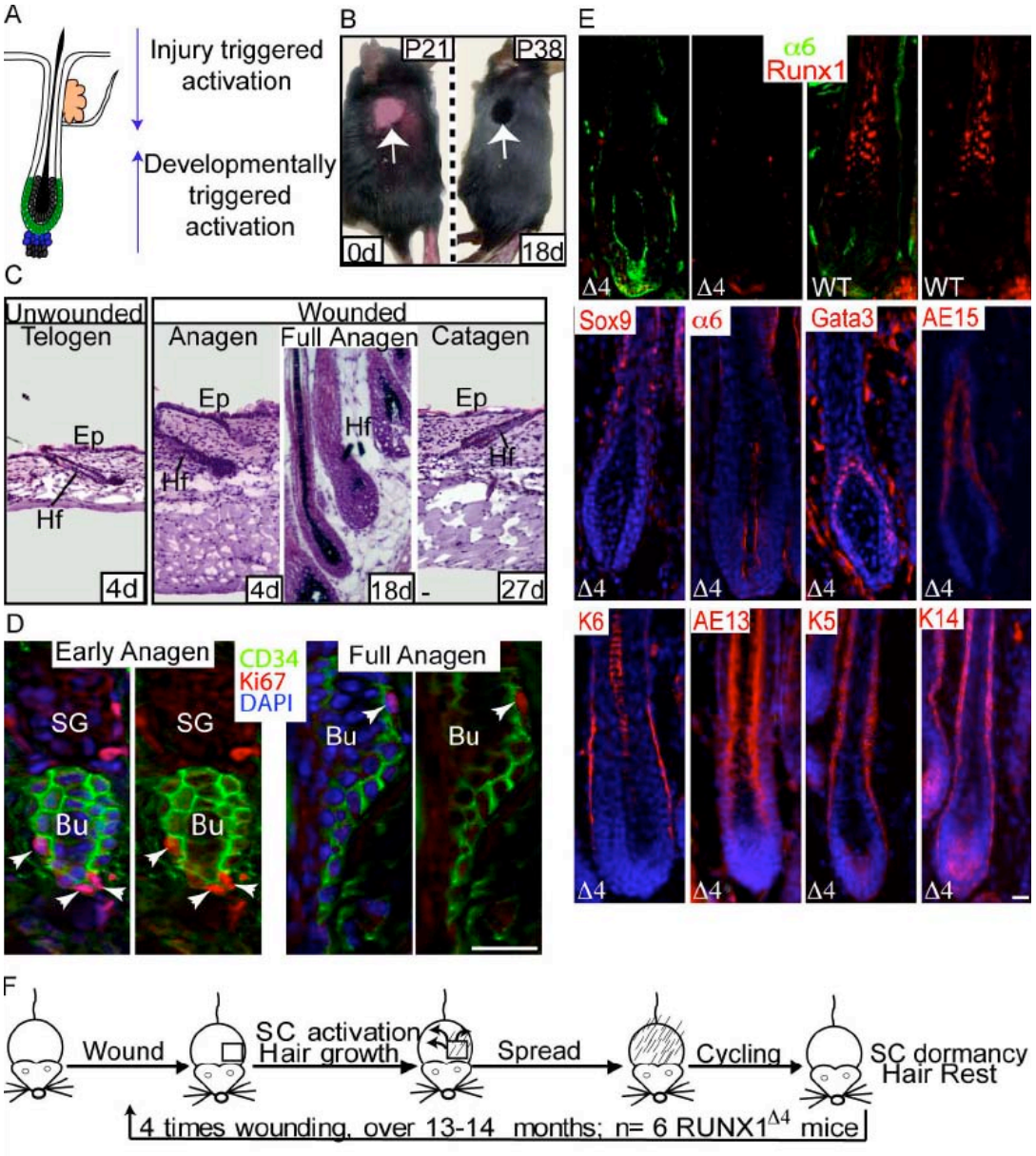
A
Injury triggered activation
Developmentally triggered activation
B
P21
P38
0d
18d
C
Unwounded
Telogen
Ep
Hf
4d
Wounded
Anagen
Full Anagen
Catagen
Ep
Hf
4d
18d
27d
D
Early Anagen
CD34
Ki67
DAPI
Full Anagen
SG
Bu
E
α6
Runx1
Δ4
WT
Sox9
α6
Gata3
AE15
K6
AE13
K5
K14
F
Wound
SC activation
Hair growth
Spread
Cycling
SC dormancy
Hair Rest
4 times wounding, over 13-14 months; n= 6 RUNX1Δ4 mice

Figure 2.13. Skin color indicates hair growth in uninjured WT and injured Δ4 mice. (A) Skin color of Δ4 and WT shaved mice at PD29 is pink (telogen) or black (anagen), respectively. (B) Hair growth spreading from injured into un-injured Δ4 skin. Skin is pink after hair pluck. Hair growth (black) and its spreading indicated by arrow. Gray color is early anagen. (C) Left: mouse at the second round of wounding shows gray skin patch in the previously wounded area (arrow) and pink skin in the newly plucked area (arrowhead). Right: same mouse 2 weeks later shows black skin indicative of hair growth in both the old (arrow) and newly (arrowhead) injured areas.

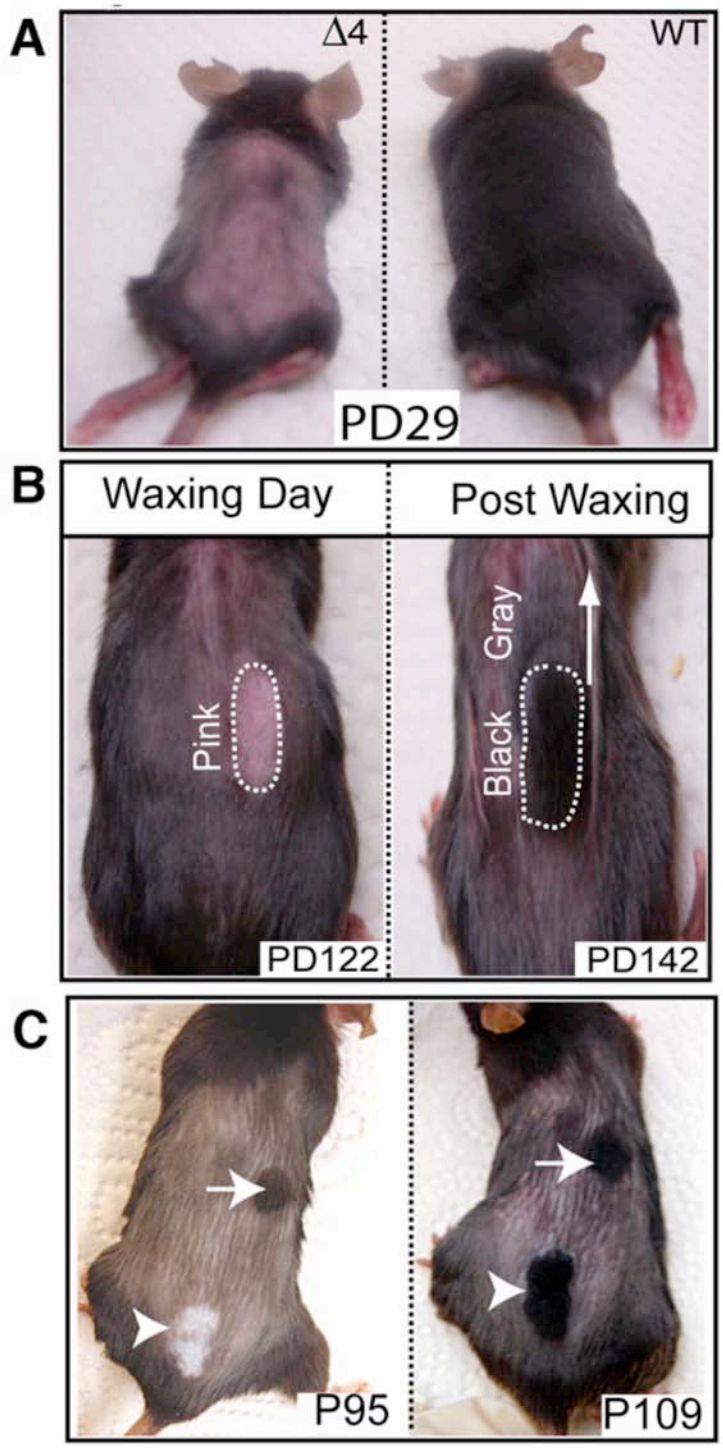
A
Δ4
WT
PD29
B
Waxing Day
Post Waxing
Pink
Gray
Black
PD122
PD142
C
P95
P109

Finally, the skin phenotype of the Runx1 mutant mice is accompanied by a severe impairment of keratinocyte proliferation *in vitro,* and by changes of expression levels in the SC compartment of factors known to regulate the quiescent phase of the hair cycle.

Runx1 regulates hair follicle SC activation

Here, we show that *Runx1*$^{\Delta 4/\Delta 4}$ mutation results in complete lack of newly differentiated hair lineages in the 1st hair cycle. Our data suggests that in Runx1$^{\Delta 4/\Delta 4}$ follicles the bulge HFSCs: a) were present and functional at the time of phenotype onset; b) together with progenitor cells remained quiescent at a key developmental activation time point; c) retained their intrinsic ability to proliferate and differentiate and produce essentially normal hairs; d) were maintained in the Runx1$^{\Delta 4/\Delta 4}$ bulge over prolonged periods of time and repeated stimulation.

The injury response of Runx1 mutant mice might be explained by alternative but less likely models that we formally acknowledge here. Although not yet demonstrated experimentally, it is possible that the bulge contains SC populations specialized to perform either normal homeostasis or injury repair. The first SC population is Runx1 dependent while the second one is not. Another possibility is that injury conditions of stressed/ischemic skin trigger the lineage conversion of a non-hair to a hair SC type. This possibility is hard to reconcile with our data showing spreading of the hair growth in un-injured areas far from the wound, a phenomenon present in both WT and mutant follicles.

Runx1 is expressed in a broad area that includes hair germ and bulge cells preceding SC activation. It is unclear whether the protein acts intrinsically in the SCs or acts on SCs through the niche. Its germ expression prior to activation correlated with the apparent effect of Runx1 disruption on increased outer root sheath survival during the catagen/telogen transition. Noteworthy, we detected Bcl2, an apoptosis regulator at increased levels in the bulge, and over-expression of Bcl2 (Nakamura et al., 2001) had a similar effect on the hair cycle as disruption of Runx1.

Although a role of Runx1 in the SC environment through secreted protein downstream targets is an attractive model, we cannot eliminate the possibility that Runx1 also functions within SCs to set the intrinsic rate of HFSC proliferation. This possibility is suggested by our *in vitro* cell culture assays, in which WT but not *Runx1*$^{\Delta 4/\Delta 4}$ HFSCs could generate large keratinocyte colonies in the time frame of our experiments. The regulation of skin epithelial cell culture growth by Runx1 warrants further investigation. In a clinical setting, achieving rapid expansion of keratinocytes in amounts useful for engineering artificial skin is extremely difficult, while it proves critical for patients with severe burns (Barrandon, 2004). As we understand more how control of epithelial SC proliferation is achieved in the tissue and how cell growth conditions perturb this balance, we will be able to apply more systematic approaches to *in vitro* SC manipulation for epidermal and hair engineering.

Is Runx1 a "stemness" gene?

Hematopoietic and hair SCs exist in tissues with distinct physiological roles and origins, that arise from different cell types of the early embryo (mesoderm and ectoderm). However, these two tissues share a fundamental functional characteristic: they regenerate continuously throughout life, and rely on adult SC activity to sustain extensive cellular turnover of their differentiated progeny cells. It is already known that blood and HF cells share common transcription factors that can regulate fate and differentiation of committed progenitor cells (DasGupta and Fuchs, 1999; Kaufman et al., 2003). Here, we suggest that a common transcription factor Runx1 carries out a developmental function at the SC level in the initiation of the adult-type (or definitive) stages in both tissues. Specifically, in blood Runx1 mutation blocks the initiation of definitive hematopoiesis in the aorta-gonado-mesonephros (Speck and Gilliland, 2002) , and in the hair follicle it impairs the onset of adult hair cycling (this work). At these stages the net result of Runx1 deletion is similar in both tissues: lack of all differentiated blood and hair cell lineages. The means of producing this effect appear to be different: Runx1 impairs SCs emergence for blood versus SCs activation for hair. These variation might underscore the divergence in the formation and/or maturation of these two kinds of tissue stem cells, which differ in both origin and environmental context, and have different relevance for the animal survival. It would be interesting to determine if the type of knockout analyzed, full for blood versus conditional for hair, might affect the Runx1 mutant phenotype in these tissues. Moreover, since the full knockout mice die shortly after the blood phenotype onset, it remains unclear whether stress and injury could eventually jump-

start a Runx1 independent program of hematopoiesis at this stage. Future work will likely bring more light to this intriguing comparison.

In summary, we uncover Runx1 as a modulator of keratinocyte proliferation, hair growth, and stem cell activation. Runx1 is needed for normal hair follicle homeostasis at the transition into the adult hair cycling stage, but not during injury repair. Here we add to the known role of Runx1 in stem cells (Speck and Gilliland, 2002), by demonstrating its role in another stem cell system besides blood, namely the hair follicle.

Acknowledgements

We thank Dr. Nancy Speck for the *Runx1*$^{Fl/Fl}$ and *Runx1*$^{LacZ/+}$ mice; Dr. Elaine Fuchs for the K14-Cre mice; Dr. Adam Glick for the K5-tTA mice; Dr. Jim Smith for help with flow cytometry; many others and especially Dr. Thomas Jessell for antibodies; our colleagues and especially Dr. Ken Kemphues, Dr. Jun Liu, and Dr. Linda Nicholson for critically reading the manuscript. The work was supported in part by NIH (AR053201).

CHAPTER 3

Runx1 is expressed in two populations of embryonic hair follicle progenitors that contribute to early hair formation and to the adult stem cell compartment

Introduction

The life of an animal is divided in two stages: tissue morphogenesis occurring mainly in the embryo, and tissue homeostasis in the adult. Many regenerative tissues contain adult tissue stem cells (TSCs), which can self-renew and differentiate throughout life (Fuchs, 2009). While the behavior and regulation of adult TSCs in homeostasis is intensively studied, the TSC origin and function in morphogenesis are largely obscure (Slack, 2008).

Intuitively, TSCs could be made from early embryonic progenitors, and subsequently generate their organ of residence, which they would maintain later on in life (Slack, 2008). However, accumulating evidence coming mostly from blood(Dzierzak and Speck, 2008; Mikkola and Orkin, 2006) and more recently from muscle development (Lepper et al., 2009; Messina and Cossu, 2009; Wang and Conboy, 2009), suggests a different model, in which the organ rudiments arise from distinct "primitive" progenitors prior or in parallel with adult TSCs (Messina and Cossu, 2009). The "primitive" progenitors are short-lived and generate the original cell types or structures of the tissue. In contrast TSCs are long-lived or "definitive" cells that are set-aside in a specialized

niche during morphogenesis to regenerate the tissue later on in life (Dzierzak and Speck, 2008). Here I examine these developmental models for tissue and stem cell generation in the mouse hair follicle using as an entry point a regulator of hematopoietic stem cell emergence, the transcription factor Ruxn1.

Skin is composed of two main compartments: an epithelial one that makes the interfollicular epidermis, the hair follicle, and the sebaceous glad; and a mesenchymal that is mainly composed of fibroblast and makes the dermis. Hair development also referred to as morphogenesis occurs in the embryo from embryonic day E14.5 to birth and continues on until postnatal day (PD)17. It consists of three phases: induction, which results in formation of a hair placode from the single layer of ectoderm upon epithelial-mesenchymal reciprocal signaling(Millar, 2002; Schmidt-Ullrich and Paus, 2005); down-growth of the placode which evolves into hair germ and next into peg; and differentiation with formation of the bulbous peg and the further mature HF (Figure 3.1A)(Millar, 2002; Muller-Rover et al., 2001; Schmidt-Ullrich and Paus, 2005; Schneider et al., 2009). The bulbous peg generates the matrix, a class of short-lived progenitors(Legue and Nicolas, 2005) , which proliferate and differentiate pushing cells upwards to generate the centrally located hair shaft, made of medulla, cortex, and cuticle. The hair shaft is surrounded by the inner root sheath (IRS), and the outer most layer, or outer root sheath (ORS) of the follicle. A fully mature follicle grows after birth to elongate the hair shaft that is continuously pushed upwards towards the skin surface (Schneider et al., 2009). The ORS is contiguous with the epidermis and is the

residence of the adult hair follicle stem cells (HFSCs). The HFSCs cluster in the upper follicle, known as "bulge", right beneath the sebum-filled cells of the sebaceous glad (SG) (Figure 3.1B).

At postnatal day (PD) 17 the hair morphogenesis ends and the adult homeostasis or hair cycle begins. The latter is characterized by morphologically distinct phases of degeneration and apoptosis (catagen), rest and quiescence (telogen) and growth and proliferation (anagen) (Schneider et al., 2009). A mesenchymal hair follicle component, the dermal papillae (DP), works in conjunction with environmental signals in anagen to activate the bulge epithelial HFSCs that re-generate the matrix. The DP further instructs the matrix to differentiate to inner layers (IL) and make a new hair shaft (Blanpain and Fuchs, 2009). The hair cycle phases occur relatively synchronously throughout the back skin of young mice.

Several molecular players such as BMP, WNT and Lhx2 regulate both morphogenesis and adult hair cycle (Millar, 2002; Rhee et al., 2006). Conversely, several transcription factors, such as Sox9, NfatC1, and Stat3 (Horsley et al., 2008; Nowak et al., 2008; Sano et al., 1999; Vidal et al., 2005), which are expressed in a sub-set of embryonic hair cells and in the adult bulge, regulate adult TSCs but not hair morphogenesis.

Figure 3.1: Schematic Representation of (A) Hair Follicle Morphogenesis and a (B) Mature Hair Follicle. A. Hair follicle morphogenesis can be divided into phases of induction, downgrowth and differentiation that can be classified into eight distinct morphological stages. The scheme shows the predominant stages at different timepoints throughout development. B.) A scheme showing a mature hair follicle with its corresponding eight concentric layers of keratinocytes.

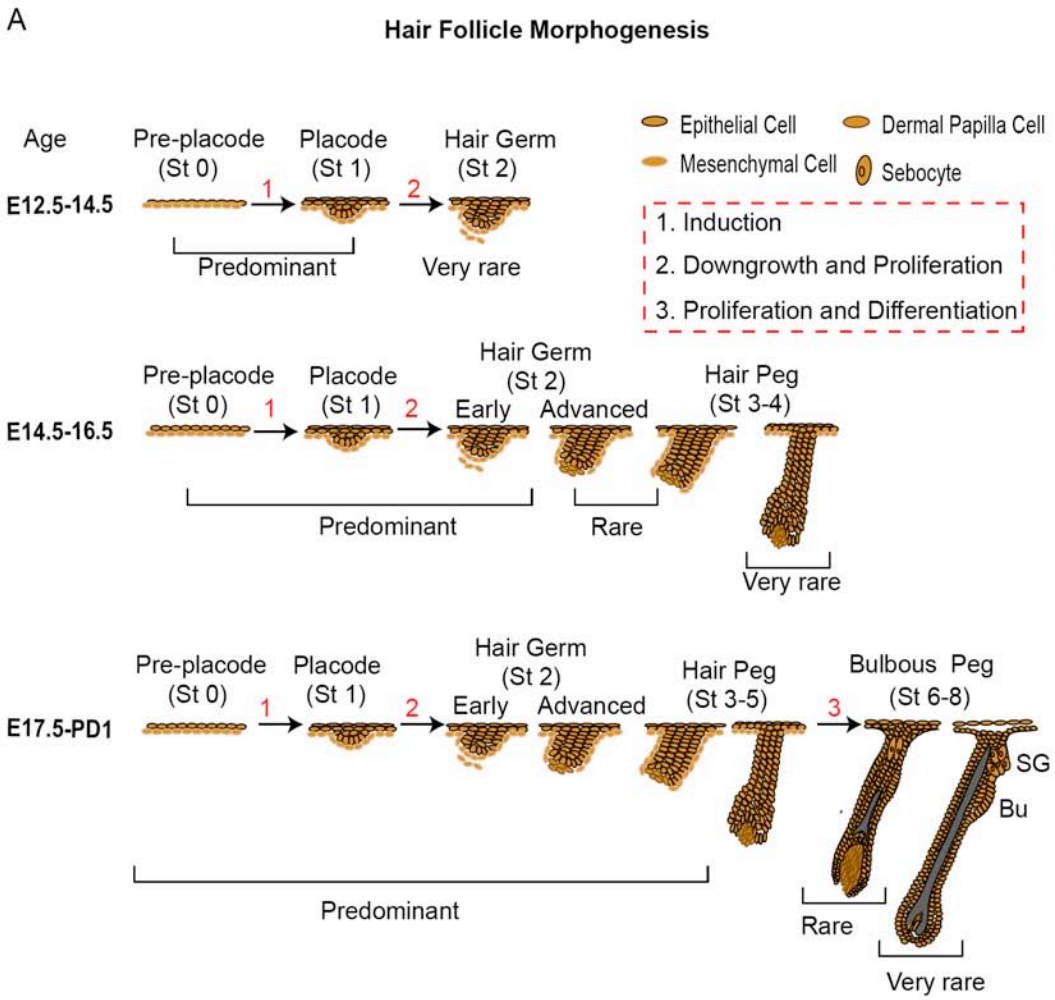
A
Hair Follicle Morphogenesis
Age
Pre-placode (St 0)
Placode (St 1)
Hair Germ (St 2)
E12.5-14.5
Predominant
Very rare
Epithelial Cell
Dermal Papilla Cell
Mesenchymal Cell
Sebocyte
1. Induction
2. Downgrowth and Proliferation
3. Proliferation and Differentiation
E14.5-16.5
Early
Advanced
Hair Peg (St 3-4)
Rare
E17.5-PD1
Bulbous Peg (St 6-8)
SG
Bu

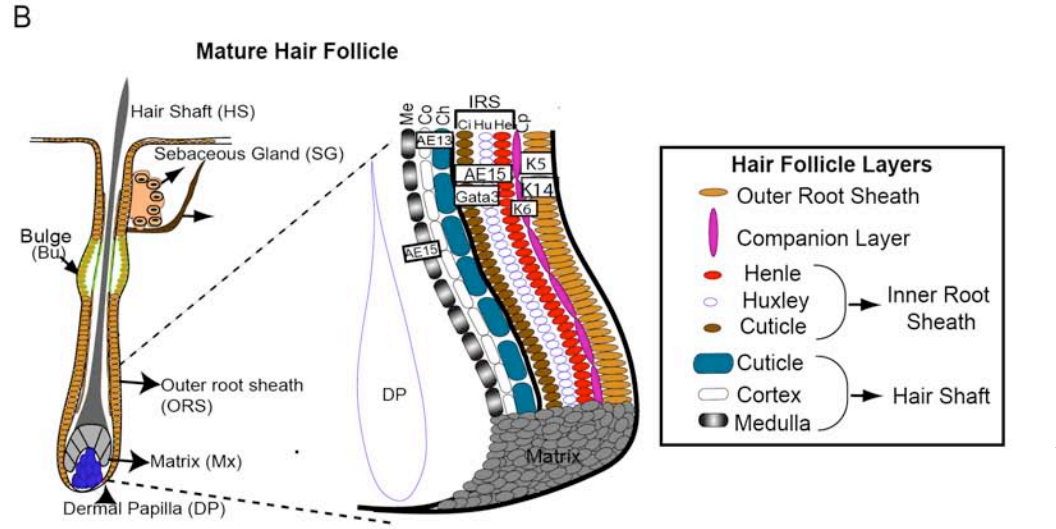
B
Mature Hair Follicle
Hair Shaft (HS)
Sebaceous Gland (SG)
Bulge (Bu)
Outer root sheath (ORS)
Matrix (Mx)
Dermal Papilla (DP)
IRS
AE13
AE15
Gata3
K5
K14
K6
DP
Matrix
Hair Follicle Layers
Outer Root Sheath
Companion Layer
Henle
Huxley
Cuticle
Inner Root Sheath
Cuticle
Cortex
Medulla
Hair Shaft

cells in the hair follicle and the potential role of Runx1 as a stem cell developmental factor. I found that Runx1 marks two classes of hair progenitors in the early hair rudiments, which appeared to contribute mainly to either "primitive" morphogenesis or to the adult HFSCs compartment. Moreover, I showed that in addition to its documented role in adult hair cycle (Osorio et al., 2008) and in terminal differentiation (Raveh et al., 2006), Runx1 is required in the skin epithelium for the timely progression of hair morphogenesis, which delayed the embryonic emergence of both the "primitive" class of progenitors as well as that of the adult HFSCs progenitors.

Materials and Methods

Mice

K14-Cre/*Runx1*$^{fl/fl}$mice were generated as previously described (Osorio et al., 2008) *Runx1*$^{+/LacZ}$ mice were maintained in the C57Bl6 background. To generate K14-Cre;Runx1fl/fl; Bat-gal reporter mice I crossed an F2 generation of Runx1fl/fl; Bat gal+ to K14-Cre selection of the reporter cKO was based on genotyping for lacZ, K14Cre and Runx1 fl/fl (Growney et al., 2005; North et al., 1999; Vasioukhin et al., 1999). I used littermates for wild type (WT)

Lineage analysis studies and X-gal Staining

Runx1CreER male were mated to Rosa26Reporter females. Day of plug was counted as E.5. Females received one daily injection for three consecutive days of tamoxifen (16ug/g body weight) and progesterone (8ug/g of body weight). At day 19.5 females were sacrificed and pups were put with K14-CreRunx1fl/fl foster mothers or tissue was prepared for further analysis. For

5-Bromo-4-chloro-3-indoxyl-beta-D-galactopyranoside (X-Gal) staining, 10μm, 20, 50 and 90μm skin sections were fixed for 1 min in 0.1% glutaraldehyde in PBS, washed 3x1 hour in cold PBS with .01% of NP40 and 100mM of Sodium Dexycholate. After incubation in X-gal solution (North et al., 1999) at 37°C for 12-16 hrs, slides were rinse in PBS and incubated for 3 hours in 1M NaCO3. Then the slides were wash in PBS, counterstained with hematoxylin and mounted in 70% glycerol.

BrdU labeling

BrdU (5-bromo-3-deoxy-uridine) (Sigma-Aldrich) was injected intraperitoneally at 25μg/g body weight in saline buffer (PBS) to pregnant dams. Females were sacrificed 3.5 hours after injection and tissue was processed for further analysis(N=6 *cKO* and 6 WT). Staining of skin sections was described (Tumbar, 2006)

Skin Grafting

Mouse work was approved by the Cornell University IACUC. Nu/Nu females were anesthesized with avertin and injected with the pain reliever ketoprofen . Each female received a piece of skin from newborn Runx1$^{CreER/fl}$;Rosa26R or Runx1$^{CreER/+}$;Rosa26R mice that were induced with tamoxifen from E12.5 to E14.5. Graft was secured with bandages and gauzes. Two weeks after grafting the bandages were removed.

Histology, immunofluorescence and BrDU staining

Skin tissue for immunofluorescence and hematoxylin and eosin staining (H&E) were described (Tumbar, 2006; Tumbar et al., 2004). For alkaline

phosphatase staining frozen tissue was fixed with 2% formaldehyde for 5 minutes washed with 100mM Tris-Base buffer 9.5 and incubated for 30 minutes in NCIB/DAB substrate. MOM Basic Kit (Vector Laboratories) was used for mouse antibodies. Nuclei were labeled by 4',6'-diamidino-2-phenylindole (DAPI). Antibodies were from (1) rat: a6 and b4-integrins (1:150), , BrdU (1:300, Abcam); (2) rabbit: β-Gal (1:2000, Cappel), Keratin 5 and Keratin 17 (1:1000, Covance), E-cadherin (1:500), LEF1(1:700, Cell Signaling, RUNX1 (1:4000, Jessel T., Columbia U.), Sox9 (rabbit, 1:500, M. Wegner, Erlangen-Nuernberg U., Germany) (Stolt, et al., 2003), Ki67 (1:100; Novocastra), AE13 (1:50, Immunoquest), GATA3 (1:100, Santa Cruz), NFATC1 (1:25; Santa Cruz) Vinculin (1:100) Phalloidin-TRed(1:250). Secondary Abs coupled to the following fluorophores: FITC, Texas-Red or Cy5 were purchased from the Jackson Laboratories. A detailed antibody staining protocol was described (Tumbar, 2006). Microscopy and image processing was done as previously described (Osorio et al., 2008).

Attachment and cell migration studies

Newborn skin was treated with dispase overnight in cold temperature. Keratinocytes were isolated as previously described and cells were plated into collagen 1, fibronectin and poly d lysine pre-coated microslides. No substrate was uses as control. For attachment studies 8-well microslide were used. Briefly, 100,000 live cells were plated per well (N=5Wts and 5cKO) and 24 hours later cells were fixed in 4% PFA and stained with vinculin, phallodin and DAPI. The total number of cells was counted per each well. Briefly, 24 pictures at 10x magnification were taken for each well (2 wells per sample) and analyzed using image J (N=5WT and 5KO).

For migration studies, 4-well collagen 1 pre coated microslide was used. One million cells were plated per well and 36 hours post plating a small scratch was made with a pipet tip. Pictures were taken at different timepoints after the wound. Wound healing was analyzed using Image J64 program.
For flow cytometry cells were isolated from E16.5 back skin stained with phycoerithrin-labeled α6-integrin (CD49f) antibody (BD Pharmingen), as described (Tumbar, 2006; Tumbar et al., 2004). Live cells were those excluding propidium iodide (PI, Sigma). Flow Cytometry was performed using BD-Biosciences FACS Aria at Cornell. RNA isolation from sorted cells and RT-PCR of cDNAs were described (Tumbar, 2006; Tumbar et al., 2004).

Western blot and Co IP

Protein extracts were from skin tissue snap-frozen in liquid N_2 and dissolved in BCS buffer (1% Triton X-100 in PBS with 10 mM EDTA, 150 mN NaCl, 1% sodium deoxycholate, and 0.1% SDS), protease inhibitors (Protease Inhibitor Cocktail Set III, Calbiochem) and PMSF. Runx1 immunoblotting was done following the protocol described in the SuperSignal chemiluminescence kit (Pierce). Distal Runx1 (J. Telfer, University of Massachusetts Amherst) was diluted at 1/1000, Lef1 (1:1000, Cell signaling).

For Co-Immunoprecipitation experiments, protein extracts were incubated at 4°C for two hours with Runx1 antibody (1:100) followed by a four hour incubation with protein A agarose beads. At the end of the incubation samples were washed 3x for 5 minutes in washing buffer (25mM Tris.HCL ph7.5, 300mM, NaCl, .1mMEDTA, 10% glycerol, .1% NP40 and 1mM DTT, 1X Protease inhibitors Cocktail III). The protein was eluted from the resin using

1X SDS loading dye and boiling it for 3 minutes. Secondary antibody anti Rabbit –HRP light chain specific (Jackson Immunoresearch).

Statistical Analyses

Data are shown as averages and standard deviations. T-Tests analyses were done with Excel 2008 (Microsoft).

Results

Runx1 is expressed in a dynamic pattern throughout hair follicle development

Previously, I documented the expression pattern and function of Runx1 in HFSC activation during adult homeostasis, but its potential implication in hair morphogenesis and adult HFSCs emergence remained unclear (Osorio et al., 2008). Using reporter mice that contained the LacZ gene inserted in the Runx1 genomic locus (North et al., 2002), Raveh and colleagues detected Runx1 expressing cells in the mesenchymal skin, including the dermal papillae (DP) and its precursors (dermal condensate) at embryonic day E14.5 and E18.5 (Raveh et al., 2006).

Although at E18.5 Runx1 was expressed in the epithelial skin in the bulbous peg, its expression in the earlier embryonic hair morphogenetic stages remained un-documented (Raveh et al., 2006). I examined Runx1 expression at different time points during embryogenesis at E12.5, E14.5, E16.5 and E17.5 using a Runx1-LacZ reporter mice (North et al., 2002) by staining frozen skin sections with X-Gal to reveal LacZ expression.

At E12.5, when skin is composed of a single layer of epithelial cells (ectoderm), I found rare X-Gal+ cells (Figure 3.2A, top left). Hair morphogenesis began at ~E14.5 with the induction of placodes for the primary type of hair (guard), and continued with a 2nd wave initiated at ~E16.5 for the intermediate hair type (awl and auchene), and with a 3rd wave at ~PD0 for the late type of hair (zigzag), as previously described(Schneider et al., 2009). Because of these overlapping hair growth waves, at any given time after ~E14.5 to newborn the HFs co-exist in the skin as a mix of morphological stages, including placodes, germs, pegs and bulbous pegs continuously progressing towards more advanced stages (Figure 3.1A). By birth all the HFs are thought to be specified (Schmidt-Ullrich and Paus, 2005)and continue to mature in postnatal life. The first hairs reach full maturity at several days after birth, while the subsequent hairs become fully mature by PD8 (Paus et al., 1999).

During these time periods, I found X-Gal+ cells in the mesenchymal compartment including the dermal condensate and papillae, as previously reported (Raveh et al., 2006). In addition, many X-Gal+ cells existed in the epithelium of the developing HFs (Figure 3.2A 1A). In the hair placode, germ, peg, and bulbous peg the X-Gal signal was strong in the upper follicle and weak and sometimes absent (especially in the placode) in lower cells of the HF. Both the high and the low Runx1 expressing populations seemed to expand as morphogenesis progresses, and the levels of X-Gal appeared higher in the bulbous peg in both the low and the high expressing cells (Figure 3.2A). Runx1 antibody staining confirmed this expression pattern (Figure 3.2B).

Interestingly, cells with high levels of Runx1 immuno-staining largely resembled the protein expression pattern of Sox9 (Figure 3.2C), a transcription factor implicated in ORS formation and in the function of adult HFSC (Nowak et al., 2008), as shown in staining of skin serial sections at E16.5-E17.5 (Figure 3.2 D and D' and data not shown). In addition, at the bulbous peg stage strong Runx1+ cells that were Sox9- were present in the upper follicle (infundibullum) as well as the lower follicle (matrix) (Figure 3.2D and D'). Moreover, the high Runx1 expressing cells also partially co-localized with Nfatc1, another adult HFSC factor (Horsley et al., 2008) detected in the bulbous peg at E17.5 (Figure 3.2E). Together these data showed that Runx1 was expressed at different levels in two possibly distinct cell subpopulations of the early hair rudiments, which might have different roles and subsequent fates in hair follicles.

Runx1+ early embryonic cells contribute to known HF divergent lineages in postnatal morphogenesis

To address the fate of cells that expressed Runx1 in early embryonic hair morphogenesis, I genetically labeled Runx1+ cells in utero and tracked the distribution of their cell progeny during post-natal morphogenesis and adult hair cycle. I employed a mouse strain that carried the Cre-ER gene inserted in the Runx1 endogenous locus (Samokhvalov et al., 2007) and the Rosa26 reporter (R26R) transgene carrying LacZ downstream of a stop codon that can be removed by Cre induction via tamoxifen administration (Soriano, 1999)

Figure 3.2: **Dynamic expression of Runx1 during embryonic hair follicle development.**

A.) X-Gal staining showing the expression of Runx1 at the different stages of embryonic hair development, arrowhead pointing out a positive cell in the placode. Skin sections were from E12.5 and E17.5 mouse embryos.

B-C.) Runx1 and Sox9 expression in the early stages of developing follicles. Immunofluorescence staining for Runx1 and E-cadherin(B) and Sox9 and a-6 Integrin (C) in E16.5 skin. Notice that the high level of expression of both proteins in the upper follicle. Arrowheads points to Runx1 expression in few cells of the placodes that are high for E-cadherin.

D.) 5uM serial section of E17.5 skin showing Sox9 and Runx1 colocolization. * hair germs

E.) Immunostaining showing Runx1 colocalization with NFATc1 in a subset of cells in the upper region of the bulbous peg.

For all immunofluorescence analysis a minimum of 3Wts and 3cKO were used per antibody. Epi: Epidermis, Der: Dermis.

Scale bars represent 10um.

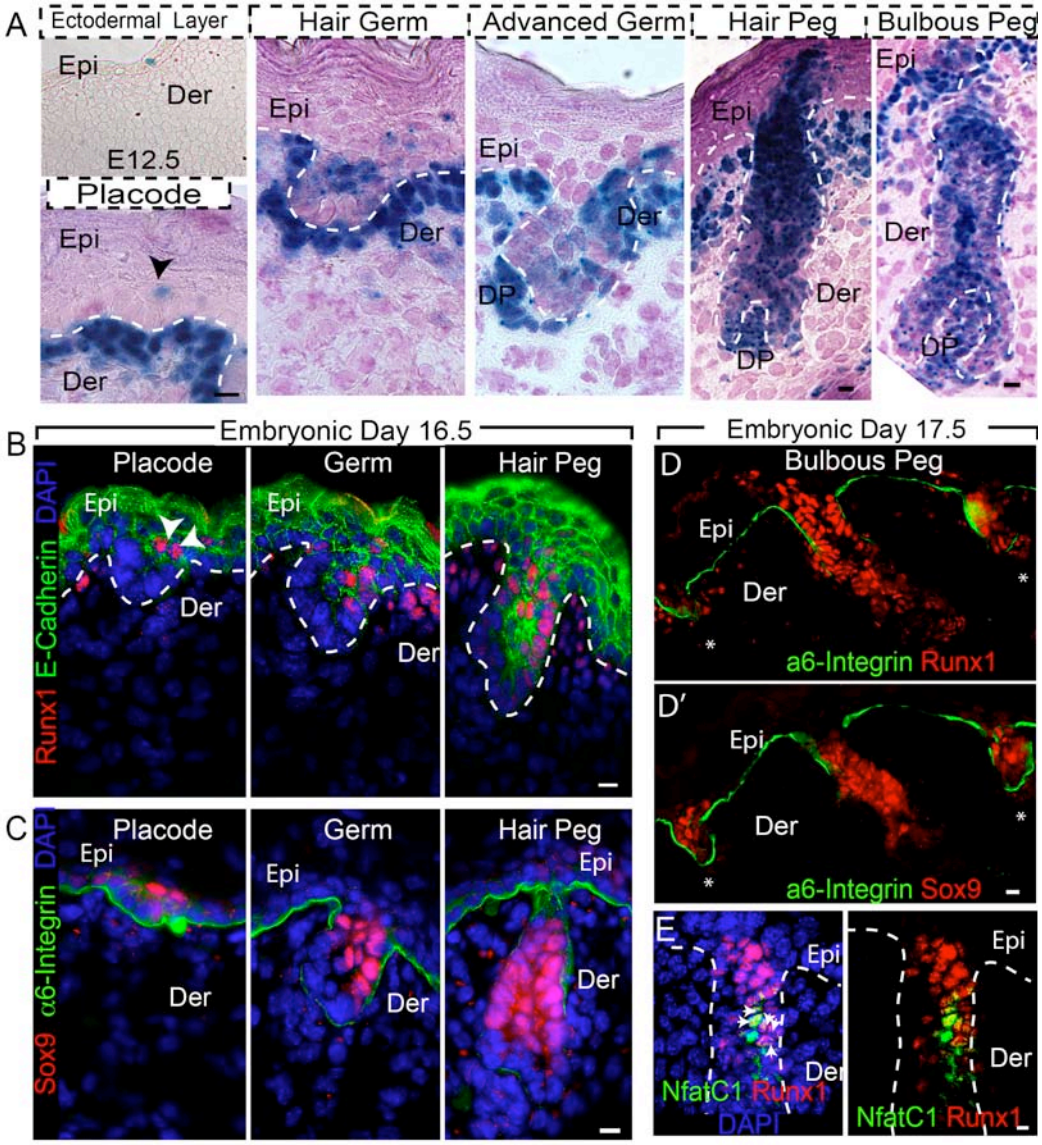
A
Ectodermal Layer
Hair Germ
Advanced Germ
Hair Peg
Bulbous Peg
Epi
Der
E12.5
Placode
DP
B
Embryonic Day 16.5
Placode
Germ
Hair Peg
DAPI
E-Cadherin
Runx1
C
α6-Integrin
Sox9
D
Embryonic Day 17.5
Bulbous Peg
a6-Integrin Runx1
D′
a6-Integrin Sox9
E
NfatC1 Runx1
DAPI

I injected tamoxifen once daily for 2, 3 and 4 consecutive days in pregnant females to optimize the labeling efficiency of the embryos, and sacrificed the embryos and pups at different time points after induction (Figure 3.3A and B). The X-gal signal was extremely weak in the embryonic skin two days after the last injection (data not shown), but by PD0 it became readily detectable, albeit still variable from cell to cell (Figure 3.3A). By PD0 mice injected at E12.5, 13.5, 14.5 showed X-Gal labeling in a noticeable fraction of the dermal cells (Figure 3.4B) and in rare DP cells of ~10% of the HFs (Figure 3.4C). Moreover, ~7% HFs contained a few X-Gal+ cells in their epithelium, as seen in 25-90um skin sections (Figure 3.4B; N=3). The low frequency of labeled HFs at PD0 was expected since only the 1st wave of hair follicles would be induced by E14.5, the last day of tamoxifen injection. That said, the Cre recombinase has been reported to work from 6-36 hours after tamoxifen induction(Zervas et al., 2004) and most likely persisted long enough to label some placodes of the second hair growth wave induced ~E16.5 (Figure 3.1A). All labeled follicles detected at PD0 showed patches of X-Gal+ and X-Gal- cells, supporting the polyclonal HF origin (Figure 3.4C). The low frequency of X-Gal+ cells in most HFs suggested that only rare cells in the hair rudiments activated the Cre recombinase.

The distribution of X-Gal+ cells in the epithelial fraction of the HF at PD0 could be classified in three main labeling patterns: (1) exclusive ORS pattern (35%), in which few X-Gal+ cells were found in the upper and/or lower ORS, and sometimes included few cells of the presumptive bulge (Figure 3.4C and E); (2) matrix and inner layer (M/IL) pattern (18%) with any X-Gal+ cells in the lower bulb and matrix cells, the hair shaft, inner root sheath, inner pre-

sebaceous gland, and/or hair canal (the inner portion of the infundibullum)(Figure 3.1B, 2C and 2E); (3) complex pattern (38%), which was a combination of both M/IL and ORS (Figure 3.4C and E). The remaining 10% labeled HF were hair pegs that had not yet developed M/IL (Figure 3.3C).

By PD5 all follicles differentiated and produced M/IL and hair shafts. The X-Gal signal was stronger than that detected at PD0. The frequency of labeled HFs was ~9% on average when analyzed in 50um sections, and was somewhat variable from mouse to mouse (5-12%; N=2 mice and ~1150 HFs). Within each mouse the three labeling patterns were still detectable by PD5, but showed a different distribution than that found at PD0: ~56% of labeled HFs had ORS exclusive pattern, ~2% M/IL and ~42% had complex (ORS and M/IL) pattern (Figure 3.4E). Thus, 98% of HFs labeled in early embryonic morphogenesis showed persistent ORS labeling pattern at the early stages of postnatal morphogenesis.

Many of the M/IL patterns showed exclusive IL with no matrix staining, and contained small patches of X-Gal+ cells, some approaching the hair canal (near the HF skin exit), where they appeared to be expelled into the shedding portion of the epidermis, the squames (Figure 2Cand S2D).

Figure 3.3: Lineage tracing of embryonic Runx1 expressing cells: induction efficiency analysis

A.) Lineage tracing labeling efficiency. X-gal staining of PD0 skin sections showing low labeling efficiency with two injection and high efficiency with four injections. B.) Plot quantifying the HF follicles shown in (A). C.) Skin section at PD0 showing X-gal staining in hair pegs. D.) Plot showing contribution to the hair canal by Runx1 expressing cells labeled during E12.5-E14.5 or E14.5 to E16.5. E.) X-gal staining showing the ORS/Bu and complex pattern in PD13 skin

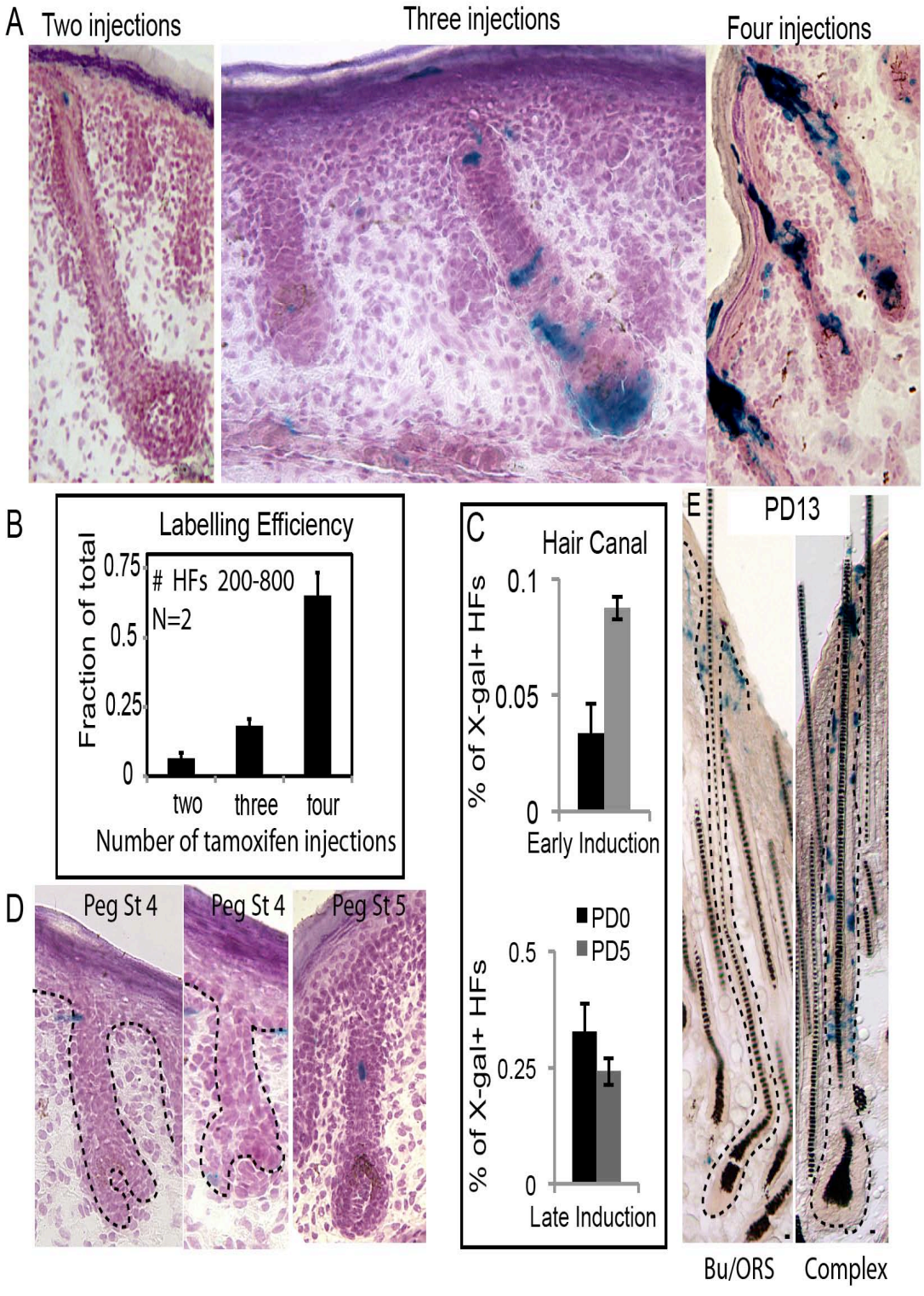
A
Two injections
Three injections
Four injections
B
Labelling Efficiency
Fraction of total
0.75
0.5
0.25
0
# HFs 200-800
N=2
two
three
four
Number of tamoxifen injections
C
Hair Canal
% of X-gal+ HFs
0.1
0.05
0
Early Induction
PD0
PD5
0.5
0.25
0
Late Induction
D
Peg St 4
Peg St 4
Peg St 5
E
PD13
Bu/ORS
Complex

Moreover, X-Gal+ cells were exclusively present in the hair canal in nearly 3x more HF at PD5 than at PD0 (.03 vs .087 Figure 3.3D), likely because X-Gal+ IL from PD0 had been pushed upward by newly generated X-Gal- cells from underneath. All these observations suggested loss of a subset of the early Runx1+ embryonic cells during early postnatal morphogenesis, from PD0 to PD5. Another formal possibility was that M/IL are not lost, but rather converted to ORS in early postnatal morphogenesis. Given published single-cell or ORS-specific lineage tracing data this possibility was less likely (see Discussion). In conclusion, Runx1+ cells from the early embryonic HF morphogenesis (placode and germ) contributed cells to both ORS and to M/IL, two populations generally considered independent during distinct times of morphogenesis (see Discussion).

Since Runx1 expression increased and became broader during late embryonic hair morphogenesis (Figure 3.2A), I assessed the fate of those Runx1+ cells by marking them via tamoxifen injections at E14.5, E15.5 and E16.5. During this period most HFs belong to the second growth wave and exist as placodes and germs, while rare HFs belong to the 1st growth wave, which had advanced to early hair pegs (Figure 3.1A). As before, in addition to genetic marking of HF at these morphological stages, a fraction of advanced pegs and bulbous pegs from ~E17.5 –E18.5 should also become marked because of prolonged Cre activity in the embryo after tamoxifen injection (Zervas et al., 2004). In line with the higher number of HFs in the skin at this stage as well as more Runx1+ cells when compared with early embryonic morphogenesis, I obtained ~3.6x more X-Gal+ HFs (25%, N=5, 1300 HFs) by PD0. Moreover, there were more X-Gal+ cells per HF than seen in the early labeling. In

addition, HFs presented complex labeling pattern (65%), M/IL labeling (27%), and only scarce ORS pattern (7%; Figure 3.4F). This distribution suggested a robust (93% of all labeled HFs) contribution to the M/IL compartments for the late class of Runx1+ HF embryonic cells. An interesting side observation was the high frequency of HFs with X-Gal+ cells in the hair canal, a region of the HF to which the late Runx1+ embryonic HF cells seemed to contribute to substantially (Figure 3.3D).

By PD5 the frequency of X-Gal+ HFs marked during late embryonic morphogenesis (E14.5, E15.5, E16.5) drastically dropped to nearly half of the PD0 level (~14%, N=2, 1200 HFs), while the distribution of the three HF labeling patterns remained roughly the same (Figure 3.4E, red bars). This suggested that cells from all the HF layers including M/IL and ORS (likely from the upper HF) were lost from the skin. This massive loss of HF cells genetically marked late but not early in embryonic morphogenesis suggested that Runx1+ early embryonic HF cells generally lived longer than their late counterparts. However, Runx1+ cells at both early and late embryonic morphogenesis contributed cells to the two divergent HF lineages: ORS and M/IL (see Discussion).

Figure 3.4: In vivo lineage tracing of embryonic Runx1 expressing cells; analysis during hair morphogenesis. A.) Scheme showing the experimental design of the tamoxifen inductions B. 90 um skin section X-gal stained at PD0 showing contribution by Runx1 expressing cells to the hair follicle, the dermal cells surrounding the upper follicle and the dermal papilla cells (arrowheads). C-D. X-gal skin sections showing the major contribution patterns observed at (C) PD0 and (D) PD5 when Runx1 expressing cells were labeled during embryogenesis.

E.) Quantification of these patterns. Noticed that 0% of the follicle had follicles that were completely blue supporting a polyclonal origin of the HF. N=2, 100 follicles analyzed per mouse.

F.) Scheme showing early (E12.5,E13.5 and E14.5) and late (E14.5, E15.5 and E16.5) induction schemes. Plot showing the contribution of the Runx1 descendants at PD0 and PD5 at both induction schemes. A minimum of two mice and 100 follicles counted per stage analyzed. Scale bar 10 uM

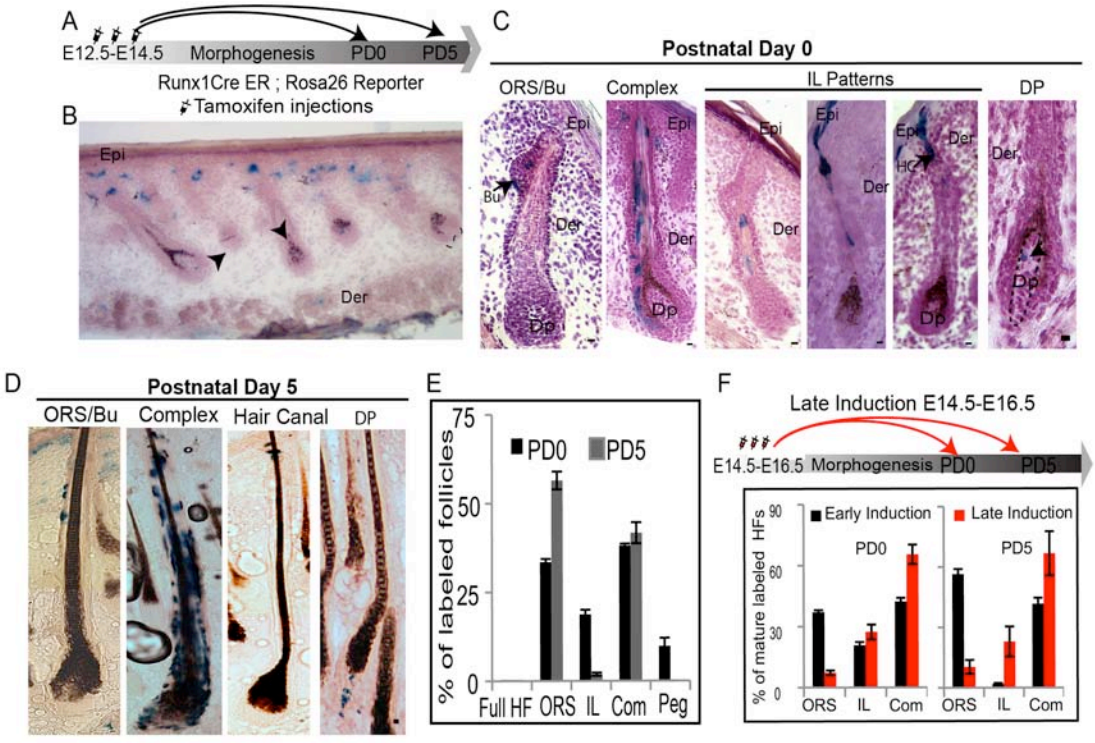
A
E12.5-E14.5
Morphogenesis
PD0
PD5
Runx1Cre ER ; Rosa26 Reporter
Tamoxifen injections
B
Epi
Der
C
Postnatal Day 0
ORS/Bu
Complex
IL Patterns
DP
Epi
Bu
Der
Dp
HC
D
Postnatal Day 5
ORS/Bu
Complex
Hair Canal
DP
E
% of labeled follicles
75
50
25
0
PD0
PD5
Full HF
ORS
IL
Com
Peg
F
Late Induction E14.5-E16.5
E14.5-E16.5
Morphogenesis
PD0
PD5
% of mature labeled HFs
90
60
30
0
Early Induction
Late Induction
PD0
PD5
ORS
IL
Com

Runx1+ early embryonic HF cells contribute to adult HFSCs

To determine if any of the Runx1+ embryonic HF cells detected in the embryonic hair rudiments contribute to the adult HFSCs compartment and to adult tissue homeostasis, I injected mice with tamoxifen during the early (E12.5, E13.5, E14.4) and late (E14.5, E15.5, E16.5) stages of embryonic hair morphogenesis (Figure 3.5A) and examined the HF X-gal labeling patterns in the skin during the adult hair cycle. In telogen (PD21-24), X-Gal+ cells were detectable in the skin in some DP cells (Figure 3.5B) and in the dermal cells that surrounded the HF (Figure 3.5C). In the epithelial compartment of the HF X-Gal+ cells were in the bulge ORS (where single cell lineage tracing data showed that the HFSCs reside;(Zhang et al., 2009), in the non-proliferative layer underneath the bulge ORS, and in the infundibullum (Figure 3B). In anagen (PD26-PD31), X-Gal+ cells were detectable in the bulge and in the bulb area including the matrix and in the differentiated IL (Figure 3.5D), as well as in the infundibullum (Figure 3.5D). These patterns were detectable in adulthood whether tamoxifen injections were done at early (E12.5-E14.5) or late (E14.5- E16.5) embryonic morphogenesis. However, I found that as seen before in morphogenesis the early Runx1+ embryonic HF cells or progenitors had a better survival rate into adulthood when compared to the late Runx1+ embryonic HF cells (Figure 3.5E). In fact, HF counting revealed a similar fraction of ~7-9% labeled follicles at PD0, PD5 and PD26 in mice injected with tamoxifen in early embryonic morphogenesis. In contrast, in mice injected in the late embryonic morphogenesis I found that only ~1/3 of the initial PD0 labeled HF still contained X-Gal+ cells in adulthood (Figure 3.5E). Thus, these data showed that Runx1+ cells in both early and late embryonic hair morphogenesis contain precursors of the adult HFSCs. In addition, the early

HF cells had a higher fraction of these permanent HF progenitors, while the late HF cells were enriched in short-term progenitors that contributed transiently only to post-natal HF morphogenesis, but not to adult homeostasis.

Delayed hair follicle morphogenesis in Runx1 epithelial skin knockout

To test the role of Runx1 in the embryonic epithelial HF cell populations, I analyzed the skin phenotype of epithelial Runx1 conditional knock out (cKO) mice, generated by crossing the K14-Cre transgenic mice (Vasioukhin et al., 1999) to the Runx1 fl/fl mice (Growney et al., 2005). Previously I reported that hair shafts emerged from the skin by PD9, but HF remained temporarily blocked in telogen from PD21 on for an extended period of time (Osorio et al., 2008). At E12.5 the K14-Cre worked only in ~50% of the undifferentiated epithelium, as showed by X-gal staining of K14-Cre; R26R embryo sections (data not shown). However, antibody staining showed that by E16.5 most of the Runx1 protein was absent in the epithelial skin (Figure 3.7A). Mice with inefficient K14-Cre activity, as shown by Runx1 antibody staining at E16.5, were not included in our analysis.

In Runx1 cKO and WT skin sections HFs were present in a mixture of morphological stages as shown by B4-integrin immunostaining, to reveal the basal layer and the ORS (Figure 3.7A), hematoxylin and eosin (not shown), or alkaline phosphatase (to reveal dermal papillae and dermal condensates; Figure 3.7 B and C). Sox9 and NFATc1, two adult stem cell factors that are expressed during morphogenesis, showed no difference in their HF expression in WT and cKO skin (Figure 3.6A and B). I also found no difference in the expression of other skin structural markers, such as Keratin-

17 and E-cadherin (Figure 3.6C and D). I found a thinning of the suprabasal layers of the skin at E16.5 (Figure 3.6E-G). However, staining for stratification markers filaggrin, keratin 1 and loricrin (not shown) showed no abnormalities in epidermal differentiation of Runx1 cKO skin (Figure 3.6E-F). Since Runx1 is not expressed in the interfollicular epidermis the epidermal thinning was likely a secondary effect from the loss of Runx1 in HFs.

Although follicles seemed to develop in the Runx1 cKO, they appeared less dense when compared to WT skin (Figure 3.7B and D). I counted the number of HFs irrespective of developmental/morphological stage in the skin and expressed it as an average per field of view (FOV). Moreover, I determined the distribution of HF patterns in 20 um back skin of cKO and WT mice section stained with alkaline phosphatase. At E16.5 WT skin analysis revealed mainly hair placodes and germs, belonging to the 2nd hair growth wave at this age, and few hair pegs, belonging to the 1st hair growth wave (Paus et al., 1999). The 1st wave represents only 2% of all the hairs in the skin(Schmidt-Ullrich and Paus, 2005). I found ~ 4 HFs/FOV in WT and ~2 HFs/FOV in cKO skin (Figure 3.7D). The total number of HFs at a given age shows directly how many placodes have been cumulatively induced in the skin from the beginning of hair morphogenesis. Therefore, these data demonstrated that ~45% of HF had not been timely induced by E16.5, and that Runx1 loss caused a developmental impairment in placode formation (Figure 3.7B).

Figure 3.5: In vivo lineage tracing of embryonic Runx1 expressing cells; analysis during adult hair cycle.

A.) Scheme showing early and late induction scheme and timepoints when skin samples were taken.

B.) X-gal staining counterstained with hematoxylin showing contribution of Runx1 expressing cells to the bulge, infundibular area and dermal papilla.

C.) 90 um section showing contribution of embryonic Runx1 expressing cells to the adult dermis.

D.) Embryonic Runx1 expressing cells contribute to hair regeneration. Anagen hair follicles shows X-gal positive cells in the bulge and in the inner layers of the new regenerated follicle.

E.)Runx1 expressing cells are long live. Plot showing that early induced Runx1 expressing cells had a better survival rate than late induced cells.

Epi: Epidermis, Der: Dermis, Dp: Dermal Papilla. Scale bars represent 10uM.

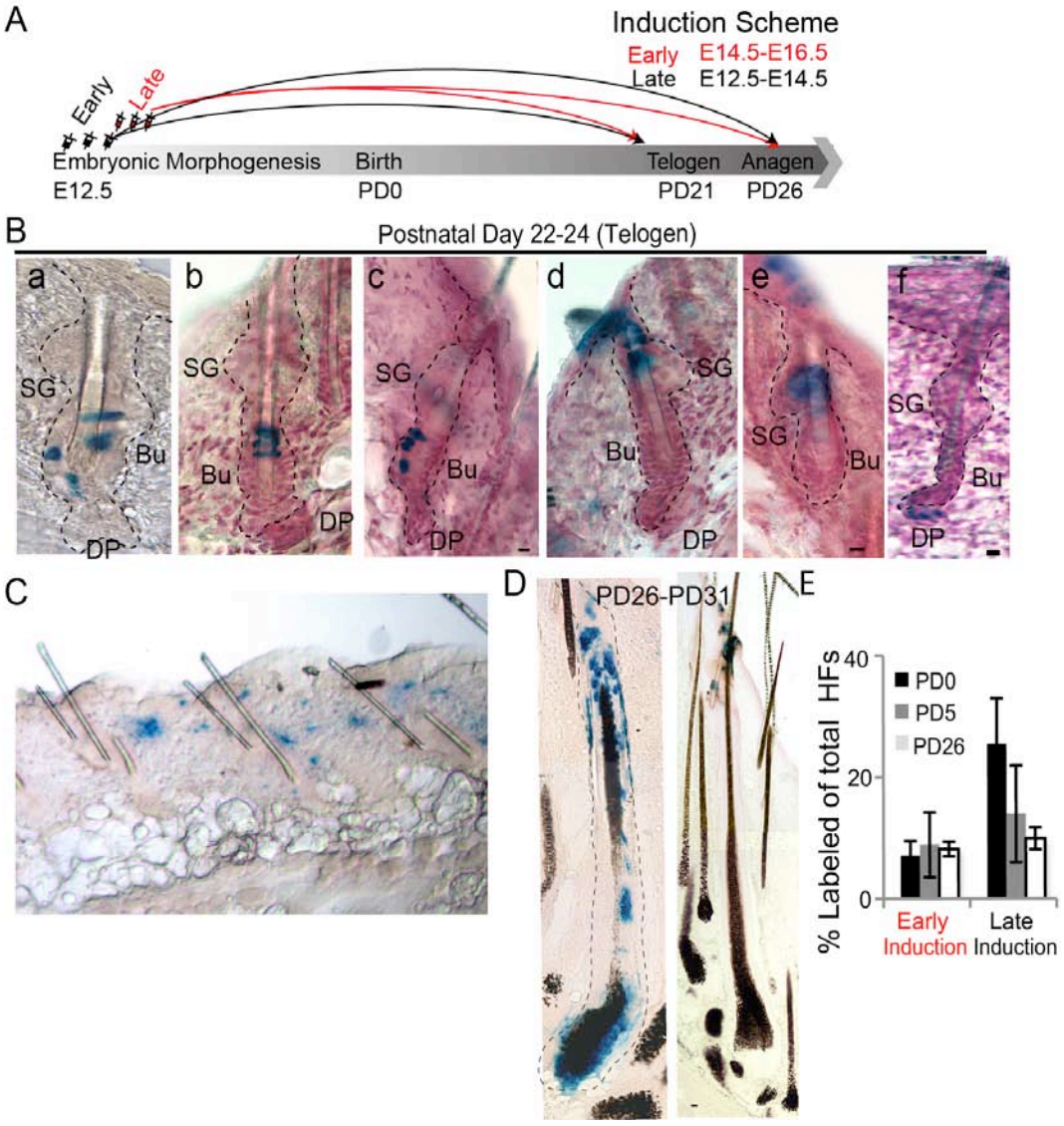
A
Induction Scheme
Early E14.5-E16.5
Late E12.5-E14.5
Early
Late
Embryonic Morphogenesis
E12.5
Birth
PD0
Telogen
PD21
Anagen
PD26
B
Postnatal Day 22-24 (Telogen)
a
b
c
d
e
f
SG
Bu
DP
C
D
PD26-PD31
E
% Labeled of total HFs
40
20
0
PD0
PD5
PD26
Early Induction
Late Induction

Figure 3.6: Normal expression of known molecular factors involved in hair morphogenesis in Runx1 cKO skin

A-D.) Immunostaining analysis at E16.5 in Runx1 cKO skin showed no abnormal expression for adult stem cell markers such as Sox9 (A) , NFATC1 (B) or other structural markers such as Keratin17(C) or E-cadherin (D).

E-F.) Thinning of the suprabasal layers in Runx1 cKO skin. E16.5 skin showed a thinning of the suprabasal layers in Runx1 cKO skin with normal stratification as represented by the normal expression of stratification markers such as keratin -1(E) and Filagrin (F).

G.) Skin measurements using imageJ at E16.5 showed thinning of the suprabasal layers in Runx1 cKO skin. N=3 WTs and 3cKOs. A minimum of 80 measurements per skin samples were done p value=.01

Epi: Epidermis. De: Dermis. Scale Bar 10uM

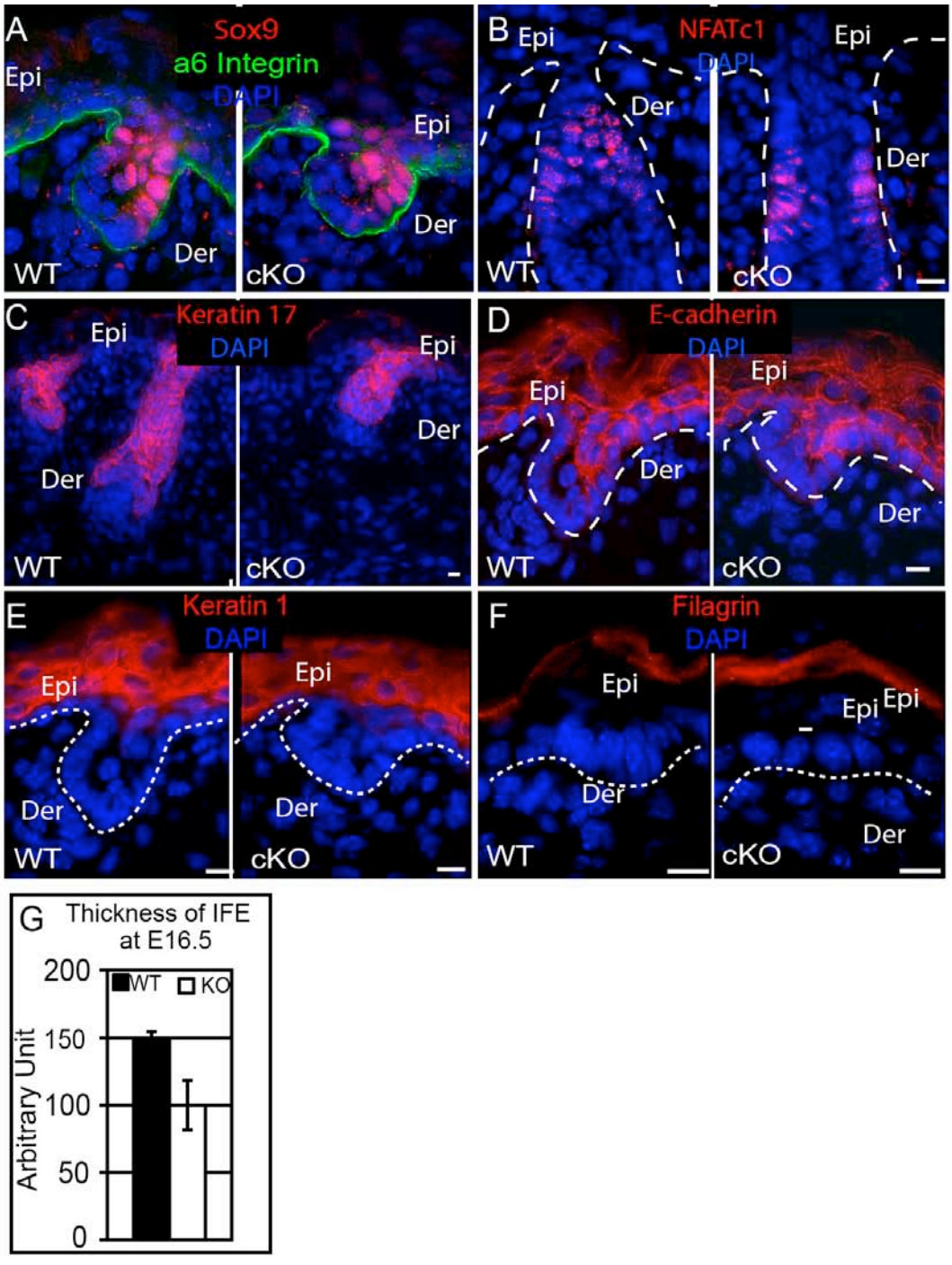
A
Sox9
a6 Integrin
DAPI
Epi
Der
WT
cKO
B
NFATc1
DAPI
C
Keratin 17
D
E-cadherin
E
Keratin 1
F
Filagrin
G
Thickness of IFE at E16.5
WT
KO
Arbitrary Unit
200
150
100
50
0

The evolution of the HF populations during morphogenesis can be expressed as the total number of HFs that passed through a particular morphological or developmental stage in their morphogenesis and can be calculated from the frequency of each morphological stage per FOV at a given time. For example, since placode (stage 1, st 1) is the most immature stage and hair peg (st 4) is the most mature stage present at E16.5 skin, the frequency of induced placodes would equal the sum of st1, 2, 3, and st4 follicles (Figure 3.7C'). Similarly the frequency of induced hair germs would equal to the sum of st2, st3 and st4 developing HFs. If the hair placode induction was delayed rather than blocked in the cKO skin, it would cause a secondary delay in all the HF developmental stages descending from the placode. Indeed, our data at E16.5 showed reduction in the frequency of occurrence of not only placodes in cKO relative to WT, but also revealed a substantial reduction in both hair germs and pegs (Figure 3.7C').

Next I asked if any of the HF developmental stages subsequent to placode induction, the down-growth and differentiation, were also directly affected by Runx1 cKO. For that I calculated the fractions of total HF that converted from placodes to germs, from germs to pegs, from pegs to bulbous pegs, etc from the beginning of morphogenesis to the time of analysis (Figure 3.7C''). The data revealed a significant impairment ($p=.01$) in the conversion of placodes (stage 1) to hair germs (stage2) upon Runx1 loss by E16.5 (Figure 3.7C''). By PD1 when the 3rd and last hair growth wave had already been initiated, I found that the total number of HFs became equal in WT and cKO (Figure 3.7D and F). Thus, HF placode induction eventually occurred in the Runx1 cKO skin. I also calculated the cumulative number of HF that passed through a

specific stage from the beginning of morphogenesis to PD1, as well as the rate of conversion from one stage to another (Figure 3.7F' and F"). First, placodes and germs (which at PD1 belong to the 3rd growth wave) were only mildly affected by Runx1 loss. The most affected seemed to appear the conversion from peg st 4 to peg st 5, which belonged to the 2nd wave of HF growth. By PD9 all HFs reached full maturity and produced hair shafts.

Lastly, I determined whether loss of Runx1 affected lineage fate specification. For this, I immunostained skin sections of PD6 and PD9 mice with markers specific for differentiated lineages such as Sox9, Gata3, AE13, Keratin 5 and Lef1. I found no difference in the pattern of expression in the cKO skin when compared to WTs suggesting that fate acquisition was not affected by the loss of Runx1 (Figure 3.8).

Collectively all of these findings suggested that Runx1 loss posed a delay in HF induction (placode formation) in embryonic morphogenesis at E16.5. This resulted in a shift or delay of the entire HF developmental program, which appeared more pronounced for the initial hair growth waves (1 and 2). In addition, Runx1 loss appeared to affect directly the HF down-growth as shown from the impaired rate of conversion from placode to hair germ and from peg to bulbous peg. However, this developmental delay was eventually overcome later in postnatal morphogenesis by PD10, when Runx1 cKO mice produced fully differentiated hairs shafts.

Figure 3.7: **Runx1 loss results in a delay in hair follicle morphogenesis.**

A.) Co-staining of hair germs with Runx1 and B4-integrin antibodies at E16.5 showed its absence in the epithelial part of the cKO germ.

B-C.) Alkaline phosphatase staining co-stained with S-red at E16.5 (B) and PD1 (C) showing a reduction in hair follicle density in Runx1 cKO skin.

D.) Plots showing the the average number of follicles per field of view (FOV) in WT and cKO skin at E16.5 and PD1. The average number of HF is cKO skin is 2.61 (N=3), while in WTs is 4.71 N=4. At PD1 the average number of HFs/FOV in cKO is 9.53 (N=4) and in WTs 10.76 (N=4) suggesting that the initial reduction in total HF number is overcome.

E-F) Loss of Runx1 results in a hair follicle developmental delay.

E.) Plots showing the HF density divided by mophogenetic stage.

E') Plot showing the evolution of HF development. The number of developing follicles that are or passed a particular developmental stage were compared in WT and cKO skin. Notice that the initial reduction in the total number of hair follicles seen in (D) results from a delay in HF induction rather than a block in hair development.

E'') Plot showing the rate of conversion of a HF in stage n of development to stage n+1 in development. Notice that the rate of conversion of stage 1 (placode) to stage 2 (germs) is decreased in Runx1 cKO skin suggesting a defect in downgrowth.

F-F'') Plot showing the HF density by stage, the evolution of hair follicle morphogenesis and the rate of conversion at PD1 skin

Epi, epidermis; De, Dermis. Scale Bars is 10uM

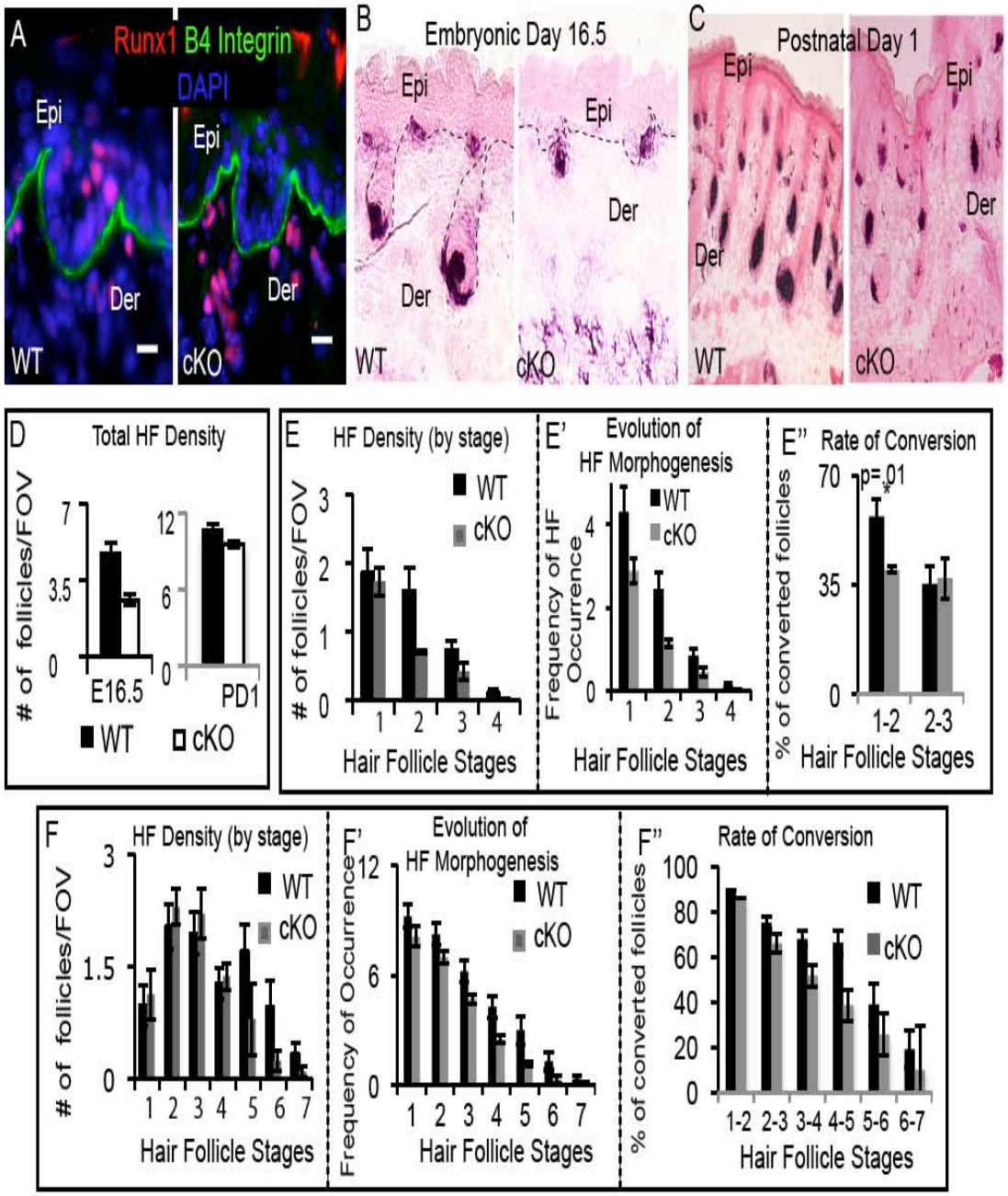
A
Runx1 B4 Integrin
DAPI
Epi
Der
WT
cKO
B
Embryonic Day 16.5
C
Postnatal Day 1
D
Total HF Density
# of follicles/FOV
E16.5
PD1
WT
cKO
E
HF Density (by stage)
Hair Follicle Stages
E'
Evolution of HF Morphogenesis
Frequency of HF Occurrence
E"
Rate of Conversion
p=.01
% of converted follicles
1-2
2-3
F
HF Density (by stage)
F'
Evolution of HF Morphogenesis
Frequency of Occurrence
F"
Rate of Conversion
1-2 2-3 3-4 4-5 5-6 6-7

Figure 3.8: Loss of Runx1 does not affect lineage fate specification. Skin section of PD6-PD9 skin show the presence of differentiation markers (red) in both WT and cKO skin. DAPI is blue. Scale bar 10uM.

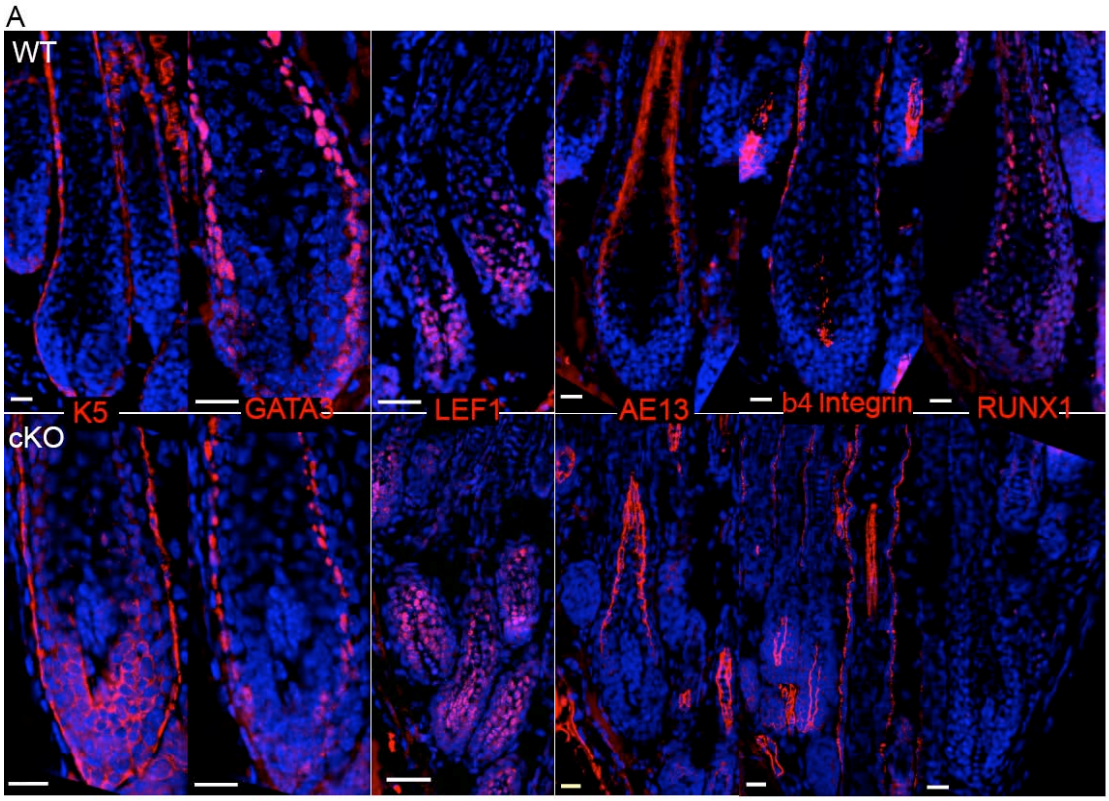
A
WT
K5
GATA3
LEF1
AE13
b4 Integrin
RUNX1
cKO

Loss of Runx1 mildly impairs embryonic HF cell proliferation

Runx1 is implicated in epithelial cells proliferation and cell cycle regulation (Hoi et al., submitted, Osorio et al., 2008), and cell proliferation occurs robustly through hair morphogenesis. Indeed, staining of E16.5 back skin for Ki67 (Figure 3.9A), a proliferative marker, and for short-term incorporation of BrdU showed ~20% difference in cKO and WT skin (Figure 3.9B). These results were true whether I analyzed basal/ORS a6-integrin+ cells sorted from the skin at E16.5 (Figure 3.9B) or skin sections in which I focused on the hair germs (Figure 3.9C and D). This mild proliferation defect was likely contributing but was probably not the entire cause of the HF developmental delay induced by Runx1 loss.

Loss of Runx1 compromises the ability of keratinocytes to adhere and migrate

The formation of the early HF rudiments require downward migration of the ectodermal cells from the single layer of ectoderm that need to become polarized and invade the underlining dermis. Staining of E16.5 back skin with keratin-5 antibody to mark the epithelial cells cytoskeleton revealed a disorganization in the early hair germs of the cKO. The cells appeared more crowded with cells and lacked the regular tiled-pavement appearance observed in the WT (Figure 3.10A). I found equal number of cells per germ in both WT and cKO , but a significantly reduced germ area in cKO (Figure 3.10B), suggesting that germ cells were produced in normal numbers but they failed to migrate down upon Runx1 loss.

Figure 3.9: Loss of Runx1 causes mild proliferation defects.

A-B.)Immunofluorescene analysis showing embryonic hair germs stained for A.) Ki67 and B.) BrDU

C.) Mild decrease rate of proliferation in the cKO E16.5 skin. Plot of a BrDU immunostaining analysis of FACS purified a6-integrin cells showing a 28% reduction in BrDU incorporation observed in cKO a6 epithelial cells. $N \geq 3$ Wt and cKO. A minimun of 250 cells counted per population.

D. Plot quantifying the average number of BrDU+ cells observed in germs (Figure 3.5B) after 3.5 hours chase. $N \geq 100$ germs WT and cKO.

Epi: Epidermis, Der: Dermis. Scale bars represent 10um.

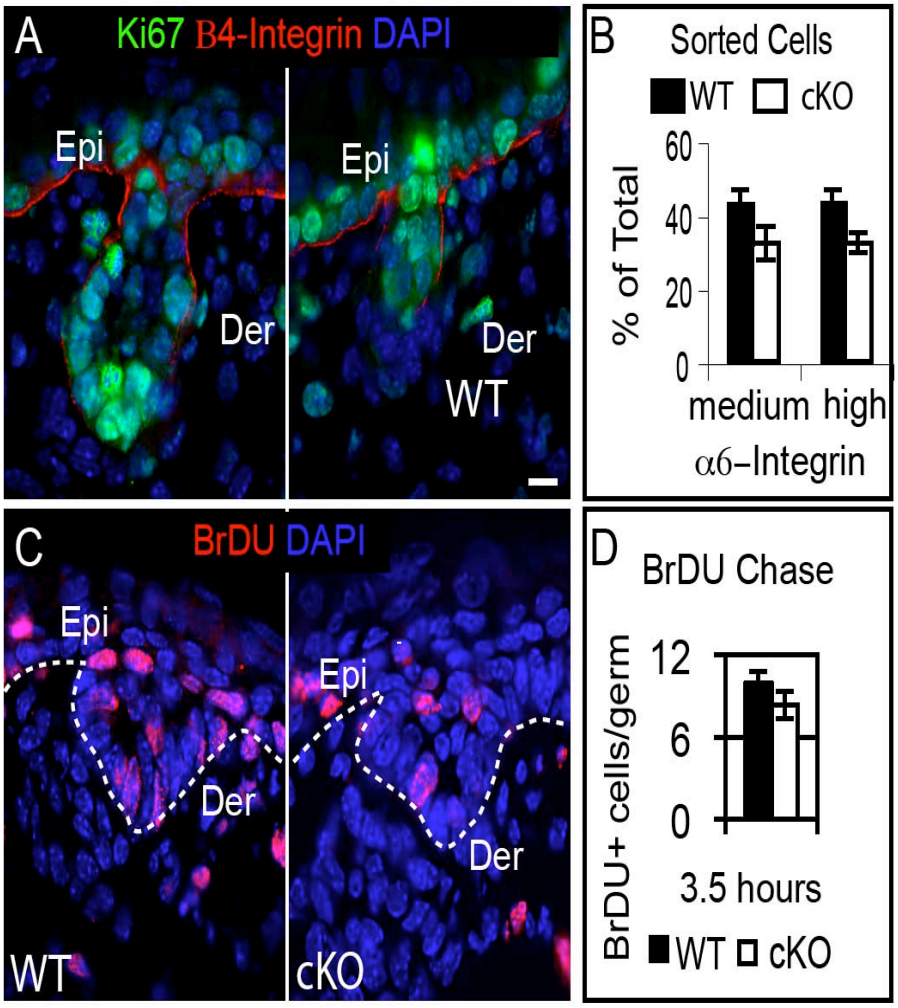
A
Ki67 B4-Integrin DAPI
Epi
Der
Epi
Der
WT
B
Sorted Cells
WT
cKO
% of Total
60
40
20
0
medium high
α6–Integrin
C
BrDU DAPI
Epi
Der
Epi
Der
WT
cKO
D
BrDU Chase
BrDU+ cells/germ
12
6
0
3.5 hours
WT
cKO

To test whether Runx1 might play a direct role in epithelial cell migration and adhesion, I isolated primary skin epithelial cells (keratinocytes) from WT and cKO newborn mice and placed them in culture. Previously I showed all of cultured keratinocytes eventually expressed Runx1, which was required for their long-term survival and proliferation (Osorio et al., 2008).

I determined whether Runx1 played a role in cell adhesion by testing the ability of epithelial skin cells (keratinocytes) to adhere and spread over a period of 24 hours after plating on different extracellular matrix (ECM) factors: fibronectin (FN), collagen 1 (Col-1) and Poly-D-Lysine (PDL). Similar to WTs, Runx1 mutant keratinocytes attached to all these different ECM substrates (Figure 3.10G).

I also looked at the ability of the cells to spread in the absence of Runx1. I focused our attention on spreading onto collagen, because keratinocytes seemed to attach best to this factor (Figure 3.10C,G and H). In a period of 24 hrs, ~85% WT and cKO cells showed "spreading", as defined by a large surface area with strong actin fibers and focal adhesion points seen in phalloidin and vincullin immunostaining (Figure 3.10D). The remaining 15% of the cells remained round with no apparent stress fiber formation during this time. In addition, I found that more Runx1 cKO keratinocytes accumulated strong stress fibers when compared to WTs, and showed a large surface area as defined by the contour of the phalloidin staining (Figure 3.10D-F and H). This effect of Runx1 loss on cell adhesion was also observed in keratinocytes plated onto a monolayer of mouse embryonic fibroblast (MEFs)

immunostained with K5, at 24 hrs (Figure 3.10F) and 96 hours (data not shown) after plating.

If Runx1 cKO keratinocytes attach more strongly and spread out more on ECM, this might also impair their cell migration ability. To test this possibility I performed scrape-wound closure in vitro assays on monolayers of primary keratinocytes freshly plated onto a collagen matrix. I photographed the wounded area using phase contrast microscopy at 0-, 8-, 12-, 24- and 31 hrs after wounding (Figure 3.10I and data not shown). To calculate the migration rate I measured the distance between wound edges (in um) for two wounds per mouse (N=4 WT and 4 cKO mice). I observed that over a period of 12 hours the distance between wound edges decreased faster in the WT than in the cKO. This was due to either slower migration or decreased proliferation in cKO cells (Figure 3.10I, K). However, when I repeated this experiment in the presence of mytomycin-C (myt-C), a potent inhibitor of cell proliferation, the cKO cells remained slower in closing the wound (Figure 3.10K). Therefore Runx1 loss resulted in impaired cell migration and adhesion in vitro, which correlated well with the high density of cells in the hair germ and the impairment in HF down-growth in vivo.

Figure 3.10: Loss of Runx1 impairs proper downgrowth *in vivo* and cell adhesion and migration *in vitro*

A.) Abnormal hair germ morphology in cKO skin. Immunostaining with K5 shows cKO gems are smaller that WTs.

B.) Analysis of hair germ. Plot of hair germ area using Image J showed reduced germ size in cKO skin. Au: Arbitrary Unit. Total number of cells per hair germ was comparable in both genotypes. Average number of cells per germ WT =27 and cKO 29 .

C.) DAPI staining of cells plated onto collagen 124 hours post plating

D-E.) Spreading defects in Runx1 mutant keratinocytes.

D.) Immunofluorescence analysis of keratinocytes plated into collagen and stained for vinculin and phalloidin. Runx1cKO keratinocytes had more stress fibers and spreaded more.

F.) Imunofluorescence analysis showing that Runx1 under normal culturing condition Runx1 cKO mutant cells plated cells spreaded more.

G.) Plot showing attachment to different ECM factors 24 hours after plating Col-1: Collagen 1, FN: Fibronectin, PDL: Poly-D-Lysine.

H.) Analysis of cell spreading in Col-1. The percent of cells that spreaded in collagen is similar in WT and cKO. However Runx1 mutant cells have a higher percentage of bigger cells.

I.) Wound healing assays in cells isolated from newborn mice showing a migration defect in Runx1 deficient cells.

J.) Plot showing the average distance keratinocytes migrated in a 12 hour period without mitomycin C and 24 hour period with mytomycin C

Epi: Epidermis, Der: Dermis. Scale bars represent 10um.

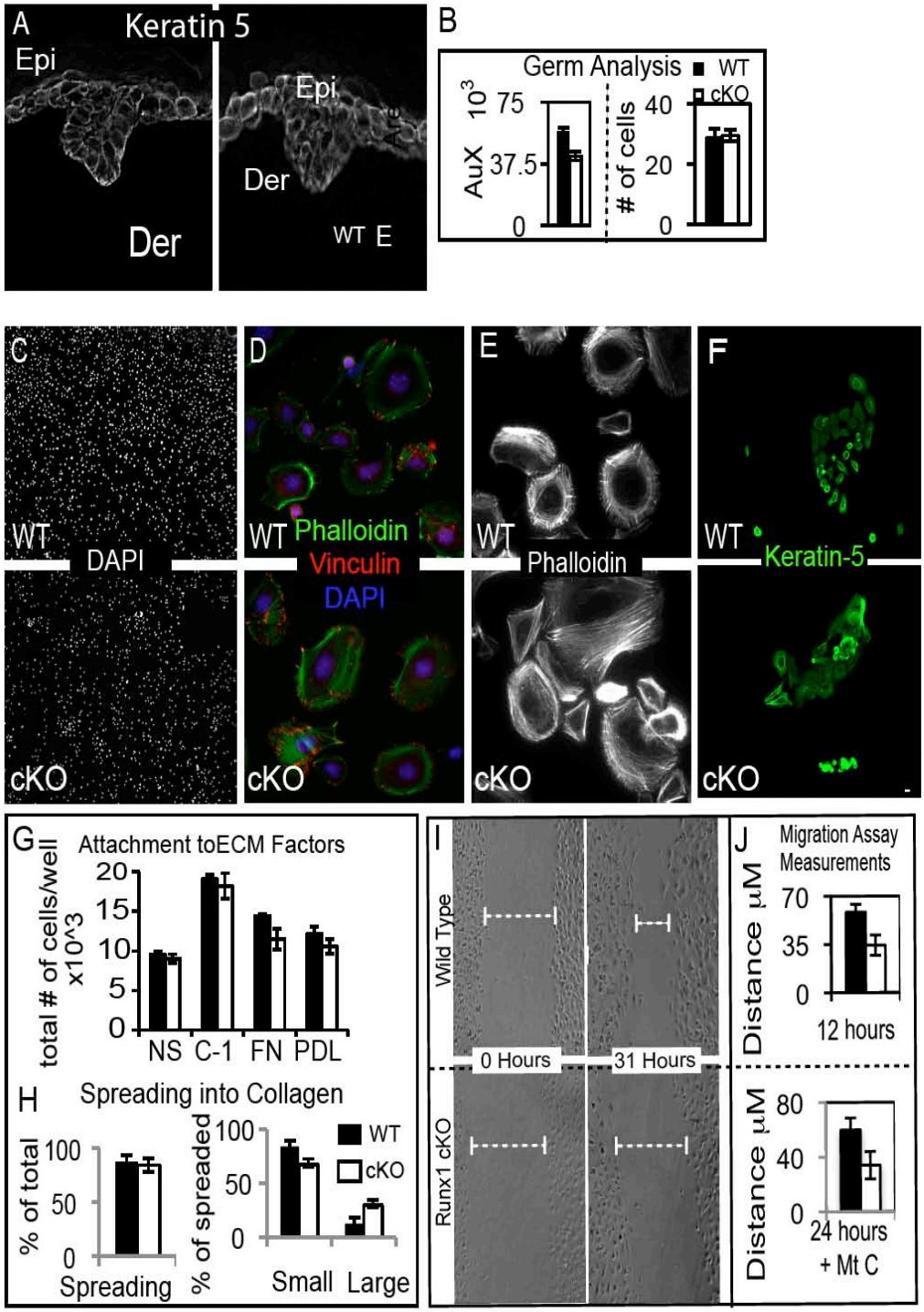
A
Keratin 5
Epi
Der
Epi
Der
WT E
B
Germ Analysis
WT
cKO
AuX 10^3
75
37.5
0
# of cells
40
20
0
C
WT
DAPI
cKO
D
WT Phalloidin
Vinculin
DAPI
cKO
E
WT
Phalloidin
cKO
F
WT
Keratin-5
cKO
G
Attachment toECM Factors
total # of cells/well x10^3
20
15
10
5
0
NS C-1 FN PDL
H
Spreading into Collagen
% of total
100
50
0
Spreading
% of spreaded
100
50
0
WT
cKO
Small Large
I
Wild Type
0 Hours
31 Hours
Runx1 cKO
J
Migration Assay Measurements
Distance µM
70
35
0
12 hours
Distance µM
80
40
0
24 hours
+ Mt C

Miss-regulated WNT signaling pathway in Runx1 cKO skin

Signaling pathways such as Bmp/TgfB, Wnt, FGFs and TNFs are known to participate in the epidermal-mesenchymal communication that occurs during embryonic hair development (Millar, 2002; Schneider et al., 2009). Since Runx1 is a transcription factor I took a candidate approach in which I tested for the mRNA expression levels of factors known to regulate hair morphogenesis (Andl et al., 2002; Botchkareva et al., 1999; Millar, 2002; Nakamura et al., 2001) as summarized in Figure3.11A. Real time PCR conducted on skin epithelial cells FACS purified from E16.5 embryos (Figure 3.11A and B) showed that of the two a6-integrin populations purified, high and medium, Runx1 was expressed in the a6 integrin^{medium} population(Figure 3.12B). Since Runx1 is expressed in the HFs but not the epidermis, this suggested that the a6 integrin^{medium} population was enriched for hair epidermal cells (Figure 3.12B and 3.11A,B). mRNA isolation and cDNA analysis by QRT-PCR revealed a change in expression for several of these factors in the a6-integrin^{medium} population (Figure 3.12C), due to Runx1 loss. However, since at E16.5 HFs are found as a mixture of developmental stages, generally less advanced in the cKO skin than in WT, it was unclear if these differences in gene expression might be a result rather than a cause of the observed Runx1 cKO HF developmental delay.

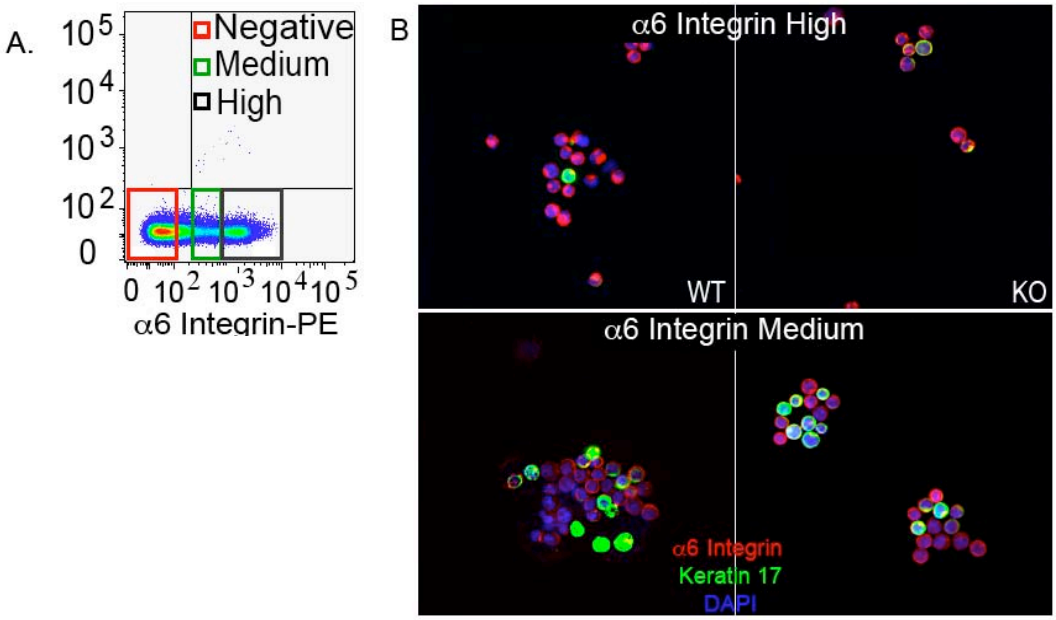

Figure 3.11: Two α6-integrin expressing populations exists in E16.5 skin.

A) FACS analysis plot showing the gates for the α6-integrin high, medium and negative population.

B.)Expression of epidermal markers on sorted cell populations. Immunofluorescence analysis showing an enrichment for Keratin 17 a hair follicle marker in the α6-integrin medium population.

To distinguish between these possibilities I focused on one of these developmental pathways, the Wnt signaling, for which available reagents including antibodies and reporter mice allowed us to examine its activity status in situ, in comparable HF developmental stages.

First, I immuno-stained skin sections for Lef1, a transactivator of Wnt target genes (Andl et al., 2002; Jamora et al., 2003; Lowry et al., 2005; Reya and Clevers, 2005), found strongly expressed at the leading edge of the developing follicle, where the Runx1 low expressing cells reside (Figure 3.12E-G). Lef1 is also weakly expressed in the upper follicle, co-localizing as well with the Runx1 high expressing cells (data not shown). In the cKO skin Lef1 showed decreased and/or diffuse levels in the hair placode, germs and pegs, especially at the leading HF edge (Figure 3.12E-G). Since Runx1 and Lef1 have been previously shown to share several binding partners (Levanon et al., 1998), it is possible that they might interact at the protein-protein level in the HF cells. To test this hypothesis, I performed co-immunopreciptation (IP), using a Runx1 specific antibody (Telfer and Rothenberg, 2001), on extracted proteins from E16.5 skin. Indeed, I found that Lef1 but not Gapdh could be co-IP using the Runx1 antibody, while control Igg could not co-IP any of these proteins (Figure 3.12D). Intriguingly, the diffusion and decrease of Lef1 staining signal was not confined to the HF epithelial compartment, but was also seen in the DP, and in the surrounding dermal cells (Figure 3.12E-F). This was not due to impaired antibody staining in the cKO as many cells in the adjacent skin regions showed bright nuclear signal (Figure 3.12E-F). These data suggested a broader paracrine effect of Runx1 loss on Lef1 protein level or nuclear localization in the skin.

To further examine in situ the effect of Runx1 loss on Wnt signaling I crossed the K14-Cre; Runx1fl/fl with Wnt signaling reporter (BAT-GAL) mice (Maretto et al., 2003). These mice carry the lacZ reporter transgene downstream of an enhancer element that contains a minimal promoter and multiple Tcf/Lef binding sites. Analysis of E18.5 and newborn back skin stained with X-Gal showed a dramatic decreased in signal in the cKO when compared to WT (Figure 3.12H,J and K). Quantification of the number of HFs with X-gal+ cells showed that 25% of all cKO counted HFs had at least one X-gal+ cell in comparison to 67% in the WT (Figure 3.12I). As seen before for Lef1, this decrease in signal was not confined to the epithelial compartment, but was also detected in the DP of the cKO HFs, many of which lacked entirely X-Gal signal (Figure 3.12H). All these results suggested that Runx1 loss in the epithelium results in a generalized decreased canonical Wnt signaling in the skin in both epithelial and mesenchymal cells.

Discussion

Here I used Runx1, a transcription factor previously implicated in adult HFSC activation (Osorio et al., 2008)and HSC emergence (Dzierzak and Speck, 2008), to investigate HFs embryonic morphogenesis and adult HFSCs emergence. First, I described Runx1 expression at different levels in two subpopulations of epithelial HF cells of the early hair rudiments. Second, I performed lineage-tracing experiments and tracked the fate of the embryonic Runx1+ cells during post-natal embryogenesis and in adulthood. Third, I examined the role of Runx1 during HF morphogenesis in a conditional epithelial knockout mouse and found that Runx1 loss delays HF induction and down-growth.

Figure 3.12: Mis-regulation of WNT signaling pathway in Runx1 cKO skin

A.) Table summarizing the name of key skin regulators and the phenotypes in the skin

B.) QPCR analysis showing expression of Runx1 in the a6-integrin high and medium population.

C.) Regulators of hair morphogenesis are misexpressed in Runx1 cKO skin. RT-PCR analysis in cDNA from a6-integrin medium population showing misregulation of known hair morphogenesis factors. N=2Wts and 2cKOs.

E-F.) Lef1 downregulation in Runx1 cKO skin. Immunostaining of Lef-1 co stain with alpha 6 integrin showing a reduction of Lef 1 in the placodes (E), germs (F) and hair peg (G) of Runx1 cKO skin when compared to WTs.

D.) Co-Immunoprecipitation using a Runx1 antibody and blotting for Lef1 showed that Runx1 and Lef1 can are found in the same protein complex in physiological conditions. N=6WTs and 6cKO

H-K.) Wnt signaling is downregulated in Runx1 cKO skin . Analysis of Lac-Z expression of cKO and WT mice that carried the BAT-GAL Wnt signaling reporters. X-gal analysis showing reduced Lac-Z activity in E18.5 skin (H), hair placodes(J) and germs (K)

I.) Quantification of D showed a 50% reduction in the number of follicles with at least one X-gal positive cell in Runx1 cKO skin . N=2Wt and 2cKO

L.) Plot showing the quantification of E-G

Epi: Epidermis, Der: Dermis. Scale bars represent 10μm.

A

Gene Name		Phenotype
FgfRIIIb	tm	Delay HF morphogenesis
Noggin	tm*	Delay HF morphogenesis, reduced HF number
Lef1	tm*	Arrested HF development
NrtKc	tm*	Delay HF morphogenesis
NT3	tm*	Delay HF morphogenesis
Noggin	K14 tg	Thickened epidermis, Increased hair density
Tgfb2	tm*	Delay HF morphogenesis, reduced HF number
Dkk1	K14 tg	Lack Hair Follicles

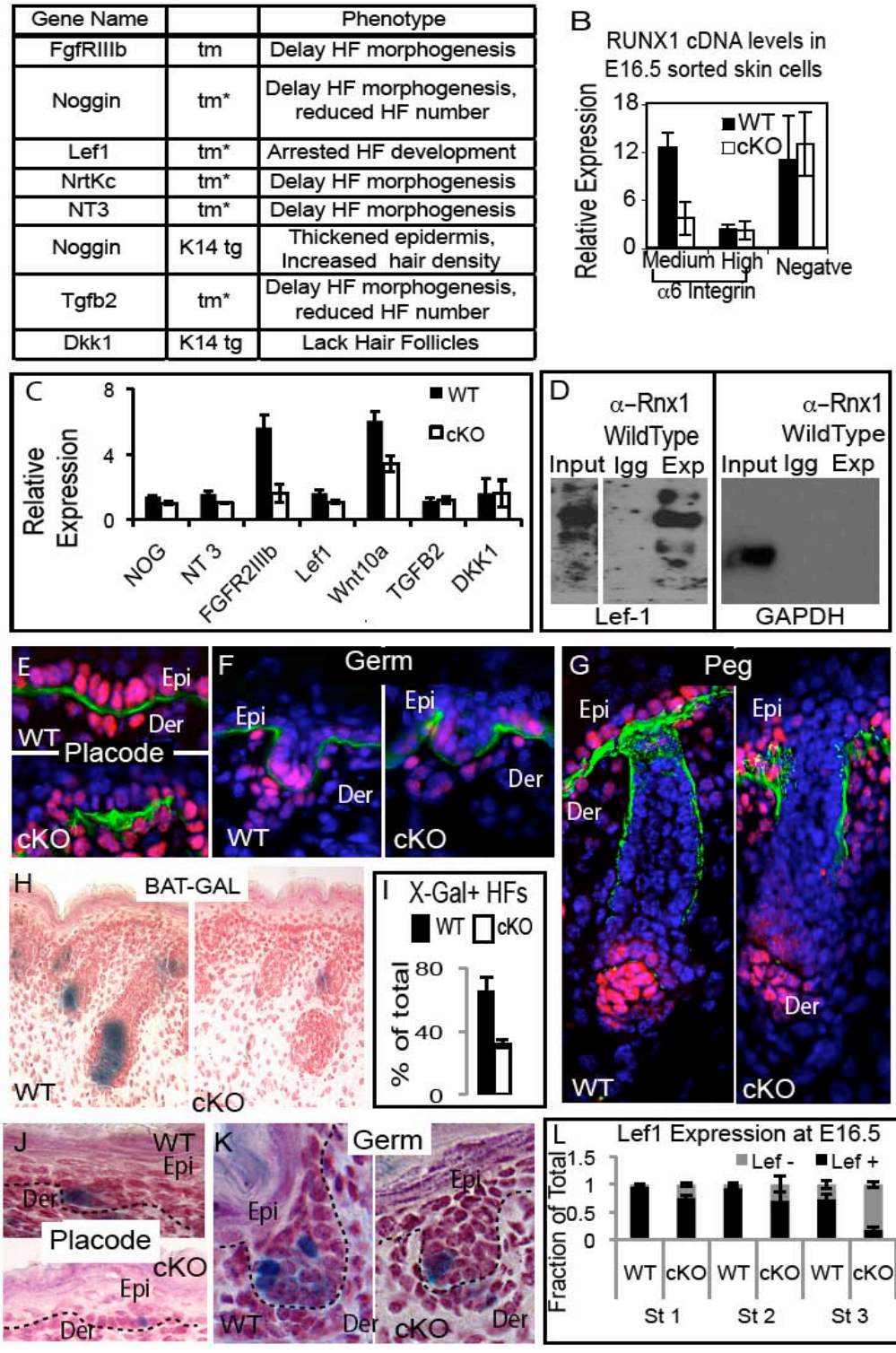

Finally, I began to uncover the mechanism of Runx1 action in the skin by: (a) identifying an in vivo interaction of Runx1 with Wnt signaling, a known positive regulator of HF morphogenesis(Andl et al., 2002); (b) implicating Runx1 in HF cell proliferation, keratinocyte cell adhesion, and cell migration.

Two populations of Runx1+ HF progenitors marking the adult HFSC embryonic precursors, and the precursors of the "primitive" hair

Previous genetic labeling via constitutive Sox9-Cre showed that exclusive marking of ORS cells in bulk did not result in progeny cell contribution to the matrix (M) and inner layers (IL), the differentiated lineages of the HF, by PD7 (Nowak et al., 2008). Second, genetic marking of single cells/HF in postnatal morphogenesis followed by lineage tracing showed exclusive labeling of either ORS M/IL cells(Legue and Nicolas, 2005) , supporting the notion that the ORS and M/IL are divergent lineages that remain independent of each other at least at discrete stages of morphogenesis. In this context, our data in which I detect a large fraction of HFs labeled in early embryonic morphogenesis presenting either ORS or M/IL labeling but not both by PD0, suggested that Runx1 was expressed in the early embryonic epithelial hair rudiments in the distinct progenitors of these lineages. The upper HF region expressing Sox9, which contains the ORS precursors (Nowak et al., 2008), also contained the high Runx1 expressing cells. Therefore it seems likely that the high Runx1 expressing cells were the precursors of ORS, leaving the low Runx1 expressing cells as the likely candidates for M/IL precursors (Figure 3.13). The presence of complex labeling patterns at PD0 and PD5 was likely due to multiple labeling events/early HF in precursors of each of the two

subpopulations, although I cannot rule out that a common Runx1+ ancestor for the two diverging progenitor populations also existed in the hair placode.

In the study by Legue et al (Legue and Nicolas, 2005), the matrix cells self-renewed and generated the IL temporarily, but failed to self-renew for the entire length of anagen and some of these progenitors were eventually lost from the skin before the end of morphogenesis(Legue and Nicolas, 2005). This loss of M/IL during postnatal morphogenesis might explain the apparent decrease in the M/IL pattern frequency from PD0 to PD5, when I marked HF cells via Runx1-CreER in early embryonic morphogenesis (Figure 3.4E). However, in our data it was unclear if all the newly made ILs at PD0 were generated from matrix cells, or were directly made from very short-lived Runx1+ progenitors that existed in the early hair rudiments. Our genetic marking of late embryonic Runx1+ HF cells (peg/bulbous peg), seem to suggest an expansion of progenitors that make the M/IL by late embryonic morphogenesis. This would be expected from the progression of HFs towards more advanced stages that culminate with production of differentiated cells. In addition, these late Runx1+ embryonic progenitors proved to have a lower survival rate than the early Runx1+ progenitors, as shown by the drop in total HF X-Gal labeling by late postnatal morphogenesis and in adulthood (Figure 3.5D). This suggested that most of the late embryonic Runx1+ progenitors were destined to contribute exclusively to hair morphogenesis (Figure 3.13 and 3.1A), resembling the "primitive" progenitors described for hematopoiesis. In contrast, the early embryonic morphogenesis HF cells survived through adulthood to contribute progeny to adult hair homeostasis and to long-lived HFSCs. In turn, this suggested that most of the early

embryonic Runx1+ progenitors were precursors of the adult HFSCs, resembling the so-called "definitive" progenitors described in hematopoiesis, which produce the adult HSCs (Dzierzak and Speck, 2008; Mikkola and Orkin, 2006).

Previous work suggested that Sox9-Cre marked ORS cells begin to contribute to M/IL after~PD7, to add progeny cells to late postnatal HF morphogenesis to postnatal morphogenesis (Nowak et al., 2008). Therefore it is possible that in later morphogenesis the Runx1+ ORS cells might also begin to contribute to M/IL. In our lineage tracing, we could still detect all types of labeling patterns at PD13, including the ORS and bulge exclusive pattern (Figure 3.3E). This might indicate that a fraction of ORS cells may remain un-utilized during morphogenesis and are kept tucked away in the upper ORS/bulge for later use in adult homeostasis. However, because of continuous loss of all marked HF labeling pattern, and substantial presence of complex patterns, I could not draw firm conclusions with respect to a potential flow of cells from the ORS into the M/IL during morphogenesis. Addressing whether "primitive" and "definitive" embryonic HF progenitors are completely independent lineages, as seen for blood and muscle (Dzierzak and Speck, 2008; Lepper et al., 2009; Messina and Cossu, 2009; Wang and Conboy, 2009), awaits inducible single cell lineage tracing of embryonic HF cells using markers that are specific to either ORS or matrix precursors. The earliest timing when HFSCs were proposed to be specified was ~E18.5, when HFs were already well formed and began to differentiate (Nowak et al., 2008) .This timing of HFSCs specification was determined by the identification of a 1st generation of slow cycling cells using an H2B-GFP pulse-chase system (Tumbar et al., 2004), in a group of cells

that are already committed to form the ORS compartment and the bulge (Nowak et al., 2008). Our data establishes the existence of a population of Runx1+ HFSCs precursors largely committed for ORS and adult homeostasis generation much prior to the E18.5 time point, at the earliest stages of hair morphogenesis in the hair placode.

Runx1 is important for the timely emergence of HFSCs precursors and of "primitive" HF progenitors

Our epithelial cKO deleted Runx1 in both subpopulations of Runx1 expressing cells in the early hair rudiments. While previously it was clear that adult HFSCs were formed in the absence of Runx1(Osorio et al., 2008) ,it was unclear if their emergence was affected in more subtle ways by Runx1 loss. In addition, it remained unclear if any effects of Runx1 loss were apparent in the embryonic hair morphogenesis. Here I showed that Runx1 loss caused a delay in placode induction therefore affecting both populations of Runx1+ progenitors, including the adult HFSC precursors as well as the "primitive" progenitors. This delay in HF emergence was efficiently overcome after birth. The "primitive" progenitors were able to produce fully differentiated hairs in late morphogenesis in the absence of Runx1. Moreover, the adult HFSCs seem to also form relatively normally by the time of 1st adult hair cycle. Although the HFSCs activation and 1st telogen-anagen transition were delayed as well by the Runx1 loss (Osorio et al., 2008),this delay was due to a direct effect of Runx1 in adulthood, and was not a consequence of developmental defects in HFSC emergence. This was demonstrated by acute deletion of Runx1 during adulthood, which recapitulated the phenotype of the constitutive epithelial KO (Hoi et al, submitted).

Figure 3.13: Model depicting the fate of embryonic epithelial Runx1 expressing cells during postanatal hair development. Genetic labeling of Runx1 expressing cells is consistent with the notion of the existence of two distinct populations existing at the early stages of hair follicle development. The primitive population will contribute to the formation of the hair during embryonic morphogenesis and will be lost from the skin postnatally. The definitive Runx1 expressing population will expand and remain undifferentiated in the ORS/Bu compartment and will contribute to the hair regeneration in the adult hair cycle.

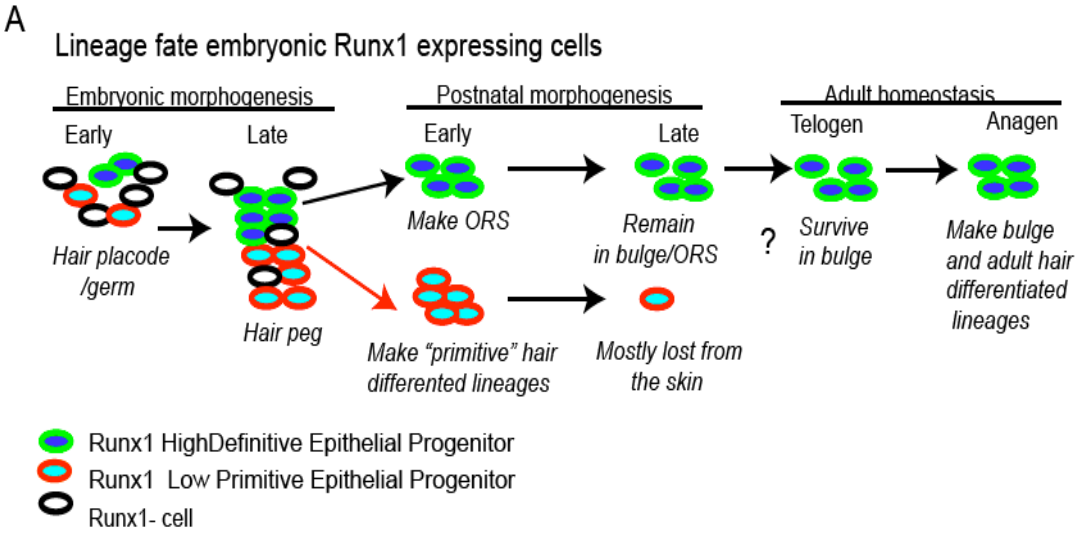
A
Lineage fate embryonic Runx1 expressing cells
Embryonic morphogenesis
Postnatal morphogenesis
Adult homeostasis
Early
Late
Early
Late
Telogen
Anagen
Hair placode /germ
Hair peg
Make ORS
Remain in bulge/ORS
?
Survive in bulge
Make bulge and adult hair differentiated lineages
Make "primitive" hair differented lineages
Mostly lost from the skin
Runx1 HighDefinitive Epithelial Progenitor
Runx1 Low Primitive Epithelial Progenitor
Runx1- cell

Mechanism of Runx1 action in HF inductive processes

The similarities in the mechanisms that control hair morphogenesis and stem cell activation during the telogen to anagen transition in adulthood (Schneider et al., 2009), appear to be also illustrated by the action of Runx1 (Osorio et al., 2008), Hoi, submitted). The telogen to anagen transition is a stage that resembles the induction and down-growth phase of hair morphogenesis in that adult stem cells migrate out from the bulge, proliferate, acquired a progenitor like state, and differentiate (Osorio et al., 2008; Zhang et al., 2009). The finding that in vitro Runx1 controls cell migration (this work) and proliferation via direct cell cycle control (Hoi et al, submitted) might explain in part why these two HF stages both characterized by down-growth and proliferation were affected by the loss of Runx1. In both cases the tissue eventually overcomes these defects (this study, Hoi et al) suggesting that other factors, such as Stat3, which showed a similar adult skin phenotype (Sano et al., 1999; Sano et al., 2000) could compensate for the loss of Runx1. A potential candidate for compensation during morphogenesis is Runx2, also expressed in the hair follicle and dermal sheath during morphogenesis (Glotzer et al., 2008). Although Runx2 is not as broadly expressed as Runx1, its ablation in the mesenchymal and epithelial compartment also delayed hair morphogenesis (Glotzer et al., 2008).

Another mechanism that might unite Runx1 action in HF morphogenesis and HF cycle is its interaction with the Wnt signaling pathway (this work). Wnt signaling regulates a variety of cellular and developmental processes in the skin including hair follicle induction, cell fate acquisition and activation of stem/progenitor cells (DasGupta et al., 2002; Gat et al., 1998; Merrill et al.,

2001; Van Mater et al., 2003). Here I showed that Runx1 promotes canonical Wnt signaling during embryogenesis and in both embryonic and adult skin Lef1 and Runx1 can be found on the same protein complexes. This is not surprising since both Runx1 and Lef1 have common interacting factors(Howcroft et al., 2005) . While down-regulating Wnt signaling in the skin is likely an important cause of HF induction delay, rescue experiments in which Wnt signaling is restored in the Runx1 cKO skin will be required in the future to firmly demonstrate the extent of Wnt contribution to the Runx1 cKO phenotype.

An intriguing finding was the apparent paracrine effect that loss of Runx1 in the epithelium had on Wnt signaling in the mesenchyme, in which both Lef1 and Bat-Gal reporter signal appeared diffuse/low. This occurred in HFs at all the developmental stages analyzed and underscores the role that Runx1 plays in the epithelial-mesenchymal interactions. Given the important role the mesenchyme plays in the induction of both HF morphogenesis (Schmidt-Ullrich and Paus, 2005)and HF cycling (Plikus et al., 2008), it is perhaps not surprising that Runx1 appears to control these inductive processes in the skin.

In conclusion, I uncovered Runx1 as an early embryonic factor expressed in the precursors of adult HFSCs, as well as in early temporary progenitors of HF morphogenesis. Moreover, Runx1 was important for the timely emergence of all HF progenitor populations, including the embryonic precursors of adult HFSCs. However, Runx1 embryonic expression in epithelial skin cells appeared dispensable for their subsequent function in postnatal life.

CHAPTER 4

CONCLUSION AND FUTURE DIRECTIONS

Adult tissue stem cells are the unique cells in the body that retain the ability to self renew and differentiate for the entire life of the organism. Malfunction of these cells leads to aging of the tissue and in some instances can lead to disease such as cancer. It is thus imperative to understand the factors that intrinsically and extrinsically regulate stem cells behavior *in vivo* and *in vitro*. This will enable to develop inexpensive tools that will allow to manipulate and to maintain adult stem cells *in vitro* such that stem cell therapy could be an accessible treatment to cure diseases like heart failure, diabetes, cancer and schizophrenia. In addition understanding the factors that affect stem cell behavior during development, adulthood and injury will allow developing drugs that will target specifically this type of cells without compromising the homeostasis on the rest of the organism.

In this dissertation I described the expression (Figure 4.1) and function (Figure 4.2) of the transcription factor Runx1 in the skin during embryonic morphogenesis and adult hair cycle regeneration. I found that Runx1 is expressed in the skin epithelia prior hair morphogenesis and since then its expression in the hair follicle is maintained throughout life. Lineage tracing analyses of the Runx1 expressing cells during the initial stages of hair development allowed discovering that the specification of adult hair follicle stem cells (HFSC) is an event that occurs during the early stages of hair morphogenesis. This finding opens a new area of investigation in which questions regarding the behavior HFSCs during embryogenesis can now be

ask. Understanding the molecular signature of embryonic HFSCs, the similarities and differences between the embryonic and adult hair follicle stem cells together with understanding the factors that affect their functionality *in vivo* and *in vitro* will not only shed light into understanding the basic behavior of stem cells but will allow determining the defects in a cancer stem cell. Addressing these questions will involve the identification of surface markers to isolate and analyze at the transcriptional level the molecular signature of embryonic HFSCs. Cross comparisons of the embryonic HFSCs microarray data with other expression data at other timepoints will allow to understand the process of stem cell maturation that occurs in any given tissue. In addition these data could also be use to identify genes that are differentially regulated in basal cell carcinoma, a type of cancer that originate from the basal layer and ORS cells. Finally genetic studies were ablating or overexpressing the function of genes during development and adulthood will help to elucidate the factors that are critical for stem cell behavior in either the embryo, the adult, or both. Answering these questions will provide molecular understanding about the basics in HFSC development and disease and will also reveal some clues about why the regeneration capacity of a tissue declines with age.

Figure 4.1: Expression of Runx1 in the skin. Scheme summarizing the expression of Runx1 throughout different developmental stages of hair follicle morphogenesis and adult hair cycle.

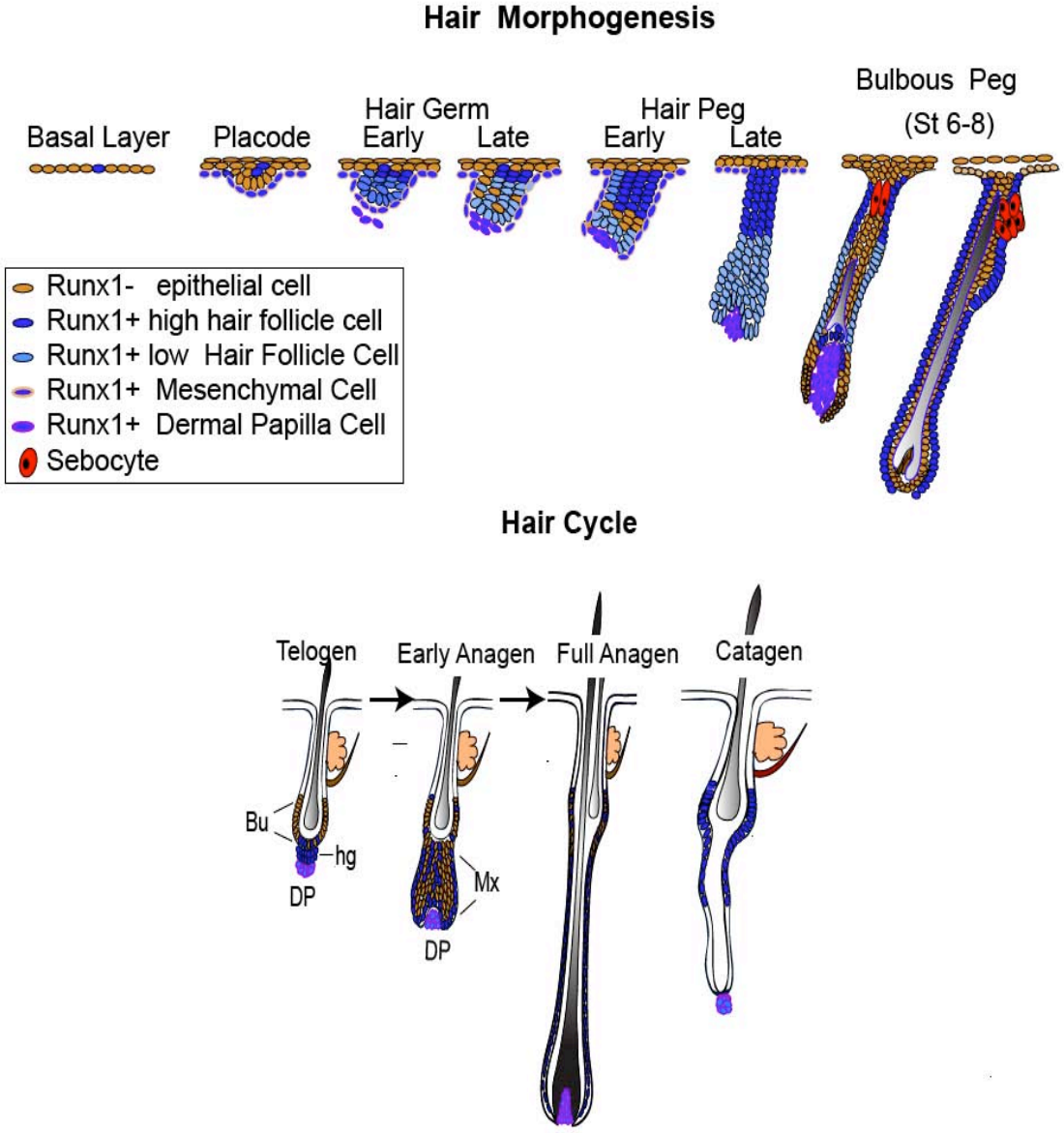
Hair Morphogenesis
Basal Layer
Placode
Hair Germ
Early
Late
Hair Peg
Early
Late
Bulbous Peg
(St 6-8)
Runx1- epithelial cell
Runx1+ high hair follicle cell
Runx1+ low Hair Follicle Cell
Runx1+ Mesenchymal Cell
Runx1+ Dermal Papilla Cell
Sebocyte
Hair Cycle
Telogen
Early Anagen
Full Anagen
Catagen
Bu
hg
DP
Mx
DP

In vitro Runx1 regulated the clonogenic activity and migration of skin keratinocytes. Still we need to understand why the clonogenic potential is affected. One possible explanation is that Runx1 directly regulates the expression of cell cycle genes and its absence results in a proliferation defect. Expression analysis in cells that have been in culture for a short period of time together with cell cycle analysis will allow determining whether Runx1 impairs a particular phase of the cell cycle and find genes that are affected by its absence. However another possible explanation for the clonogenic defect is that the culturing conditions are not suitable for the growth of these mutant cells. Addressing these questions will require changing the temperature and the CO2 content and ask whether Runx1 mutant cells can growth under these new culture conditions. In addition I described that, *in vitro,* Runx1 mutant keratinocytes are slow migrating in a collagen matrix. These results suggested that the integrin communication is altered. Whether this slow migratory response is only in a collagen matrix is unknown. Repeating the wound closure assays in other ECM factors will address this question. Moreover it would be interesting to know why Runx1 mutant keratinocytes are slow migrating *in vitro*. Migration is a multistep process that requires cell polarization, protrusion and adhesion formation and rear retraction (Ridley et al., 2003). All these steps are regulated by different factors and can be morphologically distinguished. Determining specifically which step in the migration process is affected will provide more information about the role of this gene in migration. This could be achieved by doing microscopy experiments to determine how does the shape of the cell and its movement differ in Runx1 mutant keratinocytes when compared to WTs. In addition determining whether one of the small GTPases is affected by the loss of Runx1

will allow determining which step of the migration process requires Runx1.

In vivo impairment of Runx1 delayed embryonic hair morphogenesis (Chapter 3) while during the adulthood it delayed the follicle entrance into a new hair cycle (Chapter 2). These two stages affected by Runx1 are similar in that both need to activate the processes of hair induction, downgrowth, and differentiation to form a mature hair follicle. During morphogenesis we documented that Runx1 regulated the induction and downgrowth processes without compromising lineage fate specification. Similarly during adulthood induction and downgrowth were affected by the loss of Runx1 but not lineage fate specification. It is possible that part of these *in vivo* defects observed in Runx1 cKO skin at these two stages resulted from an intrinsic defect in cell adhesion and migration. Studying the downstream targets of Runx1 *in vivo* and look whether some of the integrin signaling activators or downstream effectors are affected by the lack Runx1 will allow elucidating in more detail Runx1 function in adhesion and migration. Similarly, as previously suggested Runx1 can modulate the downgrowth process by directly regulating the expression the small GTPases or indirectly regulating their activity. Expression analysis together with Rac/CD42 and Rho activity assays will allow delineating the role of Runx1 in cell migration, *in vivo*.

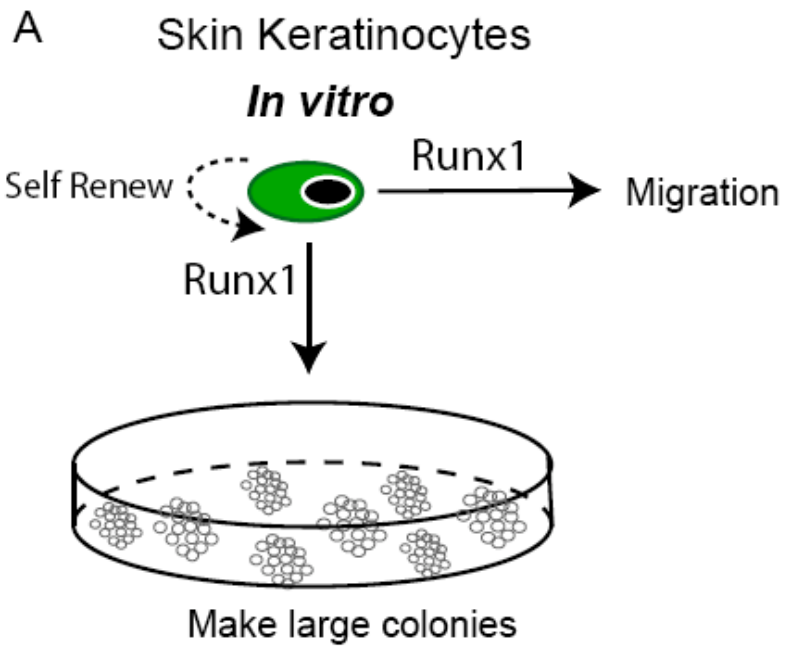

Figure 4.2: Model depicting the role of Runx1 *in vitro*. Analysis of Runx1 mutant cells show severe defects in colony forming ability which suggests and intrinsic defect in proliferation. In addition in vitro Runx1 mutant cells spread more in a collagen matrix and migrate less implicating Runx1 in cell migration.

During hair development I showed that Runx1 modulated the Wnt signaling pathway. However, it is still unknown how did Runx1 regulate the Wnt signaling. In the expression analysis of E16.5 epithelial cells we found Wnt10a to be downregulated in the absence of Runx1. This gene is highly expressed during hair development (Andl et al., 2002) yet its function hasn't been elucidated. It is possible that Runx1 directly represses or activates the transcription of several Wnt factors. Microarray array analysis together with chromatin immunoprecipation studies would allow answering this question. Yet Runx1 and Lef1 interaction at the protein level indicate that Runx1 can modulate Wnt signaling activity by enhancing transcription of Lef1/Runx1 downstream targets. In other cellular contexts it has been shown that Runx1 enhances Lef1 transcriptional activity and this function is further enhanced by the interaction with its common co-activator chaperone protein ALY (Howcroft et al., 2005). It is possible that similarly in the skin Runx1 acts with Lef1 to enhance transcription of downstream target genes. *In vitro* luciferase reporter assays could be a good tool to determine if Runx1 enhances transcription of Wnt targets genes.

Figure 4.3: Model depicting the role of Runx1 *in vivo*. Analysis of a conditional epithelial Runx1 knock out mouse line reveal its importance during hair morphogenesis and adult hair cycle. During hair morphogenesis lack or Runx1 delay the induction process, impaired downgrowth and mildly impaired proliferation but did not terminal differentiation. In an analogous stage, the telogen to anagen transition, lack of Runx1 delay stem cell activation that resulted in a hair cycle defect. These results taken together implicate Runx1 as a key regulator of the inductive processes during hair morphogenesis and homeostasis.

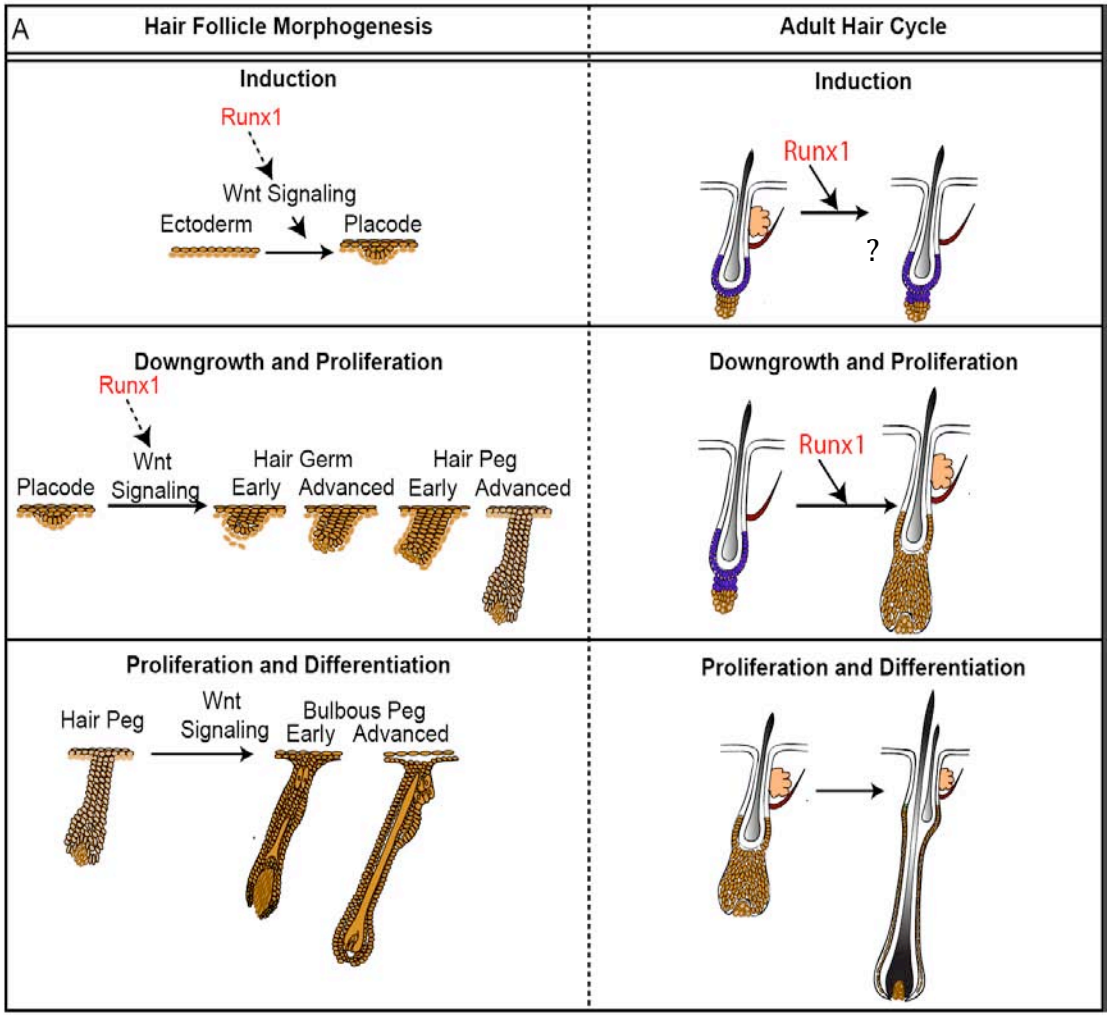
A
Hair Follicle Morphogenesis
Adult Hair Cycle
Induction
Runx1
Wnt Signaling
Ectoderm
Placode
Induction
Runx1
?
Downgrowth and Proliferation
Runx1
Wnt
Signaling
Placode
Hair Germ
Early
Advanced
Hair Peg
Early
Advanced
Downgrowth and Proliferation
Runx1
Proliferation and Differentiation
Hair Peg
Wnt
Signaling
Bulbous Peg
Early
Advanced
Proliferation and Differentiation

Another important discovery documented in this dissertation was defining the function of Runx1 in the HFSCs. Runx1 during embryogenesis was expressed in a subset of cells that eventually gave rise to the adult stem cell compartment. Moreover its role in stem cell behavior was first observed during adulthood at the telogen to anagen when the follicles failed to enter a new hair cycle due to a delay in adult HFSCs activation. However any type of injury reversed this phenotype. It has been proposed that a threshold in some "activator molecules" needs to be reached in order for the follicle to enter a new hair cycle. It is possible that Runx1 transcriptional activity is necessary to reach that threshold and in its absence reaching that threshold takes longer. Analyzing expression profiles of WT bulge cells at the telogen to anagen transition and comparing them to expression profiles of Runx1 KO bulge cells analyzed at different timepoints after the phenotype onset (example PD21, PD25, PD35 and PD40) will reveal genes that gradually accumulated in Runx1 KO bulges prior entering a new hair cycle. This analysis will provide insights into understanding the dynamic of HFSCs activation.

Besides its role as a stem cell activator in the epithelial compartment, the analysis of mosaic epithelial mesenhymal Cre Recombinase mouse strains allow me to determine that Runx1 can also regulate stem cell behavior indirectly by functioning in the dermal cells. In this phenotypic analysis I found that ablation of Runx1 in mesenchymal cells during embryogenesis but not adulthood impaired the normal function of HFSCs. Instead of regenerating a new hair follicle these cells either acquire sebocyte lineage or produce follicles with multiple shafts. Runx1 role in the dermal compartment needs to be further corroborated. Phenotypic analysis of mesenchymal Runx1

cKO mice (using a Cre Recombinase only expressed in mesenhymal compartment) will help dissect the role of Runx1 in this compartment.

In summary in this dissertation by using a combination of cell biology techniques together with the analysis of a combination of conditional and inducible KO mouse strains I defined the role of Runx1 during hair development and regeneration onset. Further studies will provide insight into how Runx1 affects these two developmental time points.

REFERENCES

Alison, M.R., and Islam, S. (2009). Attributes of adult stem cells. J Pathol *217*, 144-160.

Alonso, L., and Fuchs, E. (2003). Stem cells of the skin epithelium. Proc Natl Acad Sci U S A *100 Suppl 1*, 11830-11835.

Alonso, L., and Fuchs, E. (2006). The hair cycle. J Cell Sci *119*, 391-393.

Alvarez-Buylla, A., Kohwi, M., Nguyen, T.M., and Merkle, F.T. (2008). The heterogeneity of adult neural stem cells and the emerging complexity of their niche. Cold Spring Harb Symp Quant Biol *73*, 357-365.

Andl, T., Reddy, S.T., Gaddapara, T., and Millar, S.E. (2002). WNT signals are required for the initiation of hair follicle development. Dev Cell *2*, 643-653.

Appleford, P.J., and Woollard, A. (2009). RUNX genes find a niche in stem cell biology. J Cell Biochem *108*, 14-21.

Arnold, I., and Watt, F.M. (2001). c-Myc activation in transgenic mouse epidermis results in mobilization of stem cells and differentiation of their progeny. Curr Biol *11*, 558-568.

Bangsow, C., Rubins, N., Glusman, G., Bernstein, Y., Negreanu, V., Goldenberg, D., Lotem, J., Ben-Asher, E., Lancet, D., Levanon, D., *et al.* (2001). The RUNX3 gene--sequence, structure and regulated expression. Gene *279*, 221-232.

Barker, N., van Es, J.H., Kuipers, J., Kujala, P., van den Born, M., Cozijnsen, M., Haegebarth, A., Korving, J., Begthel, H., Peters, P.J., *et al.* (2007). Identification of stem cells in small intestine and colon by marker gene Lgr5. Nature *449*, 1003-1007.

Barrandon, A.R.a.Y. (2004). Regeneration of Epidermins from Adult Keratinocyte Stem cells. In Handbook of Stem Cells, R. Lanza, ed. (Elsevier, Inc.), pp. 763-772.

Barrandon, Y., and Green, H. (1987). Three clonal types of keratinocyte with different capacities for multiplication. Proc Natl Acad Sci U S A *84*, 2302-2306.

Benitah, S.A., Frye, M., Glogauer, M., and Watt, F.M. (2005). Stem cell depletion through epidermal deletion of Rac1. Science *309*, 933-935.

Blanpain, C., and Fuchs, E. (2006). Epidermal stem cells of the skin. Annu Rev Cell Dev Biol *22*, 339-373.

Blanpain, C., and Fuchs, E. (2007). p63: revving up epithelial stem-cell potential. Nat Cell Biol *9*, 731-733.

Blanpain, C., and Fuchs, E. (2009). Epidermal homeostasis: a balancing act of stem cells in the skin. Nat Rev Mol Cell Biol *10*, 207-217.

Blanpain, C., Lowry, W.E., Geoghegan, A., Polak, L., and Fuchs, E. (2004). Self-renewal, multipotency, and the existence of two cell populations within an epithelial stem cell niche. Cell *118*, 635-648.

Blanpain, C., Lowry, W.E., Pasolli, H.A., and Fuchs, E. (2006). Canonical notch signaling functions as a commitment switch in the epidermal lineage. Genes Dev *20*, 3022-3035.

Blau, H.M., Brazelton, T.R., and Weimann, J.M. (2001). The evolving concept of a stem cell: entity or function? Cell *105*, 829-841.

Blyth, K., Cameron, E.R., and Neil, J.C. (2005). The RUNX genes: gain or loss of function in cancer. Nat Rev Cancer *5*, 376-387.

Botchkarev, V.A. (2003). Bone morphogenetic proteins and their antagonists in skin and hair follicle biology. J Invest Dermatol *120*, 36-47.

Botchkarev, V.A., Botchkareva, N.V., Albers, K.M., Chen, L.H., Welker, P., and Paus, R. (2000a). A role for p75 neurotrophin receptor in the control of apoptosis-driven hair follicle regression. FASEB J *14*, 1931-1942.

Botchkarev, V.A., Botchkareva, N.V., Nakamura, M., Huber, O., Funa, K., Lauster, R., Paus, R., and Gilchrest, B.A. (2001a). Noggin is required for induction of the hair follicle growth phase in postnatal skin. FASEB J *15*, 2205-2214.

Botchkarev, V.A., Botchkareva, N.V., Roth, W., Nakamura, M., Chen, L.H., Herzog, W., Lindner, G., McMahon, J.A., Peters, C., Lauster, R.*, et al.* (1999a). Noggin is a mesenchymally derived stimulator of hair-follicle induction. Nat Cell Biol *1*, 158-164.

Botchkarev, V.A., Botchkareva, N.V., Sharov, A.A., Funa, K., Huber, O., and Gilchrest, B.A. (2002). Modulation of BMP signaling by noggin is required for induction of the secondary (nontylotrich) hair follicles. J Invest Dermatol *118*, 3-10.

Botchkarev, V.A., Botchkareva, N.V., Slominski, A., Roloff, B., Luger, T., and Paus, R. (1999b). Developmentally regulated expression of alpha-MSH and MC-1 receptor in C57BL/6 mouse skin suggests functions beyond pigmentation. Ann N Y Acad Sci *885*, 433-439.

Botchkarev, V.A., Botchkareva, N.V., Welker, P., Metz, M., Lewin, G.R., Subramaniam, A., Bulfone-Paus, S., Hagen, E., Braun, A., Lommatzsch, M., *et al.* (1999c). A new role for neurotrophins: involvement of brain-derived neurotrophic factor and neurotrophin-4 in hair cycle control. FASEB J *13*, 395-410.

Botchkarev, V.A., Kief, S., Paus, R., and Moll, I. (1999d). Overexpression of brain-derived neurotrophic factor increases Merkel cell number in murine skin. J Invest Dermatol *113*, 691-692.

Botchkarev, V.A., and Kishimoto, J. (2003). Molecular control of epithelial-mesenchymal interactions during hair follicle cycling. J Investig Dermatol Symp Proc *8*, 46-55.

Botchkarev, V.A., Komarova, E.A., Siebenhaar, F., Botchkareva, N.V., Komarov, P.G., Maurer, M., Gilchrest, B.A., and Gudkov, A.V. (2000b). p53 is essential for chemotherapy-induced hair loss. Cancer Res *60*, 5002-5006.

Botchkarev, V.A., Komarova, E.A., Siebenhaar, F., Botchkareva, N.V., Sharov, A.A., Komarov, P.G., Maurer, M., Gudkov, A.V., and Gilchrest, B.A. (2001b). p53 Involvement in the control of murine hair follicle regression. Am J Pathol *158*, 1913-1919.

Botchkarev, V.A., Metz, M., Botchkareva, N.V., Welker, P., Lommatzsch, M., Renz, H., and Paus, R. (1999e). Brain-derived neurotrophic factor, neurotrophin-3, and neurotrophin-4 act as "epitheliotrophins" in murine skin. Lab Invest *79*, 557-572.

Botchkarev, V.A., and Paus, R. (2003). Molecular biology of hair morphogenesis: development and cycling. J Exp Zool B Mol Dev Evol *298*, 164-180.

Botchkarev, V.A., Peters, E.M., Botchkareva, N.V., Maurer, M., and Paus, R. (1999f). Hair cycle-dependent changes in adrenergic skin innervation, and hair growth modulation by adrenergic drugs. J Invest Dermatol *113*, 878-887.

Botchkarev, V.A., and Sharov, A.A. (2004). BMP signaling in the control of skin development and hair follicle growth. Differentiation *72*, 512-526.

Botchkareva, N.V., Botchkarev, V.A., Albers, K.M., Metz, M., and Paus, R. (2000). Distinct roles for nerve growth factor and brain-derived neurotrophic factor in controlling the rate of hair follicle morphogenesis. J Invest Dermatol *114*, 314-320.

Botchkareva, N.V., Botchkarev, V.A., Chen, L.H., Lindner, G., and Paus, R. (1999a). A role for p75 neurotrophin receptor in the control of hair follicle morphogenesis. Dev Biol *216*, 135-153.

Botchkareva, N.V., Botchkarev, V.A., Metz, M., Silos-Santiago, I., and Paus, R. (1999b). Retardation of hair follicle development by the deletion of TrkC, high-affinity neurotrophin-3 receptor. J Invest Dermatol *113*, 425-427.

Botchkareva, N.V., Khlgatian, M., Longley, B.J., Botchkarev, V.A., and Gilchrest, B.A. (2001). SCF/c-kit signaling is required for cyclic regeneration of the hair pigmentation unit. FASEB J *15*, 645-658.

Braun, K.M., and Prowse, D.M. (2006). Distinct epidermal stem cell compartments are maintained by independent niche microenvironments. Stem Cell Rev *2*, 221-231.

Buckingham, M., Bajard, L., Chang, T., Daubas, P., Hadchouel, J., Meilhac, S., Montarras, D., Rocancourt, D., and Relaix, F. (2003). The formation of skeletal muscle: from somite to limb. J Anat *202*, 59-68.

Cai, J., Weiss, M.L., and Rao, M.S. (2004). In search of "stemness". Exp Hematol *32*, 585-598.

Calvi, L.M., Adams, G.B., Weibrecht, K.W., Weber, J.M., Olson, D.P., Knight, M.C., Martin, R.P., Schipani, E., Divieti, P., Bringhurst, F.R., *et al.* (2003). Osteoblastic cells regulate the haematopoietic stem cell niche. Nature *425*, 841-846.

Chen, C.L., Broom, D.C., Liu, Y., de Nooij, J.C., Li, Z., Cen, C., Samad, O.A., Jessell, T.M., Woolf, C.J., and Ma, Q. (2006). Runx1 determines nociceptive sensory neuron phenotype and is required for thermal and neuropathic pain. Neuron *49*, 365-377.

Chen, M.J., Yokomizo, T., Zeigler, B.M., Dzierzak, E., and Speck, N.A. (2009). Runx1 is required for the endothelial to haematopoietic cell transition but not thereafter. Nature *457*, 887-891.

Claudinot, S., Nicolas, M., Oshima, H., Rochat, A., and Barrandon, Y. (2005). Long-term renewal of hair follicles from clonogenic multipotent stem cells. Proc Natl Acad Sci U S A *102*, 14677-14682.

Clayton, E., Doupe, D.P., Klein, A.M., Winton, D.J., Simons, B.D., and Jones, P.H. (2007). A single type of progenitor cell maintains normal epidermis. Nature *446*, 185-189.

Conover, J.C., and Notti, R.Q. (2008). The neural stem cell niche. Cell Tissue Res *331*, 211-224.

Cotsarelis, G. (2006). Epithelial stem cells: a folliculocentric view. J Invest Dermatol *126*, 1459-1468.

Cotsarelis, G., Sun, T.T., and Lavker, R.M. (1990). Label-retaining cells reside in the bulge area of pilosebaceous unit: implications for follicular stem cells, hair cycle, and skin carcinogenesis. Cell *61*, 1329-1337.

DasGupta, R., and Fuchs, E. (1999). Multiple roles for activated LEF/TCF transcription complexes during hair follicle development and differentiation. Development *126*, 4557-4568.

DasGupta, R., Rhee, H., and Fuchs, E. (2002). A developmental conundrum: a stabilized form of beta-catenin lacking the transcriptional activation domain triggers features of hair cell fate in epidermal cells and epidermal cell fate in hair follicle cells. J Cell Biol *158*, 331-344.

Diamond, I., Owolabi, T., Marco, M., Lam, C., and Glick, A. (2000). Conditional gene expression in the epidermis of transgenic mice using the tetracycline-regulated transactivators tTA and rTA linked to the keratin 5 promoter. J Invest Dermatol *115*, 788-794.

Doherty, J.M., Geske, M.J., Stappenbeck, T.S., and Mills, J.C. (2008). Diverse adult stem cells share specific higher-order patterns of gene expression. Stem Cells *26*, 2124-2130.

Duan, X., Kang, E., Liu, C.Y., Ming, G.L., and Song, H. (2008). Development of neural stem cell in the adult brain. Curr Opin Neurobiol *18*, 108-115.

Durst, K.L., and Hiebert, S.W. (2004). Role of RUNX family members in transcriptional repression and gene silencing. Oncogene *23*, 4220-4224.

Dzierzak, E., and Speck, N.A. (2008). Of lineage and legacy: the development of mammalian hematopoietic stem cells. Nat Immunol *9*, 129-136.

Evsikov, A.V., and Solter, D. (2003). Comment on " 'Stemness': transcriptional profiling of embryonic and adult stem cells" and "a stem cell molecular signature". Science *302*, 393; author reply 393.

Ezhkova, E., Pasolli, H.A., Parker, J.S., Stokes, N., Su, I.H., Hannon, G., Tarakhovsky, A., and Fuchs, E. (2009). Ezh2 orchestrates gene expression for the stepwise differentiation of tissue-specific stem cells. Cell *136*, 1122-1135.

Fortunel, N.O., Otu, H.H., Ng, H.H., Chen, J., Mu, X., Chevassut, T., Li, X., Joseph, M., Bailey, C., Hatzfeld, J.A., *et al.* (2003). Comment on " 'Stemness': transcriptional profiling of embryonic and adult stem cells" and "a stem cell molecular signature". Science *302*, 393; author reply 393.

Fuchs, E. (2007). Scratching the surface of skin development. Nature *445*, 834-842.

Fuchs, E. (2009). The tortoise and the hair: slow-cycling cells in the stem cell race. Cell *137*, 811-819.

Fuchs, E., and Horsley, V. (2008). More than one way to skin. Genes Dev *22*, 976-985.

Fuchs, E., and Nowak, J.A. (2008). Building epithelial tissues from skin stem cells. Cold Spring Harb Symp Quant Biol *73*, 333-350.

Fuchs, E., Tumbar, T., and Guasch, G. (2004). Socializing with the neighbors: stem cells and their niche. Cell *116*, 769-778.

Fujita, Y., Nishimura, M., Taniwaki, M., Abe, T., and Okuda, T. (2001). Identification of an alternatively spliced form of the mouse AML1/RUNX1 gene transcript AML1c and its expression in early hematopoietic development. Biochem Biophys Res Commun *281*, 1248-1255.

Gambardella, L., and Barrandon, Y. (2003). The multifaceted adult epidermal stem cell. Curr Opin Cell Biol *15*, 771-777.

Gandarillas, A., and Watt, F.M. (1997). c-Myc promotes differentiation of human epidermal stem cells. Genes Dev *11*, 2869-2882.

Gat, U., DasGupta, R., Degenstein, L., and Fuchs, E. (1998). De Novo hair follicle morphogenesis and hair tumors in mice expressing a truncated beta-catenin in skin. Cell *95*, 605-614.

Ghazizadeh, S., and Taichman, L.B. (2001). Multiple classes of stem cells in cutaneous epithelium: a lineage analysis of adult mouse skin. EMBO J *20*, 1215-1222.

Glotzer, D.J., Zelzer, E., and Olsen, B.R. (2008). Impaired skin and hair follicle development in Runx2 deficient mice. Dev Biol *315*, 459-473.

Growney, J.D., Shigematsu, H., Li, Z., Lee, B.H., Adelsperger, J., Rowan, R., Curley, D.P., Kutok, J.L., Akashi, K., Williams, I.R., *et al.* (2005). Loss of Runx1 perturbs adult hematopoiesis and is associated with a myeloproliferative phenotype. Blood *106*, 494-504.

Hayashi, S., and McMahon, A.P. (2002). Efficient recombination in diverse tissues by a tamoxifen-inducible form of Cre: a tool for temporally regulated gene activation/inactivation in the mouse. Dev Biol *244*, 305-318.

Hock, H., Hamblen, M.J., Rooke, H.M., Schindler, J.W., Saleque, S., Fujiwara, Y., and Orkin, S.H. (2004a). Gfi-1 restricts proliferation and preserves functional integrity of haematopoietic stem cells. Nature *431*, 1002-1007.

Hock, H., Meade, E., Medeiros, S., Schindler, J.W., Valk, P.J., Fujiwara, Y., and Orkin, S.H. (2004b). Tel/Etv6 is an essential and selective regulator of adult hematopoietic stem cell survival. Genes Dev *18*, 2336-2341.

Hoi, C., Lee, S.E., Lu, Shu., McDermitt, D.J., Osorio, K.M., Piskun, C., Peters, R., Paus, R., and Tumbar, T. Runx1 directly promotes proliferation of hair follicle stem cells and epithelial tumor formation in mouse skin. manuscript in submission.

Horsley, V., Aliprantis, A.O., Polak, L., Glimcher, L.H., and Fuchs, E. (2008). NFATc1 balances quiescence and proliferation of skin stem cells. Cell *132*, 299-310.

Horsley, V., O'Carroll, D., Tooze, R., Ohinata, Y., Saitou, M., Obukhanych, T., Nussenzweig, M., Tarakhovsky, A., and Fuchs, E. (2006). Blimp1 defines a progenitor population that governs cellular input to the sebaceous gland. Cell *126*, 597-609.

Howcroft, T.K., Weissman, J.D., Gegonne, A., and Singer, D.S. (2005). A T lymphocyte-specific transcription complex containing RUNX1 activates MHC class I expression. J Immunol *174*, 2106-2115.

Huelsken, J., Vogel, R., Erdmann, B., Cotsarelis, G., and Birchmeier, W. (2001). beta-Catenin controls hair follicle morphogenesis and stem cell differentiation in the skin. Cell *105*, 533-545.

Ichikawa, M., Asai, T., Chiba, S., Kurokawa, M., and Ogawa, S. (2004a). Runx1/AML-1 ranks as a master regulator of adult hematopoiesis. Cell Cycle *3*, 722-724.

Ichikawa, M., Asai, T., Saito, T., Seo, S., Yamazaki, I., Yamagata, T., Mitani, K., Chiba, S., Ogawa, S., Kurokawa, M., *et al.* (2004b). AML-1 is required for megakaryocytic maturation and lymphocytic differentiation, but not for maintenance of hematopoietic stem cells in adult hematopoiesis. Nat Med *10*, 299-304.

Inoue, K., Ozaki, S., Shiga, T., Ito, K., Masuda, T., Okado, N., Iseda, T., Kawaguchi, S., Ogawa, M., Bae, S.C., *et al.* (2002). Runx3 controls the axonal projection of proprioceptive dorsal root ganglion neurons. Nat Neurosci *5*, 946-954.

Ivanova, N.B., Dimos, J.T., Schaniel, C., Hackney, J.A., Moore, K.A., and Lemischka, I.R. (2002). A stem cell molecular signature. Science *298*, 601-604.

Jamora, C., DasGupta, R., Kocieniewski, P., and Fuchs, E. (2003). Links between signal transduction, transcription and adhesion in epithelial bud development. Nature *422*, 317-322.

Jensen, K.B., Collins, C.A., Nascimento, E., Tan, D.W., Frye, M., Itami, S., and Watt, F.M. (2009). Lrig1 expression defines a distinct multipotent stem cell population in mammalian epidermis. Cell Stem Cell *4*, 427-439.

Joyner, A.L., and Zervas, M. (2006). Genetic inducible fate mapping in mouse: establishing genetic lineages and defining genetic neuroanatomy in the nervous system. Dev Dyn *235*, 2376-2385.

Kaufman, C.K., Zhou, P., Pasolli, H.A., Rendl, M., Bolotin, D., Lim, K.C., Dai, X., Alegre, M.L., and Fuchs, E. (2003). GATA-3: an unexpected regulator of cell lineage determination in skin. Genes Dev *17*, 2108-2122.

Kim, I., Saunders, T.L., and Morrison, S.J. (2007). Sox17 dependence distinguishes the transcriptional regulation of fetal from adult hematopoietic stem cells. Cell *130*, 470-483.

Kobielak, K., Pasolli, H.A., Alonso, L., Polak, L., and Fuchs, E. (2003). Defining BMP functions in the hair follicle by conditional ablation of BMP receptor IA. J Cell Biol *163*, 609-623.

Kobielak, K., Stokes, N., de la Cruz, J., Polak, L., and Fuchs, E. (2007). Loss of a quiescent niche but not follicle stem cells in the absence of bone morphogenetic protein signaling. Proc Natl Acad Sci U S A *104*, 10063-10068.

Komori, T., Yagi, H., Nomura, S., Yamaguchi, A., Sasaki, K., Deguchi, K., Shimizu, Y., Bronson, R.T., Gao, Y.H., Inada, M., *et al.* (1997). Targeted disruption of Cbfa1 results in a complete lack of bone formation owing to maturational arrest of osteoblasts. Cell *89*, 755-764.

Koster, M.I., Dai, D., Marinari, B., Sano, Y., Costanzo, A., Karin, M., and Roop, D.R. (2007a). p63 induces key target genes required for epidermal morphogenesis. Proc Natl Acad Sci U S A *104*, 3255-3260.

Koster, M.I., Dai, D., and Roop, D.R. (2007b). Conflicting roles for p63 in skin development and carcinogenesis. Cell Cycle *6*, 269-273.

Koster, M.I., and Roop, D.R. (2007). Mechanisms regulating epithelial stratification. Annu Rev Cell Dev Biol *23*, 93-113.

Kriegstein, A., and Alvarez-Buylla, A. (2009). The glial nature of embryonic and adult neural stem cells. Annu Rev Neurosci *32*, 149-184.

Kuang, S., Gillespie, M.A., and Rudnicki, M.A. (2008). Niche regulation of muscle satellite cell self-renewal and differentiation. Cell Stem Cell *2*, 22-31.

Kulessa, H., Turk, G., and Hogan, B.L. (2000). Inhibition of Bmp signaling affects growth and differentiation in the anagen hair follicle. EMBO J *19*, 6664-6674.

Kurek, D., Garinis, G.A., van Doorninck, J.H., van der Wees, J., and Grosveld, F.G. (2007). Transcriptome and phenotypic analysis reveals Gata3-dependent signalling pathways in murine hair follicles. Development *134*, 261-272.

Laird, D.J., von Andrian, U.H., and Wagers, A.J. (2008). Stem cell trafficking in tissue development, growth, and disease. Cell *132*, 612-630.

Legue, E., and Nicolas, J.F. (2005). Hair follicle renewal: organization of stem cells in the matrix and the role of stereotyped lineages and behaviors. Development *132*, 4143-4154.

Lensch, M.W., Daheron, L., and Schlaeger, T.M. (2006). Pluripotent stem cells and their niches. Stem Cell Rev *2*, 185-201.

Lepper, C., Conway, S.J., and Fan, C.M. (2009). Adult satellite cells and embryonic muscle progenitors have distinct genetic requirements. Nature *460*, 627-631.

Levanon, D., Bettoun, D., Harris-Cerruti, C., Woolf, E., Negreanu, V., Eilam, R., Bernstein, Y., Goldenberg, D., Xiao, C., Fliegauf, M., *et al.* (2002). The Runx3 transcription factor regulates development and survival of TrkC dorsal root ganglia neurons. EMBO J *21*, 3454-3463.

Levanon, D., Brenner, O., Negreanu, V., Bettoun, D., Woolf, E., Eilam, R., Lotem, J., Gat, U., Otto, F., Speck, N., *et al.* (2001). Spatial and temporal expression pattern of Runx3 (Aml2) and Runx1 (Aml1) indicates non-redundant functions during mouse embryogenesis. Mech Dev *109*, 413-417.

Levanon, D., Goldstein, R.E., Bernstein, Y., Tang, H., Goldenberg, D., Stifani, S., Paroush, Z., and Groner, Y. (1998). Transcriptional repression by AML1

and LEF-1 is mediated by the TLE/Groucho corepressors. Proc Natl Acad Sci U S A *95*, 11590-11595.

Levy, V., Lindon, C., Harfe, B.D., and Morgan, B.A. (2005). Distinct stem cell populations regenerate the follicle and interfollicular epidermis. Dev Cell *9*, 855-861.

Li, L., and Xie, T. (2005). Stem cell niche: structure and function. Annu Rev Cell Dev Biol *21*, 605-631.

Li, Q.L., Ito, K., Sakakura, C., Fukamachi, H., Inoue, K., Chi, X.Z., Lee, K.Y., Nomura, S., Lee, C.W., Han, S.B., *et al.* (2002). Causal relationship between the loss of RUNX3 expression and gastric cancer. Cell *109*, 113-124.

Lowry, W.E., Blanpain, C., Nowak, J.A., Guasch, G., Lewis, L., and Fuchs, E. (2005). Defining the impact of beta-catenin/Tcf transactivation on epithelial stem cells. Genes Dev *19*, 1596-1611.

Magerl, M., Tobin, D.J., Muller-Rover, S., Hagen, E., Lindner, G., McKay, I.A., and Paus, R. (2001). Patterns of proliferation and apoptosis during murine hair follicle morphogenesis. J Invest Dermatol *116*, 947-955.

Maretto, S., Cordenonsi, M., Dupont, S., Braghetta, P., Broccoli, V., Hassan, A.B., Volpin, D., Bressan, G.M., and Piccolo, S. (2003). Mapping Wnt/beta-catenin signaling during mouse development and in colorectal tumors. Proc Natl Acad Sci U S A *100*, 3299-3304.

Merkle, F.T., and Alvarez-Buylla, A. (2006). Neural stem cells in mammalian development. Curr Opin Cell Biol *18*, 704-709.

Merrill, B.J., Gat, U., DasGupta, R., and Fuchs, E. (2001). Tcf3 and Lef1 regulate lineage differentiation of multipotent stem cells in skin. Genes Dev *15*, 1688-1705.

Messina, G., and Cossu, G. (2009). The origin of embryonic and fetal myoblasts: a role of Pax3 and Pax7. Genes Dev *23*, 902-905.

Mikhail, F.M., Sinha, K.K., Saunthararajah, Y., and Nucifora, G. (2006). Normal and transforming functions of RUNX1: a perspective. J Cell Physiol *207*, 582-593.

Mikkers, H., and Frisen, J. (2005). Deconstructing stemness. Embo J *24*, 2715-2719.

Mikkola, H.K., and Orkin, S.H. (2006). The journey of developing hematopoietic stem cells. Development *133*, 3733-3744.

Millar, S.E. (2002). Molecular mechanisms regulating hair follicle development. J Invest Dermatol *118*, 216-225.

Mills, A.A., Zheng, B., Wang, X.J., Vogel, H., Roop, D.R., and Bradley, A. (1999). p63 is a p53 homologue required for limb and epidermal morphogenesis. Nature *398*, 708-713.

Molofsky, A.V., Pardal, R., Iwashita, T., Park, I.K., Clarke, M.F., and Morrison, S.J. (2003). Bmi-1 dependence distinguishes neural stem cell self-renewal from progenitor proliferation. Nature *425*, 962-967.

Molofsky, A.V., Pardal, R., and Morrison, S.J. (2004). Diverse mechanisms regulate stem cell self-renewal. Curr Opin Cell Biol *16*, 700-707.

Moore, K.A., and Lemischka, I.R. (2006). Stem cells and their niches. Science *311*, 1880-1885.

Morris, R.J., Liu, Y., Marles, L., Yang, Z., Trempus, C., Li, S., Lin, J.S., Sawicki, J.A., and Cotsarelis, G. (2004). Capturing and profiling adult hair follicle stem cells. Nat Biotechnol *22*, 411-417.

Muller-Rover, S., Handjiski, B., van der Veen, C., Eichmuller, S., Foitzik, K., McKay, I.A., Stenn, K.S., and Paus, R. (2001). A comprehensive guide for the accurate classification of murine hair follicles in distinct hair cycle stages. J Invest Dermatol *117*, 3-15.

Muller-Rover, S., Tokura, Y., Welker, P., Furukawa, F., Wakita, H., Takigawa, M., and Paus, R. (1999). E- and P-cadherin expression during murine hair follicle morphogenesis and cycling. Exp Dermatol *8*, 237-246.

Nakamura, M., Sundberg, J.P., and Paus, R. (2001). Mutant laboratory mice with abnormalities in hair follicle morphogenesis, cycling, and/or structure: annotated tables. Exp Dermatol *10*, 369-390.

Nguyen, H., Rendl, M., and Fuchs, E. (2006). Tcf3 governs stem cell features and represses cell fate determination in skin. Cell *127*, 171-183.

North, T., Gu, T.L., Stacy, T., Wang, Q., Howard, L., Binder, M., Marin-Padilla, M., and Speck, N.A. (1999). Cbfa2 is required for the formation of intra-aortic hematopoietic clusters. Development *126*, 2563-2575.

North, T.E., de Bruijn, M.F., Stacy, T., Talebian, L., Lind, E., Robin, C., Binder, M., Dzierzak, E., and Speck, N.A. (2002). Runx1 expression marks long-term repopulating hematopoietic stem cells in the midgestation mouse embryo. Immunity *16*, 661-672.

Nowak, J.A., Polak, L., Pasolli, H.A., and Fuchs, E. (2008). Hair follicle stem cells are specified and function in early skin morphogenesis. Cell Stem Cell *3*, 33-43.

Okuda, T., van Deursen, J., Hiebert, S.W., Grosveld, G., and Downing, J.R. (1996). AML1, the target of multiple chromosomal translocations in human leukemia, is essential for normal fetal liver hematopoiesis. Cell *84*, 321-330.

Oshima, H., Rochat, A., Kedzia, C., Kobayashi, K., and Barrandon, Y. (2001). Morphogenesis and renewal of hair follicles from adult multipotent stem cells. Cell *104*, 233-245.

Osorio, K.M., Lee, S.E., McDermitt, D.J., Waghmare, S.K., Zhang, Y.V., Woo, H.N., and Tumbar, T. (2008). Runx1 modulates developmental, but not injury-driven, hair follicle stem cell activation. Development *135*, 1059-1068.

Otto, A., Collins-Hooper, H., and Patel, K. (2009). The origin, molecular regulation and therapeutic potential of myogenic stem cell populations. J Anat.

Otto, F., Lubbert, M., and Stock, M. (2003). Upstream and downstream targets of RUNX proteins. J Cell Biochem *89*, 9-18.

Pan, Y., Lin, M.H., Tian, X., Cheng, H.T., Gridley, T., Shen, J., and Kopan, R. (2004). gamma-secretase functions through Notch signaling to maintain skin appendages but is not required for their patterning or initial morphogenesis. Dev Cell *7*, 731-743.

Panteleyev, A.A., Jahoda, C.A., and Christiano, A.M. (2001). Hair follicle predetermination. J Cell Sci *114*, 3419-3431.

Park, I.K., Qian, D., Kiel, M., Becker, M.W., Pihalja, M., Weissman, I.L., Morrison, S.J., and Clarke, M.F. (2003). Bmi-1 is required for maintenance of adult self-renewing haematopoietic stem cells. Nature *423*, 302-305.

Paus, R., Muller-Rover, S., Van Der Veen, C., Maurer, M., Eichmuller, S., Ling, G., Hofmann, U., Foitzik, K., Mecklenburg, L., and Handjiski, B. (1999). A comprehensive guide for the recognition and classification of distinct stages of hair follicle morphogenesis. J Invest Dermatol *113*, 523-532.

Perez-Moreno, M., Jamora, C., and Fuchs, E. (2003). Sticky business: orchestrating cellular signals at adherens junctions. Cell *112*, 535-548.

Plikus, M.V., Mayer, J.A., de la Cruz, D., Baker, R.E., Maini, P.K., Maxson, R., and Chuong, C.M. (2008). Cyclic dermal BMP signalling regulates stem cell activation during hair regeneration. Nature *451*, 340-344.

Poblet, E., Jimenez, F., de Cabo, C., Prieto-Martin, A., and Sanchez-Prieto, R. (2005). The calcium-binding protein calretinin is a marker of the companion cell layer of the human hair follicle. Br J Dermatol *152*, 1316-1320.

Rachel, J.D., and Jamora, J.J. (2003). Skin rejuvenation regimens: a profilometry and histopathologic study. Arch Facial Plast Surg *5*, 145-149.

Ramalho-Santos, M., Yoon, S., Matsuzaki, Y., Mulligan, R.C., and Melton, D.A. (2002). "Stemness": transcriptional profiling of embryonic and adult stem cells. Science *298*, 597-600.

Raveh, E., Cohen, S., Levanon, D., Groner, Y., and Gat, U. (2005). Runx3 is involved in hair shape determination. Dev Dyn *233*, 1478-1487.

Raveh, E., Cohen, S., Levanon, D., Negreanu, V., Groner, Y., and Gat, U. (2006). Dynamic expression of Runx1 in skin affects hair structure. Mech Dev *123*, 842-850.

Rendl, M., Polak, L., and Fuchs, E. (2008). BMP signaling in dermal papilla cells is required for their hair follicle-inductive properties. Genes Dev *22*, 543-557.

Reya, T., and Clevers, H. (2005). Wnt signalling in stem cells and cancer. Nature *434*, 843-850.

Rhee, H., Polak, L., and Fuchs, E. (2006). Lhx2 maintains stem cell character in hair follicles. Science *312*, 1946-1949.

Ridley, A.J., Schwartz, M.A., Burridge, K., Firtel, R.A., Ginsberg, M.H., Borisy, G., Parsons, J.T., and Horwitz, A.R. (2003). Cell migration: integrating signals from front to back. Science *302*, 1704-1709.

Rivolta, M.N., and Holley, M.C. (1998). GATA3 is downregulated during hair cell differentiation in the mouse cochlea. J Neurocytol *27*, 637-647.

Rushton, D.H. (2002). Nutritional factors and hair loss. Clin Exp Dermatol *27*, 396-404.

Samokhvalov, I.M., Samokhvalova, N.I., and Nishikawa, S. (2007). Cell tracing shows the contribution of the yolk sac to adult haematopoiesis. Nature *446*, 1056-1061.

Sano, S., Itami, S., Takeda, K., Tarutani, M., Yamaguchi, Y., Miura, H., Yoshikawa, K., Akira, S., and Takeda, J. (1999). Keratinocyte-specific ablation of Stat3 exhibits impaired skin remodeling, but does not affect skin morphogenesis. Embo J *18*, 4657-4668.

Sano, S., Kira, M., Takagi, S., Yoshikawa, K., Takeda, J., and Itami, S. (2000). Two distinct signaling pathways in hair cycle induction: Stat3-dependent and -independent pathways. Proc Natl Acad Sci U S A *97*, 13824-13829.

Schmidt-Ullrich, R., and Paus, R. (2005). Molecular principles of hair follicle induction and morphogenesis. Bioessays *27*, 247-261.

Schneider, M.R., Schmidt-Ullrich, R., and Paus, R. (2009). The hair follicle as a dynamic miniorgan. Curr Biol *19*, R132-142.

Silva-Vargas, V., Lo Celso, C., Giangreco, A., Ofstad, T., Prowse, D.M., Braun, K.M., and Watt, F.M. (2005). Beta-catenin and Hedgehog signal strength can specify number and location of hair follicles in adult epidermis without recruitment of bulge stem cells. Dev Cell *9*, 121-131.

Slack, J.M. (2008). Origin of stem cells in organogenesis. Science *322*, 1498-1501.

Soma, T., Ishimatsu-Tsuji, Y., Tajima, M., and Kishimoto, J. (2006). Runx1 transcription factor is involved in the regulation of KAP5 gene expression in human hair follicles. J Dermatol Sci *41*, 221-224.

Soriano, P. (1999). Generalized lacZ expression with the ROSA26 Cre reporter strain. Nat Genet *21*, 70-71.

Speck, N.A., and Gilliland, D.G. (2002). Core-binding factors in haematopoiesis and leukaemia. Nat Rev Cancer *2*, 502-513.

Speck, N.A., Peeters, M., Dzierzak, E. (2002). Development of the vertebrate hematopoietic system. In Mouse development, J. Rossant, Tam, P., ed. (Academic Press), pp. 191-210.

Spradling, A., Drummond-Barbosa, D., and Kai, T. (2001). Stem cells find their niche. Nature *414*, 98-104.

Taylor, G., Lehrer, M.S., Jensen, P.J., Sun, T.T., and Lavker, R.M. (2000). Involvement of follicular stem cells in forming not only the follicle but also the epidermis. Cell *102*, 451-461.

Telfer, J.C., and Rothenberg, E.V. (2001). Expression and function of a stem cell promoter for the murine CBFalpha2 gene: distinct roles and regulation in natural killer and T cell development. Dev Biol *229*, 363-382.

Theriault, F.M., Nuthall, H.N., Dong, Z., Lo, R., Barnabe-Heider, F., Miller, F.D., and Stifani, S. (2005). Role for Runx1 in the proliferation and neuronal differentiation of selected progenitor cells in the mammalian nervous system. J Neurosci *25*, 2050-2061.

Theriault, F.M., Roy, P., and Stifani, S. (2004). AML1/Runx1 is important for the development of hindbrain cholinergic branchiovisceral motor neurons and selected cranial sensory neurons. Proc Natl Acad Sci U S A *101*, 10343-10348.

Topley, G.I., Okuyama, R., Gonzales, J.G., Conti, C., and Dotto, G.P. (1999). p21(WAF1/Cip1) functions as a suppressor of malignant skin tumor formation and a determinant of keratinocyte stem-cell potential. Proc Natl Acad Sci U S A *96*, 9089-9094.

Trempus, C.S., Morris, R.J., Bortner, C.D., Cotsarelis, G., Faircloth, R.S., Reece, J.M., and Tennant, R.W. (2003). Enrichment for living murine keratinocytes from the hair follicle bulge with the cell surface marker CD34. J Invest Dermatol *120*, 501-511.

Tumbar, T. (2006). Epithelial skin stem cells. Methods Enzymol *419*, 73-99.

Tumbar, T., Guasch, G., Greco, V., Blanpain, C., Lowry, W.E., Rendl, M., and Fuchs, E. (2004). Defining the epithelial stem cell niche in skin. Science *303*, 359-363.

van Genderen, C., Okamura, R.M., Farinas, I., Quo, R.G., Parslow, T.G., Bruhn, L., and Grosschedl, R. (1994). Development of several organs that require inductive epithelial-mesenchymal interactions is impaired in LEF-1-deficient mice. Genes Dev *8*, 2691-2703.

Van Mater, D., Kolligs, F.T., Dlugosz, A.A., and Fearon, E.R. (2003). Transient activation of beta -catenin signaling in cutaneous keratinocytes is sufficient to trigger the active growth phase of the hair cycle in mice. Genes Dev *17*, 1219-1224.

Vasioukhin, V., Degenstein, L., Wise, B., and Fuchs, E. (1999). The magical touch: genome targeting in epidermal stem cells induced by tamoxifen application to mouse skin. Proc Natl Acad Sci U S A *96*, 8551-8556.

Vicente-Manzanares, M., Choi, C.K., and Horwitz, A.R. (2009). Integrins in cell migration--the actin connection. J Cell Sci *122*, 199-206.

Vidal, V.P., Chaboissier, M.C., Lutzkendorf, S., Cotsarelis, G., Mill, P., Hui, C.C., Ortonne, N., Ortonne, J.P., and Schedl, A. (2005). Sox9 is essential for outer root sheath differentiation and the formation of the hair stem cell compartment. Curr Biol *15*, 1340-1351.

Vogel, G. (2003). Stem cells. 'Stemness' genes still elusive. Science *302*, 371.

Waghmare, S.K., Bansal, R., Lee, J., Zhang, Y.V., McDermitt, D.J., and Tumbar, T. (2008). Quantitative proliferation dynamics and random chromosome segregation of hair follicle stem cells. EMBO J *27*, 1309-1320.

Waikel, R.L., Kawachi, Y., Waikel, P.A., Wang, X.J., and Roop, D.R. (2001). Deregulated expression of c-Myc depletes epidermal stem cells. Nat Genet *28*, 165-168.

Walker, M.R., Patel, K.K., and Stappenbeck, T.S. (2009). The stem cell niche. J Pathol *217*, 169-180.

Wang, J., and Conboy, I. (2009). Embryonic vs. Adult Myogenesis: Challenging the 'Regeneration Recapitulates Development' Paradigm. J Mol Cell Biol.

Wang, L.C., Liu, Z.Y., Gambardella, L., Delacour, A., Shapiro, R., Yang, J., Sizing, I., Rayhorn, P., Garber, E.A., Benjamin, C.D., *et al.* (2000). Regular articles: conditional disruption of hedgehog signaling pathway defines its critical role in hair development and regeneration. J Invest Dermatol *114*, 901-908.

Wang, Q., Stacy, T., Binder, M., Marin-Padilla, M., Sharpe, A.H., and Speck, N.A. (1996). Disruption of the Cbfa2 gene causes necrosis and hemorrhaging in the central nervous system and blocks definitive hematopoiesis. Proc Natl Acad Sci U S A *93*, 3444-3449.

Wang, X., Blagden, C., Fan, J., Nowak, S.J., Taniuchi, I., Littman, D.R., and Burden, S.J. (2005). Runx1 prevents wasting, myofibrillar disorganization, and autophagy of skeletal muscle. Genes Dev *19*, 1715-1722.

Watt, F.M., and Hogan, B.L. (2000). Out of Eden: stem cells and their niches. Science *287*, 1427-1430.

Yang, A., Schweitzer, R., Sun, D., Kaghad, M., Walker, N., Bronson, R.T., Tabin, C., Sharpe, A., Caput, D., Crum, C., *et al.* (1999). p63 is essential for regenerative proliferation in limb, craniofacial and epithelial development. Nature *398*, 714-718.

Yang, L., Wang, L., and Yang, X. (2009). Disruption of Smad4 in mouse epidermis leads to depletion of follicle stem cells. Mol Biol Cell *20*, 882-890.

Yi, R., Poy, M.N., Stoffel, M., and Fuchs, E. (2008). A skin microRNA promotes differentiation by repressing 'stemness'. Nature *452*, 225-229.

Young, H.E., and Black, A.C., Jr. (2004). Adult stem cells. Anat Rec A Discov Mol Cell Evol Biol *276*, 75-102.

Zervas, M., Millet, S., Ahn, S., and Joyner, A.L. (2004). Cell behaviors and genetic lineages of the mesencephalon and rhombomere 1. Neuron *43*, 345-357.

Zhang, J., Niu, C., Ye, L., Huang, H., He, X., Tong, W.G., Ross, J., Haug, J., Johnson, T., Feng, J.Q., *et al.* (2003). Identification of the haematopoietic stem cell niche and control of the niche size. Nature *425*, 836-841.

Zhang, Y.V., Cheong, J., Ciapurin, N., McDermitt, D.J., and Tumbar, T. (2009). Distinct Self-Renewal and Differentiation Phases in the Niche of Infrequently Dividing Hair Follicle Stem Cells. Cell Stem Cell.

Zhong, J., Pevny, L., and Snider, W.D. (2006). "Runx"ing towards sensory differentiation. Neuron *49*, 325-327.

Zhou, P., Byrne, C., Jacobs, J., and Fuchs, E. (1995). Lymphoid enhancer factor 1 directs hair follicle patterning and epithelial cell fate. Genes Dev *9*, 700-713.